PL-TR--95-1013

PL-TR--
95-1013

DATA REPORT OF HYPERVELOCITY MICRO-PARTICLE IMPACT LIGHT FLASH DATA AND MOS IMPACT DETECTOR OUTPUT

Patrick J. Serna

June 1995

Final Report

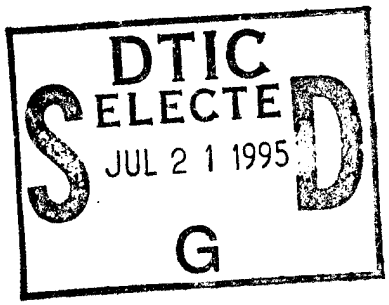

PHILLIPS LABORATORY
Advanced Weapons and Survivability Directorate
AIR FORCE MATERIEL COMMAND
KIRTLAND AIR FORCE BASE, NM 87117-5776

PL-TR-95-1013

This final report was prepared by the Phillips Laboratory, Kirtland Air Force Base, New Mexico, under Job Order 5797ABAB. The Laboratory Project Officer-In-Charge was Mr. Patrick J. Serna (WSCH).

When Government drawings, specifications, or other data are used for any purpose other than in connection with a definitely Government-related procurement, the United States Government incurs no responsibility or other obligation whatsoever. The fact that the Government may have formulated or in any way supplied the said drawings, specifications, or other data, is not to be regarded by implication, or otherwise in any manner construed, as licensing the holder, or any other person or corporation; or as conveying any rights or permission to manufacture, use, or sell any patented invention that may in any way be related thereto.

This report has been authored by an employee of the United States Government. Accordingly, the United States Government retains a non-exclusive, royalty-free license to publish or reproduce the material contained herein, or allow others to do so, for the United States Government purposes.

This report has been reviewed by the Public Affairs Office and is releasable to the National Technical Information Service (NTIS). At NTIS, it will be available to the general public, including foreign nationals.

If your address has changed, if you wish to be removed from the mailing list, or if your organization no longer employs the addressee, please notify PL/WSC, Kirtland AFB, NM 87117-6008 to help maintain a current mailing list.

This technical report has been reviewed and is approved for publication.

Patrick J. Serna

PATRICK J. SERNA
Project Officer

FOR THE COMMANDER

Firooz A. Allahdadi

FIROOZ A. ALLAHDADI
Space Kinetic Impact/Debris Branch, Chief

William G. Heckathorn

WILLIAM G. HECKATHORN, Col, USAF
Director, Advanced Weapons and
Survivability Directorate

DO NOT RETURN COPIES OF THIS REPORT UNLESS CONTRACTUAL OBLIGATIONS OR NOTICE ON A SPECIFIC DOCUMENT REQUIRES THAT IT BE RETURNED

REPORT DOCUMENTATION PAGE

Form Approved
OMB No. 0704-0188

1. AGENCY USE ONLY *(Leave blank)*	2. REPORT DATE	3. REPORT TYPE AND DATES COVERED
	June 1995	FINAL, May 94 - May 95

4. TITLE AND SUBTITLE

Data Report of Hypervelocity Micro-Particle Impact Light Flash Data and MOS Impact Detector Output

5. FUNDING NUMBERS

C: none G: none
PE: 62601F
PR: 5797
TA: AB
WU: AB

6. AUTHOR(S)

Patrick J. Serna

7. PERFORMING ORGANIZATION NAME(S) AND ADDRESS(ES)

Phillips Laboratory/WSCH
3550 Aberdeen Ave., SE
Kirtland AFB, NM 87117-5776

8. PERFORMING ORGANIZATION REPORT NUMBER

PL-TR-95--1013

9. SPONSORING / MONITORING AGENCY NAME(S) AND ADDRESS(ES)

10. SPONSORING / MONITORING AGENCY REPORT NUMBER

11. SUPPLEMENTARY NOTES

Prepared as a companion data report to a separate report to be published by F. Allahdadi, D. Medina, M. Long, and P. Serna

12a. DISTRIBUTION / AVAILABILITY STATEMENT

Approved For Public Release; Distribution Is Unlimited

12b. DISTRIBUTION CODE

13. ABSTRACT *(Maximum 200 words)*

A series of hypervelocity impact tests were conducted at the Max-Plank Institut fur Kernphysik, Heidelberg, Germany using the Institut's 2 MV Van De Graaff micro-particle accelerator. The purpose of this experimental effort was to collect impact flash data resulting from hypervelocity impact events. The results of these test experiments are to be correlated with actual waveforms obtained from on-orbit systems. Furthermore, these experimental results will supplement ongoing theoretical predictions being conducted within the Phillips Laboratory by the Space Kinetic Impact/Debris Branch (PL/WSCD). This report only describes the instrumentation configuration and presents data collected from light flash measurements and a MOS micro-particle impact detector. An analysis of the acquired light flash data is contained in a separate report authored by Allahdadi, Medina, Serna, and Long. Iron particles in the mass range of 1×10^{-15} to 8×10^{-18} kg were accelerated to velocities between 7 and 38 km/sec. Three targets were used for these impact test: spacecraft optical lens, spacecraft optical sunshade, and MOS spacecraft micro-particle impact detector. The hypervelocity particle impacted the lens and micro-particle impact detector targets normal to the target surface. The sunshade was impacted at a 25 degree angle measured from the particle direction of flight.

14. SUBJECT TERMS

Micro-Particle, Hypervelocity, Light Flash, Hypervelocity Impact, Micro-Particle Detector

15. NUMBER OF PAGES

130

16. PRICE CODE

17. SECURITY CLASSIFICATION OF REPORT	18. SECURITY CLASSIFICATION OF THIS PAGE	19. SECURITY CLASSIFICATION OF ABSTRACT	20. LIMITATION OF ABSTRACT
UNCLASSIFIED	UNCLASSIFIED	UNCLASSIFIED	UNLIMITED

CONTENTS

FIGURES

FIGURES (CONTINUED)

TABLES

1.0 INTRODUCTION

Phillips Laboratory and Max-Plank Institut personnel conducted a series of hypervelocity impact tests at the Max-Plank Institut fur Kernphysik, Heidelberg, Germany using the Institut's 2 MV Van De Graaff micro-particle accelerator. A detailed description of the Van De Graaff was published by Fechtig (Ref. 1).

The purpose of this experimental effort was to collect impact flash data resulting from hypervelocity impact events. The results of these test experiments are to be correlated with actual waveforms obtained from on-orbit systems. Furthermore, these experimental results will supplement ongoing theoretical predictions being conducted within the Phillips Laboratory by the Space Kinetic Impact/Debris Branch (PL/WSCD). This report only describes the instrumentation configuration and presents data collected from light flash measurements and a MOS micro-particle impact detector. A complete analysis of the acquired data is contained in a separate Phillips Laboratory report to be published by Allahdadi, Medina, Serna, and Long.

Iron particles in the mass range of 1×10^{-15} to 8×10^{-18} kg were accelerated to velocities between 7 and 38 km/sec, with the majority of particles accelerated in the 7-12 km/sec range. Three targets were used for the impact tests: spacecraft optical lens, spacecraft optical sunshade, and spacecraft micro-particle impact detector. The hypervelocity particle impacted the lens and micro-particle impact detector targets normal to the target surface. The sunshade was impacted at a 25 degree angle measured from the particle direction of flight.

The instrumentation system for measuring the light flash from iron particles impacting the lens and sunshade targets consisted of two independent light flash detectors: photomultiplier and photo-diode.* Post test data analysis revealed that the photomultiplier provided higher quality data than the photo-diode data. As a result, this data report will only discuss the photomultiplier data and will not discuss specifics of the photo-diode system or data. The output from the photomultiplier, photo-diode, and micro-particle impact detector were recorded using a Nicolet digitizing oscilloscope system. The Van De Graaff instrumentation system provided a data trigger for the Nicolet digitizing oscilloscope.

The three targets were installed in the Van De Graaff vacuum chamber that maintained vacuum at approximately 10^{-6} Torr.

---

* Browning J., Spalding R., Sandia National Laboratory, Kirtland AFB, NM, private communication, 1994.

The impact tests were divided into five series of tests. The first and second series consisted of forty-four impact tests with a positive 700 volt bias applied to the lens and sunshade targets. The third and fourth series consisted of fifty-nine impact tests with a 700 volt bias removed from the lens and sunshade targets. The 700 volt bias was removed and applied to the lens and sunshade targets to simulate a natural space environment and to determine if the 700 volt bias affected the impact light flash intensity.

The fifth test series consisted of twenty impacts on the MOS micro-particle impact detector. Appendices A through E present raw photomultiplier and micro-particle detector output signals recorded for each impact test. Appendix F contains five tables which summarize the recorded impact data. Table 1 summarizes the impact test series.

Table 1. Impact Test Series

Impact Test Series	Impact Test Number	Target	700 Volt Bias Applied?
1	A6-A20	Lens	Yes
2	F7-F20	Sunshade	Yes
2	G1-G14	Sunshade	Yes
3	A1-A5	Lens	No
3	B3-B20	Lens	No
4	C1-C3	Sunshade	No
4	C5-C20	Sunshade	No
4	E10-E20	Sunshade	No
4	F1-F6	Sunshade	No
5	D1-D20	Micro-particle Impact Detector	No

2.0 IMPACT TEST INSTRUMENTATION and CONFIGURATION

2.1 Light Flash Instrumentation and Configuration

Shown in figures 1 and 2 are the light flash instrumentation configuration. Figure 3 shows the light flash instrumentation electronic schematics.

The light flash instrumentation included a THORN EMI photomultiplier tube model 9813B, photo-diodes, and associated electronics.

The photomultiplier had a bialkali spectral response and a standard borosilicate window type B. The photomultiplier tube was used with an EG&G ORTEC photomultiplier base model 269. The photomultiplier was negatively biased using a standard laboratory high voltage power supply. Bias voltages ranged from -1,700 volts to -2,000 volts. Photomultiplier anode output voltage will respond in the negative direction with increasing light intensity.

The voltage output of the photomultiplier and the photo-diodes were recorded using a Nicolet digitizing oscilloscope, model number 4094C and Nicolet floppy disk data recording system F-43.

The photomultiplier and photo-diodes were mounted such that they viewed the mounted target through a 100 mm diameter vacuum atmospheric window port. Care was taken to ensure that there were no light leaks into the photomultiplier and photo-diodes mounting apparatus during the hypervelocity impact experiments.

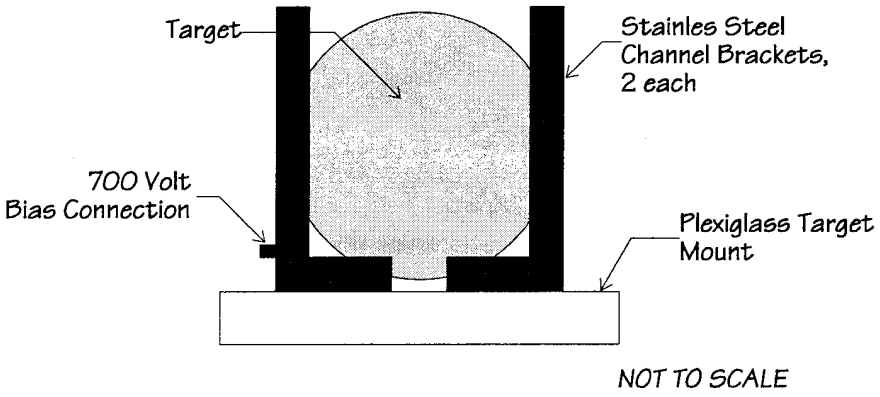

Figure 1. Target Holder, Impact Side

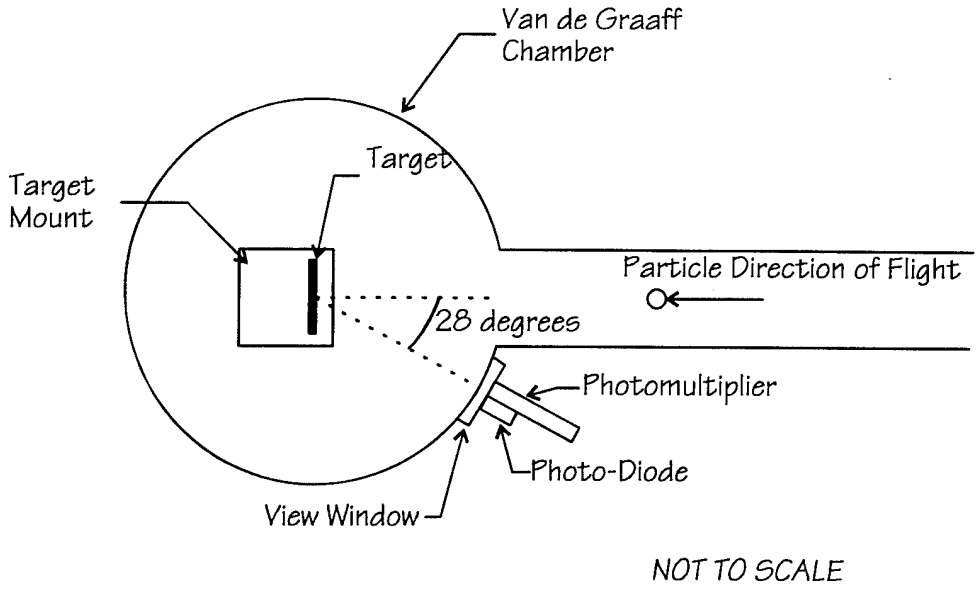

(a) Lens Normal Impact

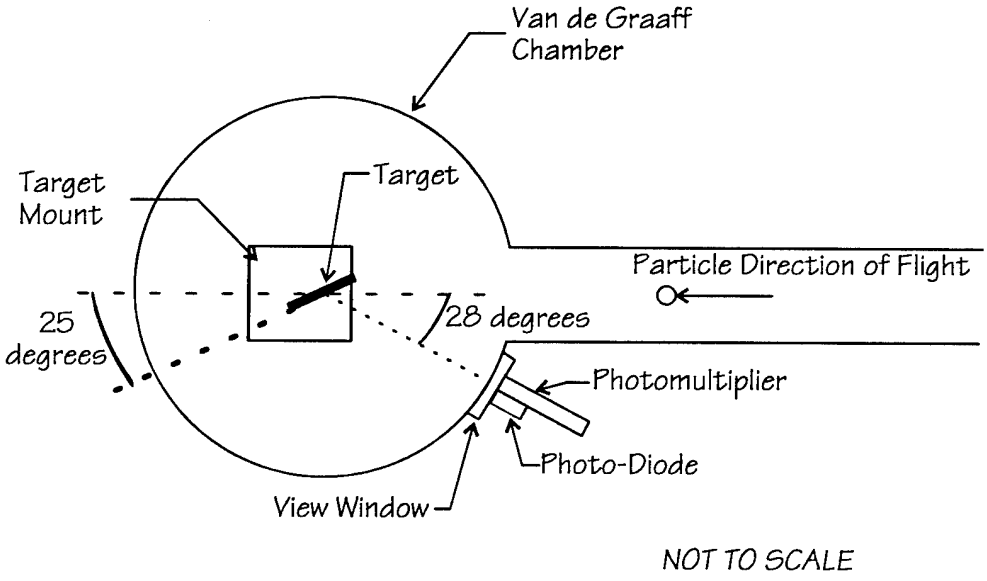

(b) Sunshade 25 Degree Impact

Figure 2. Instrumentation Configuration

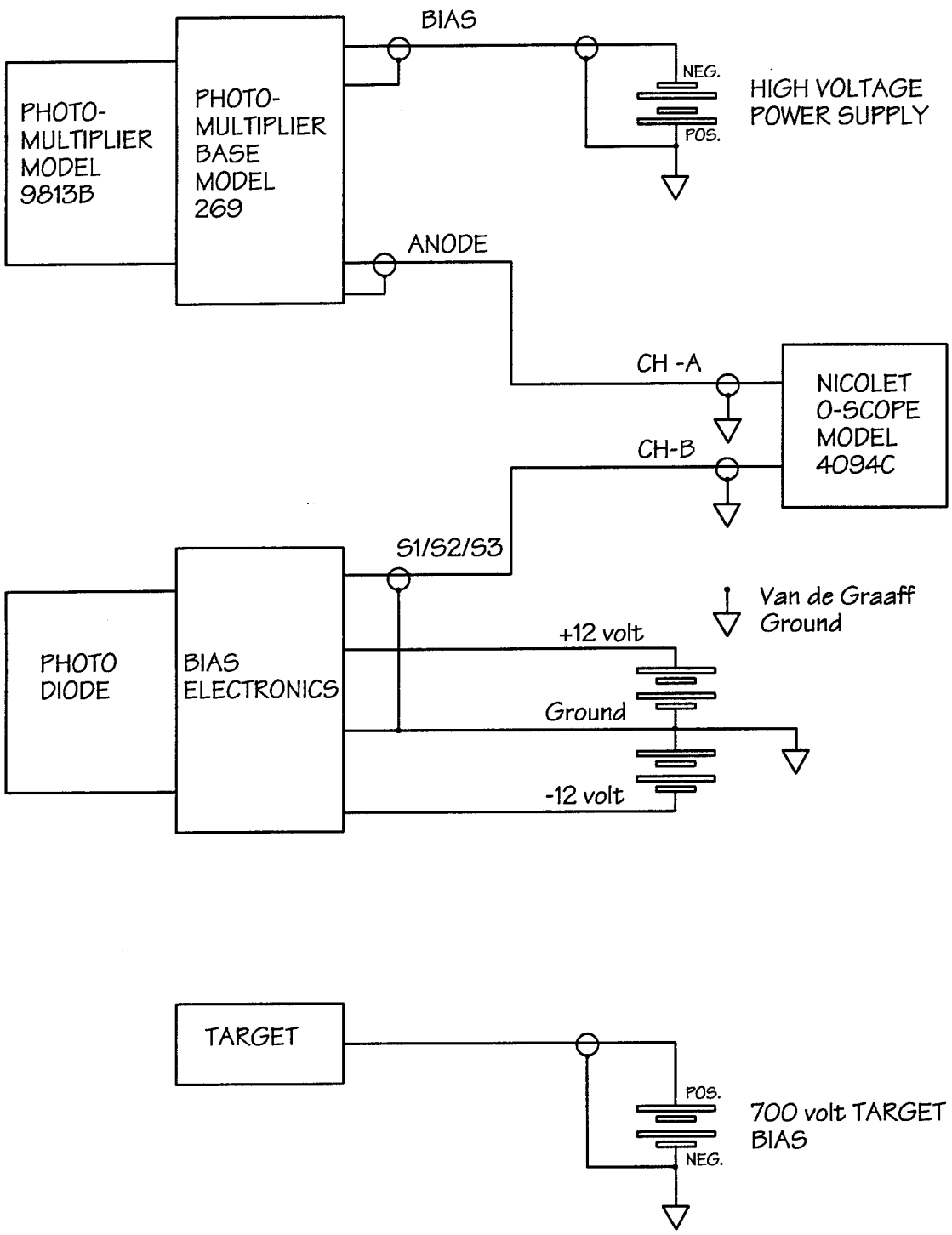

Figure 3. Light Flash Instrumentation Schematic

2.2 Micro-Particle Detector Instrumentation and Configuration

The micro-particle detectors were MOS capacitor impact detectors provided by North Carolina State University (Ref. 2). Specifics of the detectors, other than a general overview, will not be discussed in this report. However, a complete description can be found in reports authored by Kassel and Wortman (Refs. 2 and 3).

The detectors consist of a parallel plate capacitor with a dielectric thickness of 1.0 micron and a top surface thickness of 0.1 micron. A bias voltage is applied across the capacitor, resulting in a charged capacitor. When particles impact the top surface of the detector, a discharge occurs. This discharge can be monitored and recorded.

The detectors used in this experiment were identical to the detectors that were flown on the Clementine Mission (Ref 4).

A schematic of the bias circuitry is shown in figure 4.

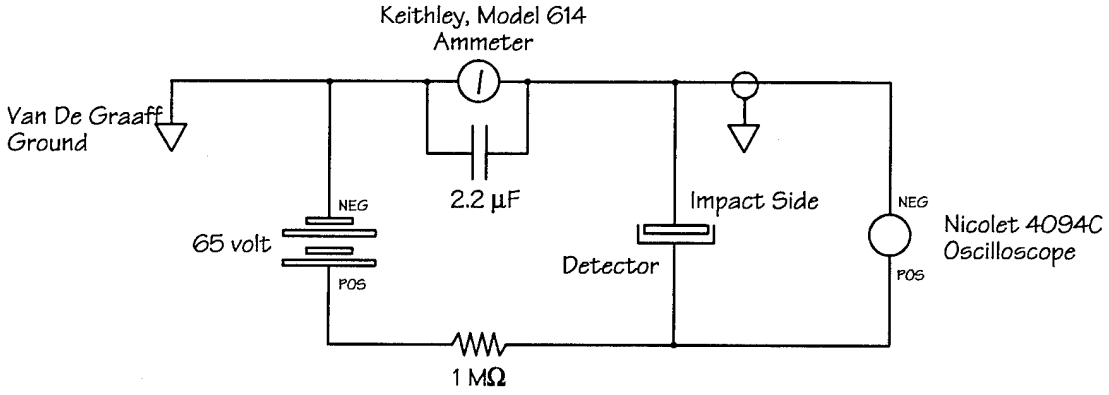

Figure 4. Micro-Particle Detector Bias Circuitry

The detectors, approximately 3.0 inches by 1.5 inches, were mounted on a 0.375 inch thick aluminum mounting block. Dow Corning RTV number 734 was used to adhere the detectors to the aluminum mounting block. Rubber gloves and tweezers were used while handling and mounting the detectors. A small amount of RTV was evenly spread across the aluminum mounting block just prior to placing the detector on the mounting block. The aluminum mounting block is shown in figure 5.

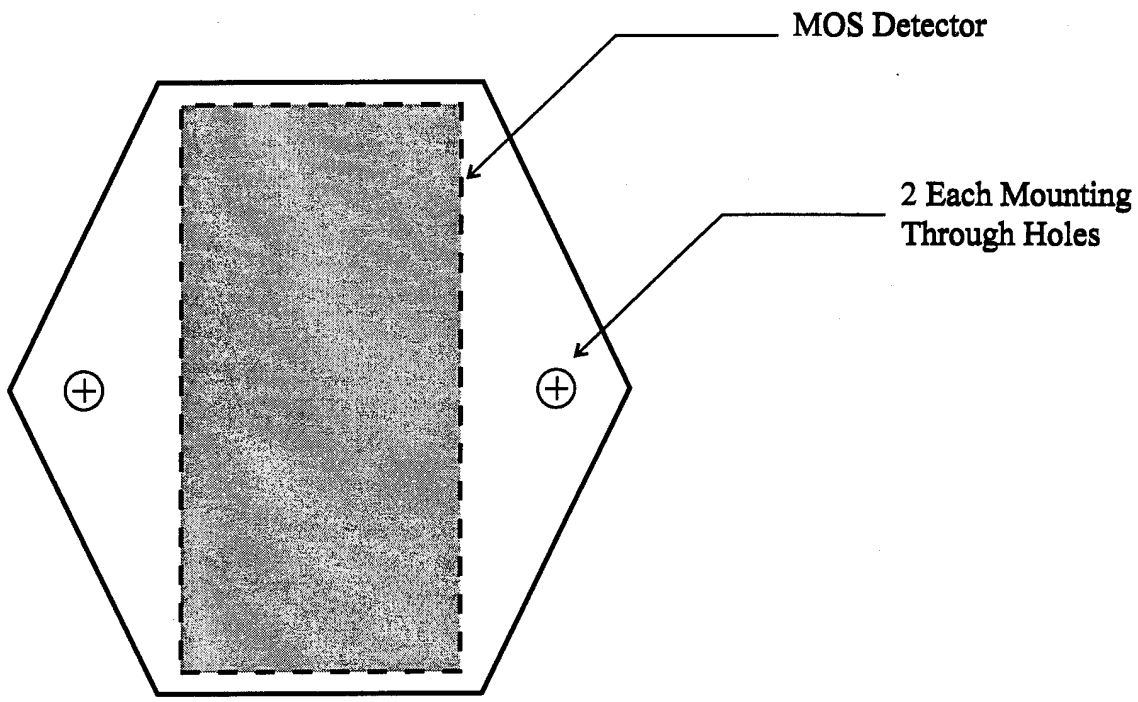

Figure 5. Micro-Particle Mounting Block

Prior to impact testing, operational tests were conducted on each detector. However, only one detector was used during impact testing, serial number 0523-10-2. Capacitance of the impact tested single detector was 87.9 x 10^{-9} farads.

For each impact test, the micro-particle detector output was recorded using a Nicolet 4094C oscilloscope and associated floppy disk recorder.

2.3 LIGHT EMITTING DIODE (LED) LIGHT SOURCE SIMULATION

An LED was attached to the target holder in a manner that could be viewed by the photomultiplier. Using a standard laboratory LED bias system, the LED was pulsed on and off as simulation of an impact light flash. This simulation was used to verify that the photomultiplier instrumentation system was configured correctly. An electrical schematic of the LED light flash simulation system is shown in figure 6.

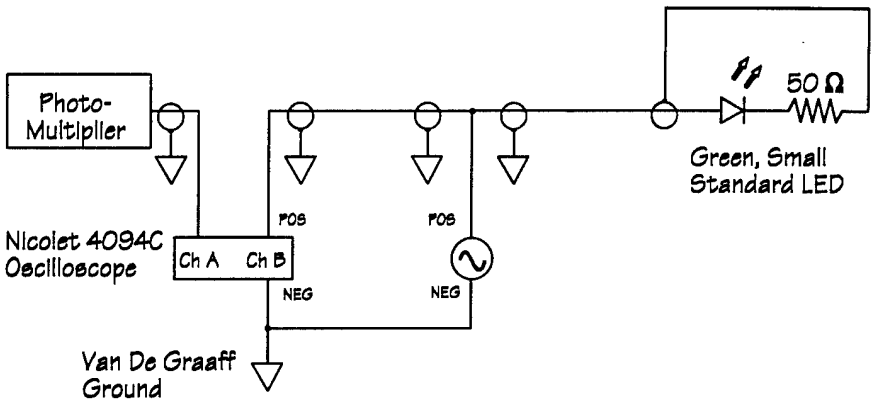

Figure 6. Light Flash Simulation Electrical Configuration

Shown in figure 7 is the recorded single pulse that was used to pulse the LED on and off. Figure 8 shows the recorded photomultiplier response to the LED light flash simulation.

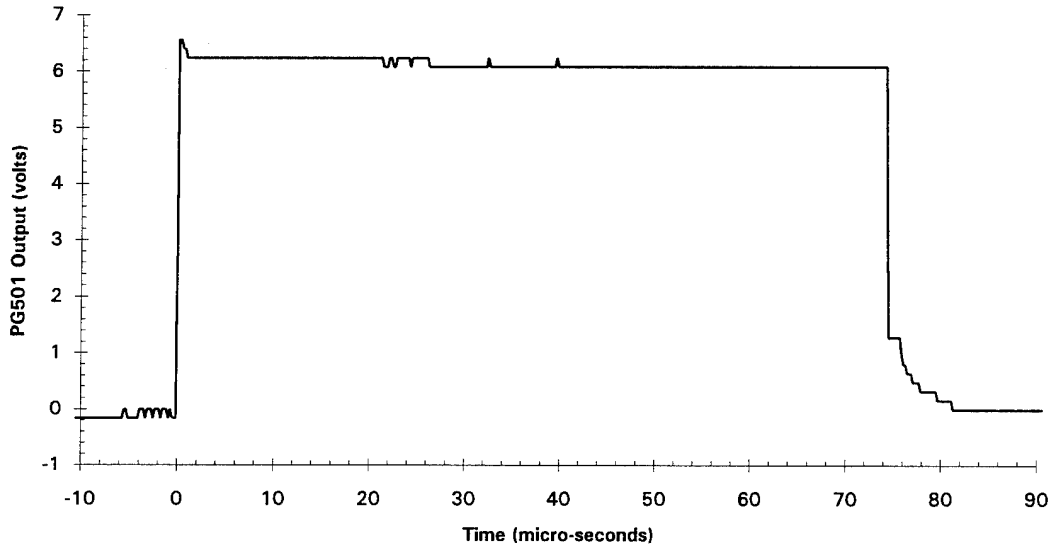

Figure 7. Output Of Pulse Generator. See Figure 6

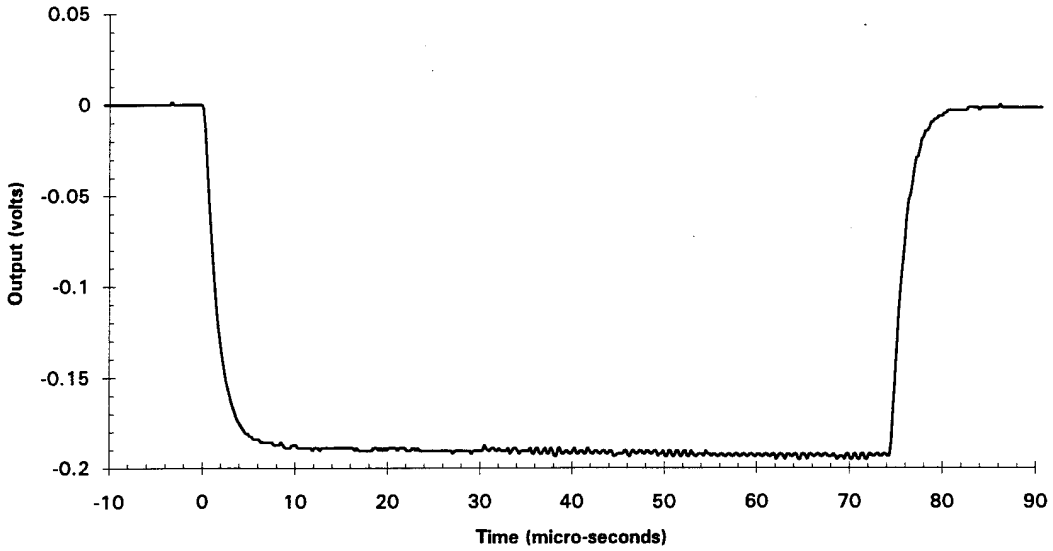

Figure 8. Photomultiplier Response To Pulse Shown In Figure 7

3.0 PHOTOMULTIPLIER CALIBRATION

3.1 Relative Calibration Factor

The general method described in RCA Photomultiplier Handbook, PMT-62, was used to determine a relative calibration factor for the photomultiplier tube (Ref. 5). The following description focuses primarily on the calculation method as it relates to this particular experiment. A more complete discussion of the general method is described in the RCA handbook.

A light source will radiate power as expressed by the following equation:

$$P = P_o \int_0^\infty W(\lambda) d\lambda \qquad (1)$$

where

P = total power radiating from a light source

P_o = peak power per unit wavelength at the peak of the relative spectral radiation characteristic of a light source, W(λ)

$W(\lambda)$ = spectral characteristic of light source, normalized to unity at the peak

λ = wavelength

Photocathode current resulting from light incident on the photomultiplier can be expressed as follows:

$$I_k = \sigma(0.9P_o)\int_0^\infty W(\lambda)R(\lambda)d\lambda \qquad (2)$$

where

σ = radiant sensitivity of the photocathode at the peak of the spectral response curve (amperes per watt)

$R(\lambda)$ = relative photocathode spectral response normalized to unity at the peak

0.9 = fractional transmission characteristic of window port, 0.32 - 0.62 microns (Ref. 6)

Solving equation 1 for peak power per unit wavelength, P_o, yields the following expression:

$$P_o = \frac{P}{\int_0^\infty W(\lambda)d\lambda} \qquad (3)$$

Substituting equation 3 into equation 2 yields an alternative expression for the photocathode current. The resulting expression follows:

$$I_k = 0.9\sigma P \frac{\int_0^\infty W(\lambda)R(\lambda)d\lambda}{\int_0^\infty W(\lambda)d\lambda} \qquad (4)$$

Solving equation 4 for P, the total power radiating from the impact light flash, yields the following expression:

$$P = \frac{I_k}{0.9\sigma}\left[\frac{\int_0^\infty W(\lambda)d\lambda}{\int_0^\infty W(\lambda)R(\lambda)d\lambda}\right] \qquad (5)$$

A matching factor, M, can be defined as the ratio of the two integrals in equation 5. The matching factor is expressed as follows:

$$M = \frac{\int_0^\infty W(\lambda)d\lambda}{\int_0^\infty W(\lambda)R(\lambda)d\lambda} \tag{6}$$

Equation 5 can be re-written using the matching factor, M, resulting in the following expression:

$$P = \frac{I_k}{0.9\sigma} M \tag{7}$$

The single unknown in equation 7 is the spectral characteristic of the impact light flash, $W(\lambda)$. For this experiment, $W(\lambda)$, is assumed to be that of a blackbody source. With this assumption the total power of the light flash, P, can be calculated. The author uses the spectral characteristics of a blackbody source based on previous work conducted by Friichtenicht (Ref 7). In Friichtenicht, the experimenters suggested that the source of light caused by hypervelocity impact was similar to a blackbody source. However, the author recognizes that this assumption does not truly represent the spectral characteristic of the impact light flash.

The radiant sensitivity, σ, of the photocathode at the peak of the photomultiplier spectral response was calculated and normalized to unity using the photomultiplier spectral response characteristics published by the photomultiplier manufacture and the following standard photomultiplier expression for wavelengths between 0.32 and 0.62 microns in increments of 0.02 microns (Ref. 8).

$$\sigma = \frac{(Q.E.)\lambda}{123.96} \tag{8}$$

where

$Q.E.$= photomultiplier quantum efficiency

λ = wavelength at peak of spectral response curve

123.96 = unit conversion factor

Radiant sensitivity, σ, of the photomultiplier at the peak of the spectral response curve was calculated to be 4.5×10^{-8} amperes/watt.

The photomultiplier spectral response curve derived using equation 8 is shown in figure 9.

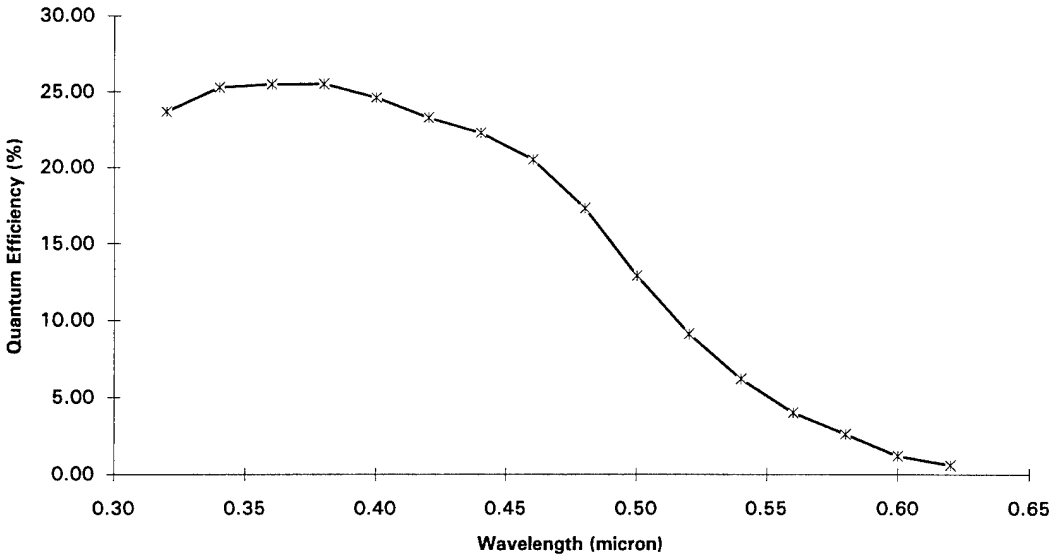

Figure 9. Photomultiplier Spectral Response Curve

The spectral characteristic of the light flash, $W(\lambda)$, was calculated assuming a blackbody source at 4,000°K. The blackbody temperature of 4,000°K was used based on earlier work conducted by TRW Systems (Ref. 7).

Figure 10 shows the spectral characteristics of the assumed light flash, $W(\lambda)$, and the photomultiplier, $R(\lambda)$, both normalized to unity. The blackbody spectral response was normalized to unity using wavelength limits from zero to infinity. As a result, the peak of the blackbody curve occurs at a wavelength well beyond the spectral response of the photomultiplier. Figure 10 only shows spectral responses for wavelengths between 0.32 and 0.62 microns.

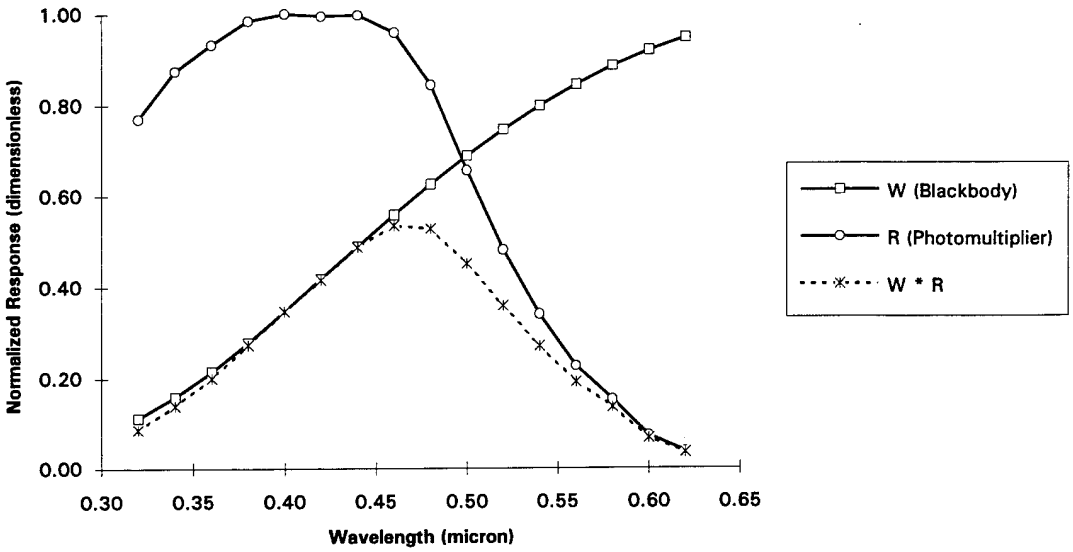

Figure 10. Spectral Response Characteristics of Assumed Blackbody and Photomultiplier, Normalized to Unity

Using data curves shown in figure 10 and equation 6 the matching factor, M, was calculated to be 1.903 (dimensionless).

The cathode current, I_k, is calculated from the measured photomultiplier anode voltage using the following expression:

$$I_A = GI_k \tag{9}$$

where

I_A = photomultiplier tube anode current

G = photomultiplier tube gain

An equation describing the effective power detected by the photomultiplier must account for the distance between the photomultiplier and the light flash and the effective detecting area of the photomultiplier. The relative light flash power, P_x, as detected by the photomultiplier can be expressed as follows:

$$P_x = P\left[\frac{m^2}{4\pi r^2}\right] \tag{10}$$

where

P_x = light flash power detected by photomultiplier

m^2 = effective detection area of photomultiplier

r = distance from the impact light flash to the photomultiplier

Substituting equation 7 into equation 10 yields the following equation for the relative light flash power detected by the photomultiplier.

$$P_x = \left[\frac{I_k M}{0.9\sigma}\right]\left[\frac{m^2}{4\pi r^2}\right] \tag{11}$$

where

M = 1.903 (dimensionless)

$\sigma = 4.5 \times 10^{-8}$ amperes/watt

$m^2 = 1.7 \times 10^{-3}$ m2

$r^2 = 5.1 \times 10^{-2}$ m2

3.2 Typical Light Flash Power and Energy Calculation

The first step in calculating relative light flash power and energy, as detected at the photomultiplier, is to calculate cathode current, I_k, using measured anode voltage. Anode current can be calculated by dividing the anode voltage by the termination resistance. During this experiment the equivalent anode termination resistance was 500 kilo-ohms. Cathode current, I_k, can then be calculated by dividing the anode current by the gain of the photomultiplier. Table 2 lists the photomultiplier gain that was used for each hypervelocity impact for this experiment. Shown in figure 11 is a typical anode voltage time plot for a single hypervelocity impact.

Table 2. Photomultiplier Bias Voltage and Gain

Impact Number	Photomultiplier Bias Voltage	Photomultiplier Gain
A1 - A5	2,000	2×10^7
A6 - A20	2,000	2×10^7
B3	1,500	5×10^5
B4 - B20	2,000	2×10^7
C1	1,500	5×10^5
C2 - C3	1,700	3×10^6
C4	2,000	2×10^7
C5 - C20	1,800	5×10^6
E10 - E20	2,000	2×10^7
F1 - F6	2,000	2×10^7
F7 - F20	2,000	2×10^7
G1 - G14	2,000	2×10^7

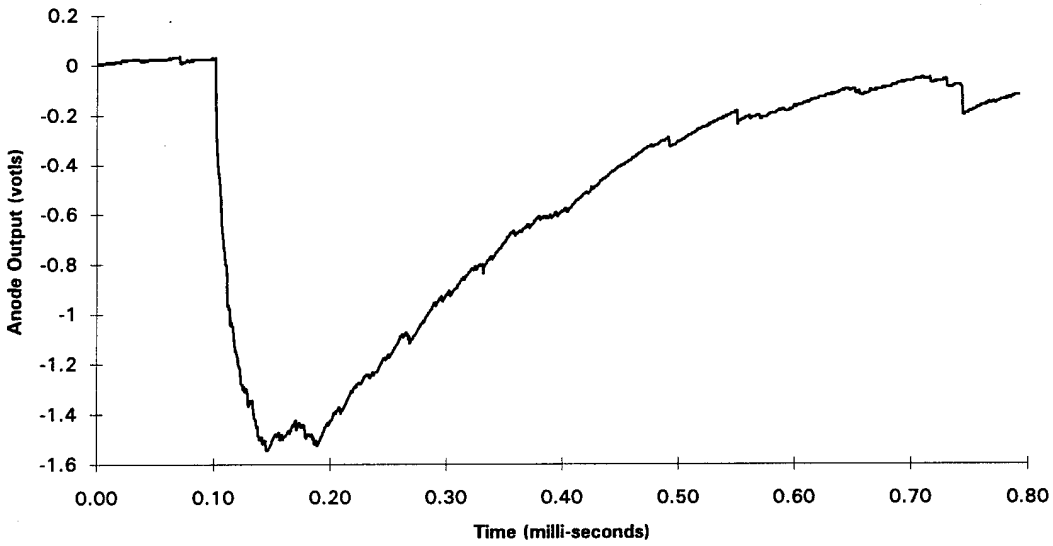

Figure 11. Voltage Time Plot, Impact Test Number A4

The calculated cathode current, I_k, can now be incorporated into equation 11, resulting in a determination of relative light flash power. Figure 12 shows a power versus time plot for the hypervelocity impact shown in figure 11.

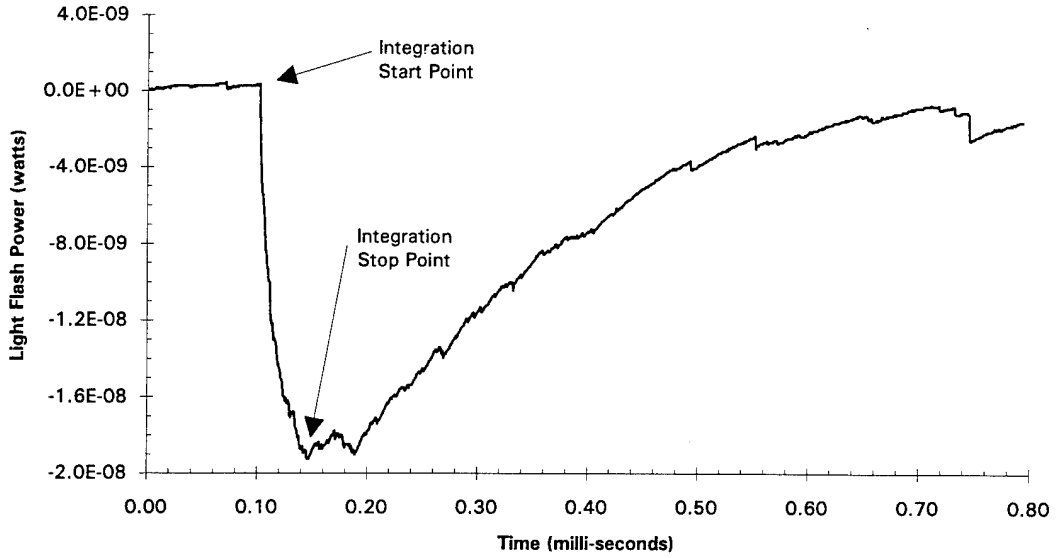

Figure 12. Power Time Plot, Impact Test Number A4

Relative light flash energy was calculated by integrating the light flash power curve over time. Prior to integration, a start and stop point for each hypervelocity impact power curve was manually identified. The integration start point was the point where the photomultiplier signal began to significantly change in amplitude. The integration stop point was the point where the photomultiplier signal significantly changed slope and where the hypervelocity impact light flash could no longer reasonably contribute to impact light energy. Shown in figure 12 are typical integration start and stop points. Additionally, the integration stop and start points were used to determine the photomultiplier signal rise time.

For the hypervelocity impact shown in figure 11, the following parameters were calculated:

Relative Light Flash Power = 1.91×10^{-8} watts
Relative Light Flash Energy = 8.19×10^{-13} joules
Rise Time = 43.2 micro-seconds

It is important to stress that the power and energy calculations assume the light flash spectral characteristics are that of a blackbody source. Because of this assumption, power and energy results are relative to a blackbody source and do not represent a precise measure of light flash power or energy.*

---

* Spalding R., Sandia National Laboratory, Kirtland AFB, NM, private communication, 1994.

4.0 IMPACT TEST RESULTS

4.1 Particle Mass, Diameter, and Velocity Data

Particle velocity was determined by the Van De Graaff internal measurement system by measuring particle time of flight between two known points.*

Particle mass was determined using one of the following two methods,

method 1: use of equation 12; or

$$qu = \frac{1}{2}mv^2 \tag{12}$$

where

q = particle charge. A standard laboratory charge amplifier and fine grid system was used to measure the particle charge

u = accelerating voltage of Van De Graaff

m = particle mass

v = particle velocity

method 2: an average of the value provided by the Van De Graaff internal measurement system and the value calculated from equation 12.

---

* Schafer G., Max-Plank Institut fur Kernphysik, Heildelberg, Germany, private communication, 1994.

Particle diameter was determined using one of the following two methods,

method 1: use of equation 13; or

$$\rho = \frac{mass}{volume} \tag{13}$$

method 2: an average of the value provided by the Van De Graaff internal measurement system and the value calculated from equation 13.

Table 3 tabulates the method used to determine particle mass and diameter for each hypervelocity impact.

Table 3. Particle Mass and Diameter Measurement Method

Impact Test Number	Method Used To Determine Particle Mass	Method Used To Determine Particle Diameter
A1-A20	Equation 12	Equation 13
B3-B20	Equation 12	Equation 13
C1-C20	Equation 12	Equation 13
D1-D20	Van De Graaff Value	Van De Graaff Value
E10-E20	Average	Average
F1-F20	Average	Average
G1-G20	Average	Average

A +700 volt bias was removed and applied to the lens and sunshade targets in an effort to simulate a natural space environment and to determine if a +700 volt bias affected the impact light flash energy. However, the +700 volt bias has no effect or correlation to the impacting particle diameter, mass, or velocity.

Figures 13 and 14 show mass, diameter, and velocity data for impacts associated with the lens target.

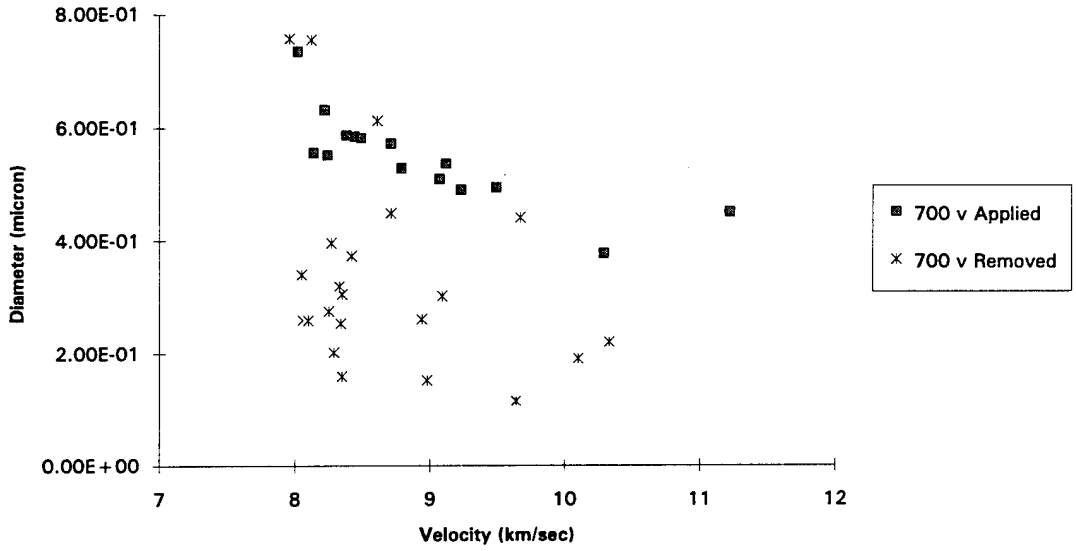

Figure 13. Diameter versus Velocity For Lens Target

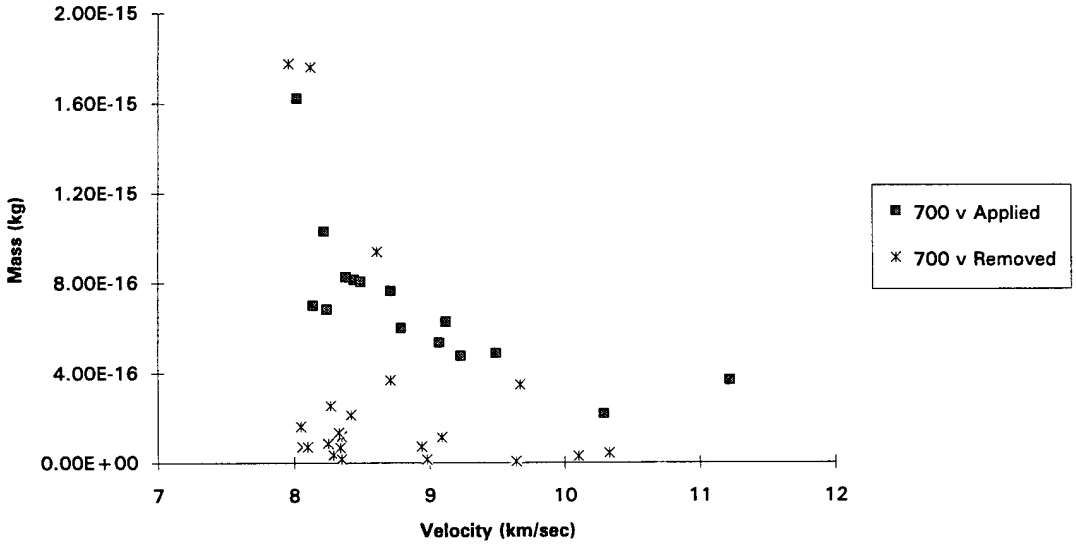

Figure 14. Mass versus Velocity For Lens Target

Figures 15 and 16 show mass, diameter, and velocity data for impacts associated with the sunshade target.

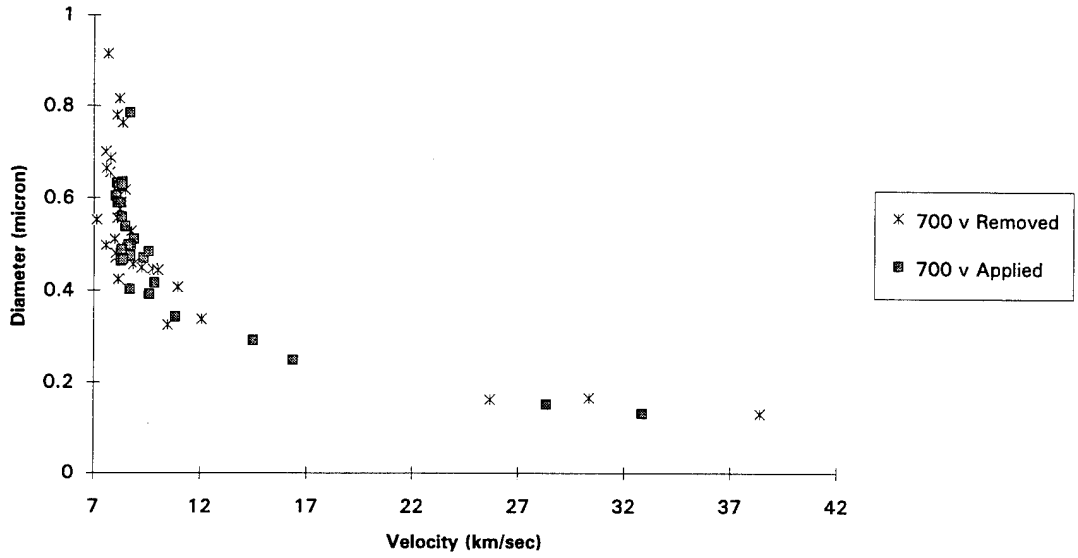

Figure 15. Diameter versus Velocity For Sunshade Target

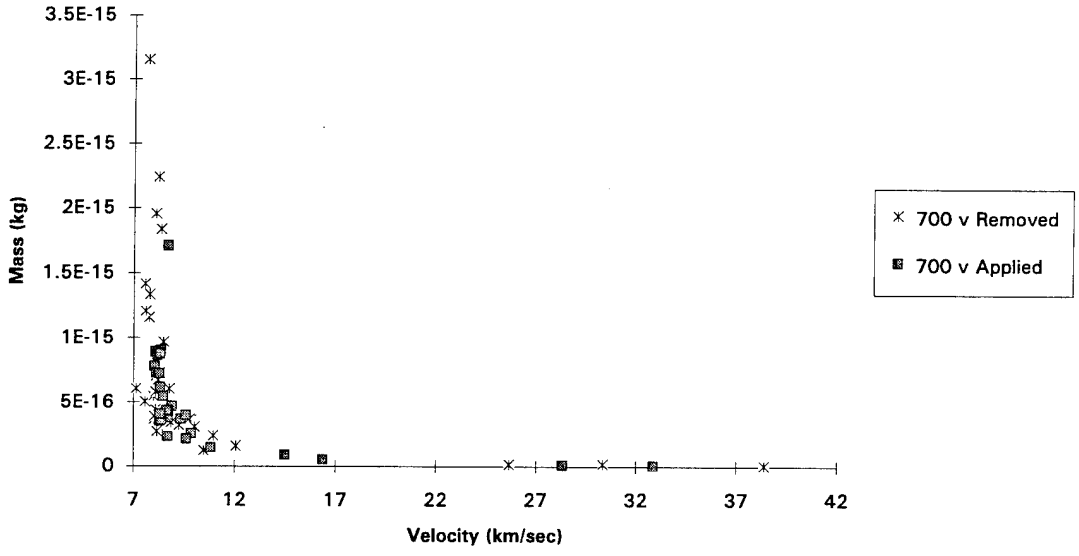

Figure 16. Mass versus Velocity For Sunshade Target

Figures 17 and 18 show mass, diameter, and velocity data for impacts associated with the micro-particle detector target.

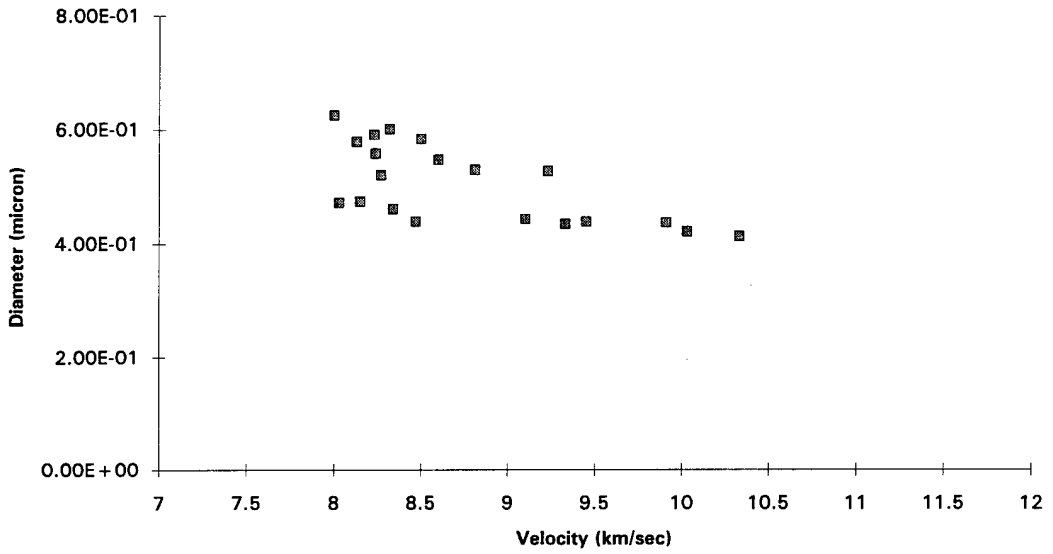

Figure 17. Diameter versus Velocity For Micro-Particle Detector Target

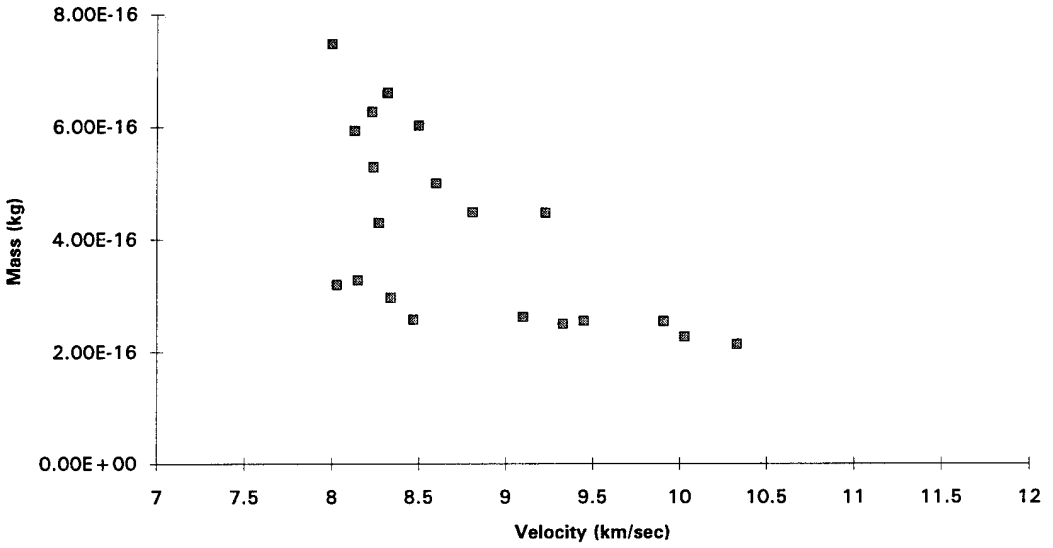

Figure 18. Mass versus Velocity For Micro-Particle Detector Target

4.2 Light Flash Power and Energy Results

Using the procedure described in section 3.0 of this report, relative light flash power and energy was determined for each hypervelocity impact and are shown in the following figures.

Figures 19 through 21 show lens data and figures 22 through 24 show sunshade data.

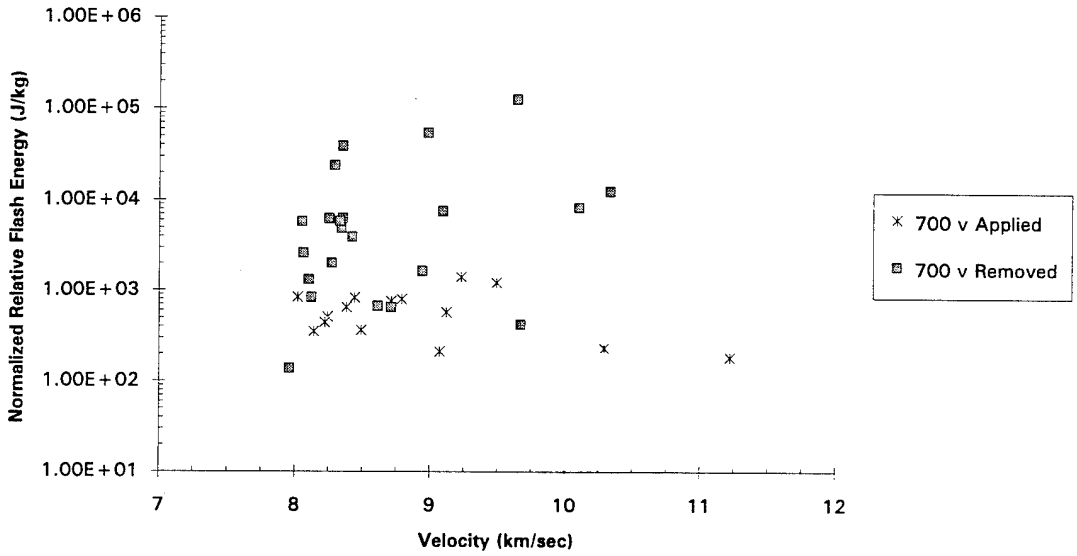

Figure 19. Relative Light Flash Energy Normalized to Particle Mass, Lens Target

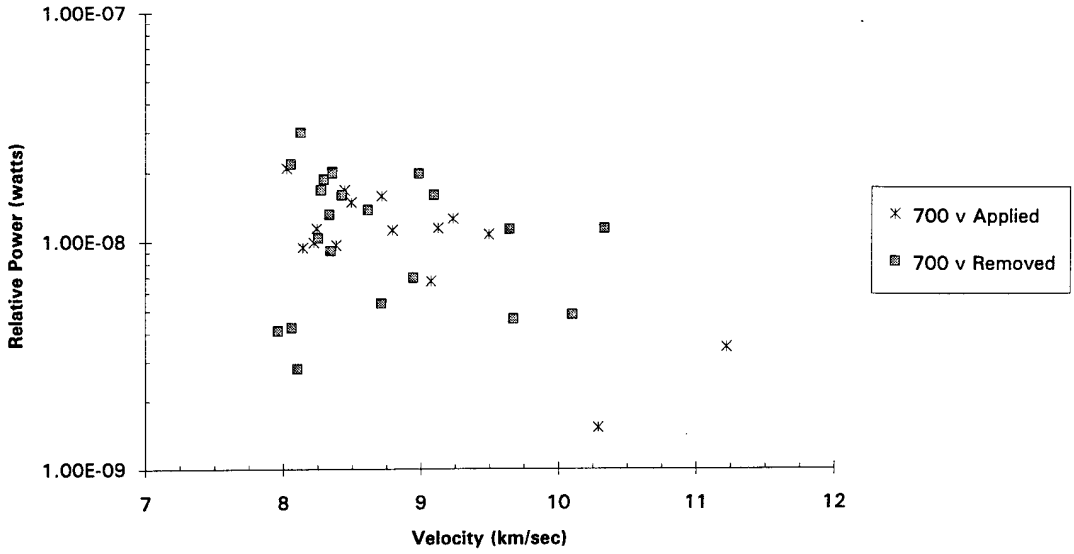

Figure 20. Relative Light Flash Power, Lens Target

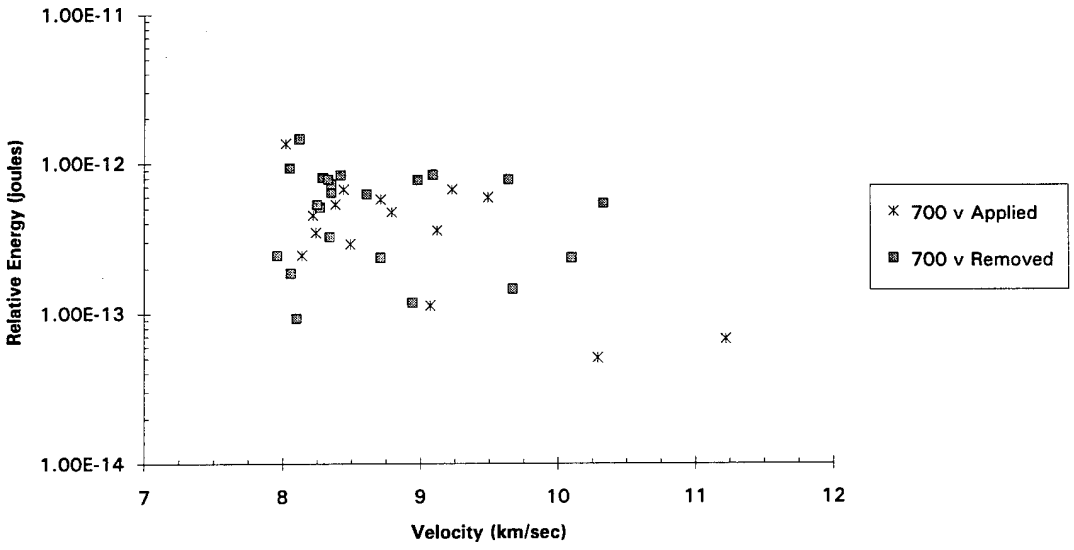

Figure 21. Relative Light Flash Energy, Lens Target

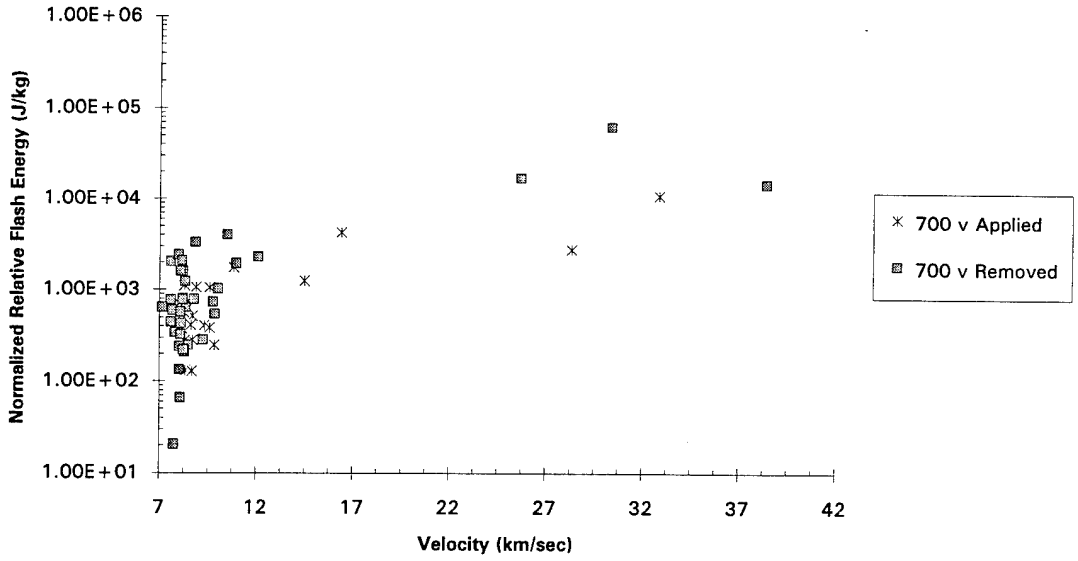

Figure 22. Relative Light Flash Energy Normalized to Particle Mass, Sunshade Target

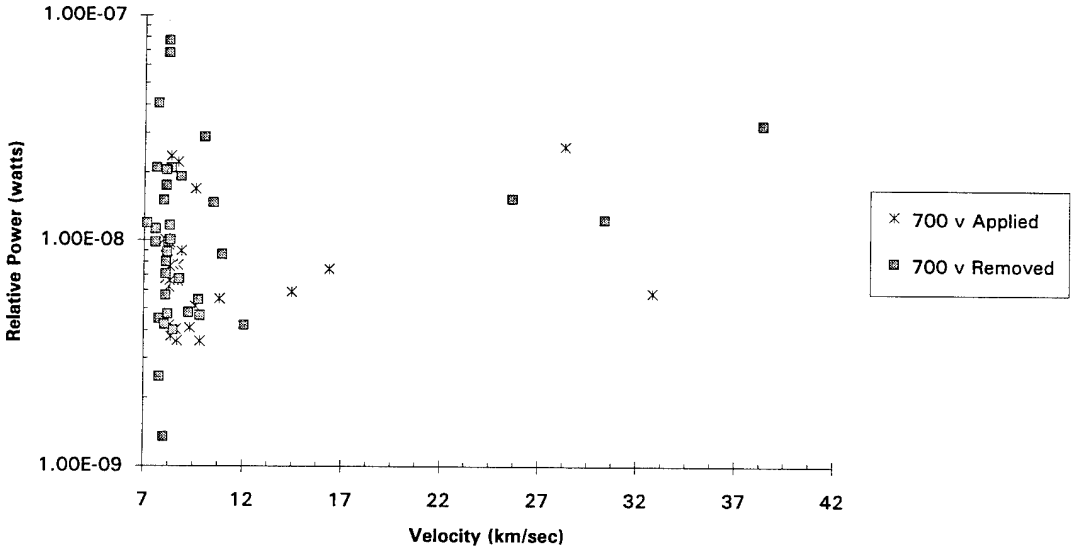

Figure 23. Relative Light Flash Power, Sunshade Target

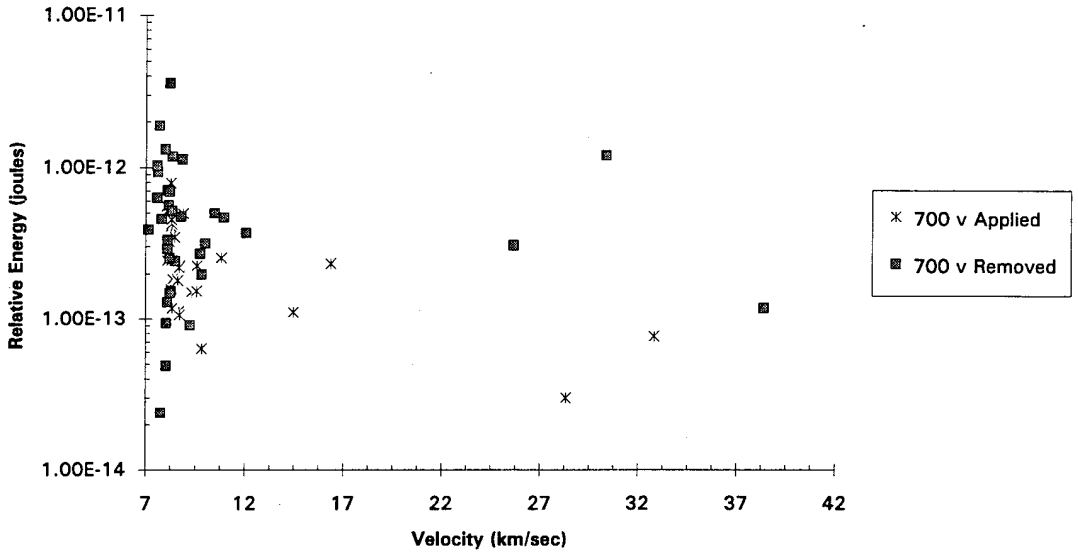

Figure 24. Relative Light Flash Energy, Sunshade Target

4.3 Micro-Particle Detector Data

A typical micro-particle detector output wave form is shown in figure 25. The complete set of detector output versus particle velocity is shown in figure 26. A complete set of micro-particle detector output wave forms are included in appendix A.

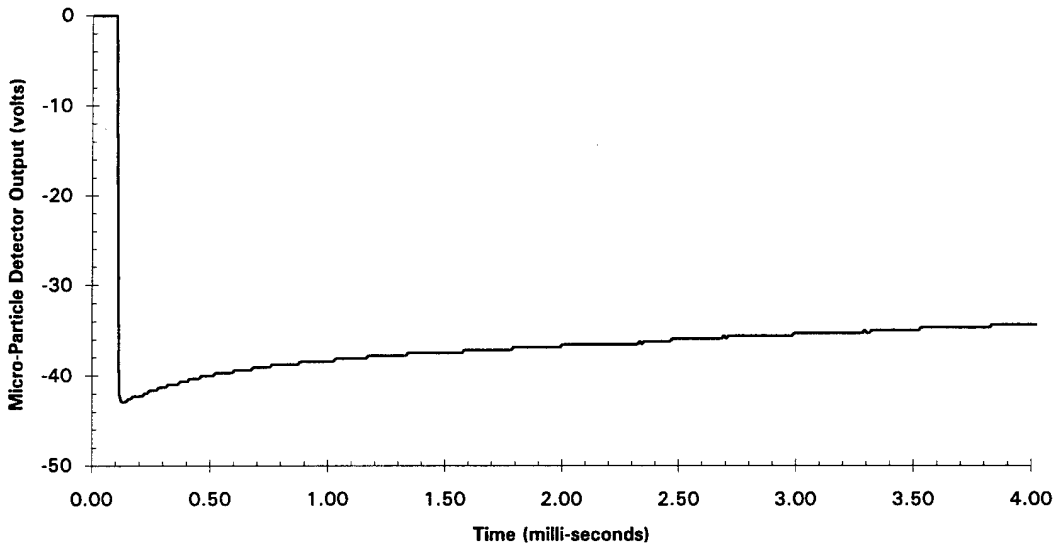

Figure 25. Typical Micro-Particle Detector Output Wave Form With Time Limited To 4.0 milli-seconds

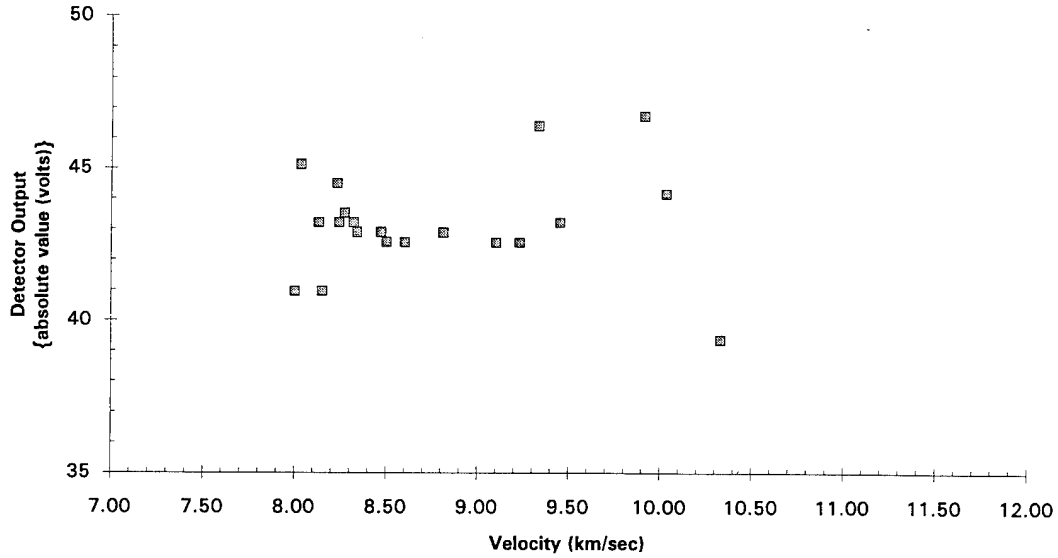

Figure 26. Micro-Particle Detector Output versus Particle Velocity

Plotted in figure 27 is the detector output normalized to mass versus particle velocity.

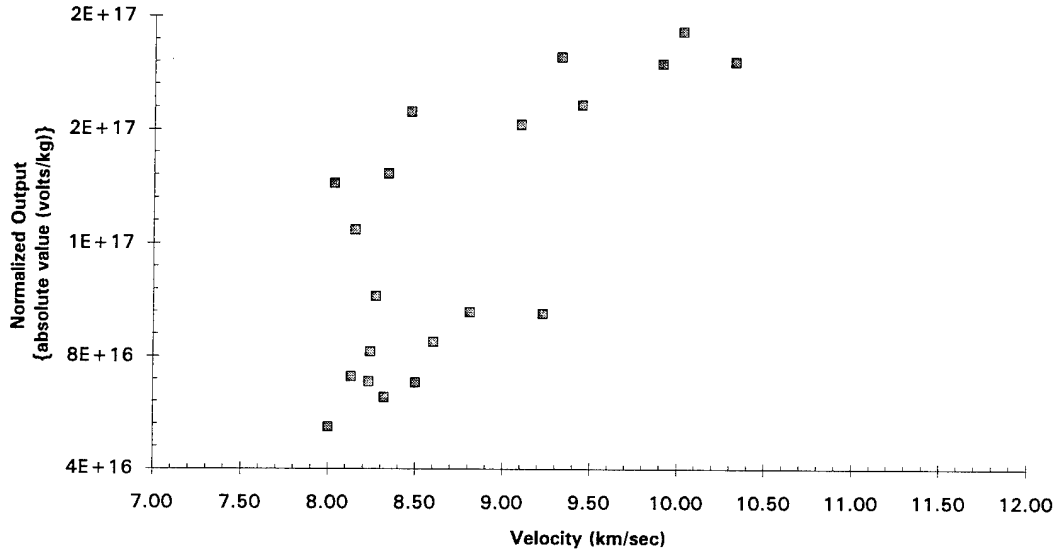

Figure 27. Detector Output Normalized to Mass versus Particle Velocity

5.0 LIGHT FLASH COMPARISONS

5.1 Comparison of Light Flash Energy Results

Similar light flash experiments were conducted at the University of Kent and the Max-Plank Institut fur Kernphysik and were documented in two reports authored by McDonnell and Eichhorn (Refs. 9 and 10). In both experiments, light flash energy caused by microparticle hypervelocity impact was measured and presented as light flash energy normalized to particle mass.

The McDonnell experiment accelerated microparticles by means of a Van De Graaff dust accelerator using particles with masses between 10^{-14} and 10^{-18} kg and with velocities between 2 and 50 km/sec. The Eichhorn experiment also accelerated microparticles by means of a Van De Graaff dust accelerator but used particles with masses between 10^{-9} and 10^{-16} kg and velocities between 0.5 and 35 km/sec.

The McDonnell experiment used iron particles and a molybdenum target. Eichhorn used iron, aluminum and tungsten particles with a gold target.

Shown in figure 28 is an estimated data spread for the Eichhorn reported data of iron, aluminum and tungsten particles impacting a gold target as a single data set for particle velocities in the range between 7 and 12 km/sec (Ref 10, figure 3.b). The Eichhorn estimated data spread was created by the author of this report and consisted of approximately 45 data points.

McDonnell parametrically described his data with a straight line on a logarithmic scale using the following equation:

$$\frac{energy}{mass} = 0.27x(velocity)^{3.95}\left(\frac{J}{kg}\right)\left(\frac{km}{\sec}\right) \qquad (14)$$

Shown in figure 28 is an estimated data spread of the McDonnell reported data created by the author of this report consisting of approximately 16 data points.

Shown in figure 28 is a partial light flash energy data set from this experiment for particle velocities in the range between 7 and 12 km/sec. Although this experiment collected some data points beyond a particle velocity of 12 km/sec, the majority of data points were between particle velocities of 7 and 12 km/sec. For this reason, only data for particle velocities between 7 and 12 km/sec are shown in figure 28.

The purpose of figure 28 is to show a comparison of data collected by McDonnell, Eichhorn, and Phillips Laboratory. Data shown in figure 28 indicates that normalized light flash energy data from three independent experiments resulted in similar and favorably comparable light flash energy results within a velocity range of 7 to 12 km/sec.

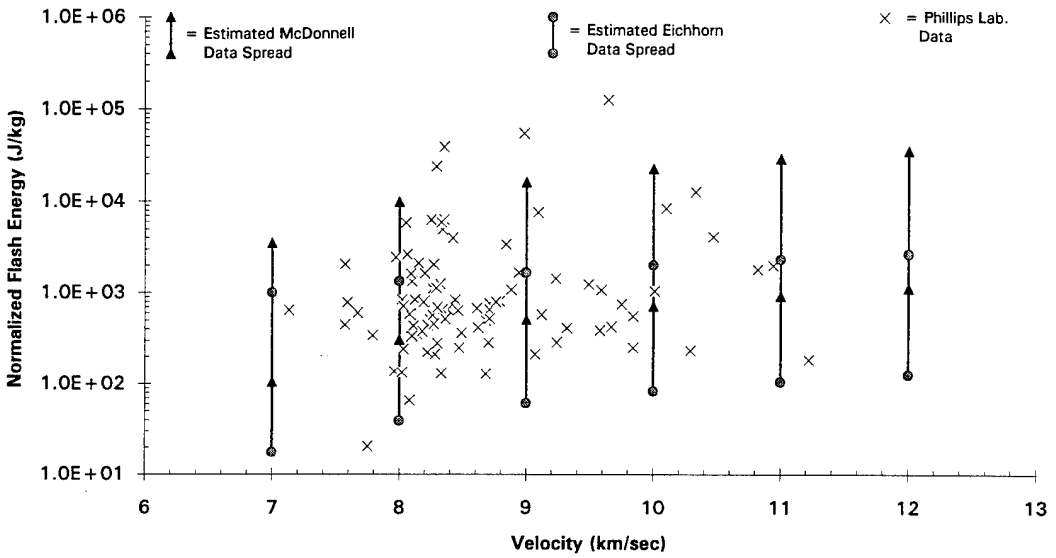

Figure 28. Normalized Light Flash Energy Data From McDonnell, Eichhorn, and Phillips Laboratory Experiments

5.2 Light Flash Rise Time

As described in section 3.0 of this report, photomultiplier signal rise time was determined by measuring time between the integration start and stop points. Rise time is typically measured as 10-90%, however, the experimenter elected to use 0-100% rise time.

Shown in figure 29 is the photomultiplier signal rise time data for the lens and sunshade targets.

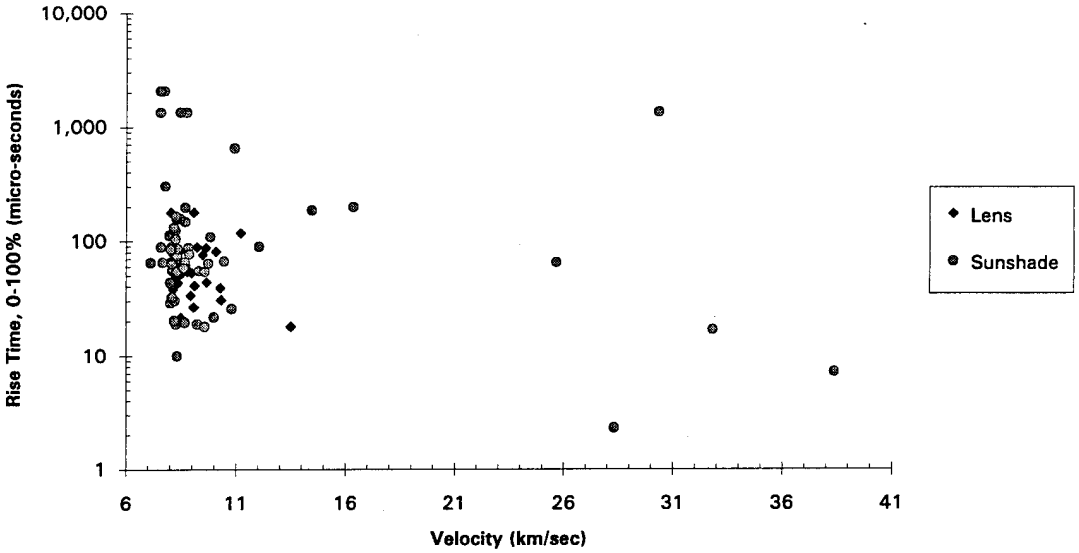

Figure 29. Rise Time Data For Lens and Sunshade Targets

6.0 LED LIGHT SOURCE SIMULATION RESULTS

The manufacture of the photomultiplier reports that the photomultiplier has a typical response time of 46 nano-seconds (Ref 8). The photomultiplier rise time shown in figure 8 was limited by the LED response and the instrumentation system. From figure 8, the rise time of the photomultiplier instrumentation system was determined to be at least 4.5 micro-seconds.

An impact light flash that has a rise time slower than 4.5 micro-seconds will be accurately detected by the photomultiplier instrumentation system. As shown in figure 29, all recorded impact flash data had rise times slower than 4.5 micro-seconds with the exception of one sunshade data point that occurred at approximately 28 km/sec. For the interest of completeness, the experimenters included the single data point that occurred at approximately 28 km/sec, however, the validity of the data point is suspect.

The result of the LED simulation was that the photomultiplier instrumentation system was properly configured and had a rise time of at least 4.5 micro-seconds.

7.0 MICRO-PARTICLE DETECTOR IMPACT CRATER MEASUREMENTS

Using an Amray Scanning Electron Microscope, Model 1830, Phillips Laboratory personnel detected and recorded several impact craters on the micro-particle detector that was used for this series of hypervelocity impacts.* Typical impact craters are shown in figures 30 through 32.

The crater diameter in figure 30 is approximately 14.5 microns. Figure 31 shows a crater inside diameter of approximately 12.5 microns. And, figure 32 is an enlarged image of the crater shown in figure 31. As seen in figures 30 and 31, the outer most ring is solidified ejecta and the inner most ring is the actual impact crater.

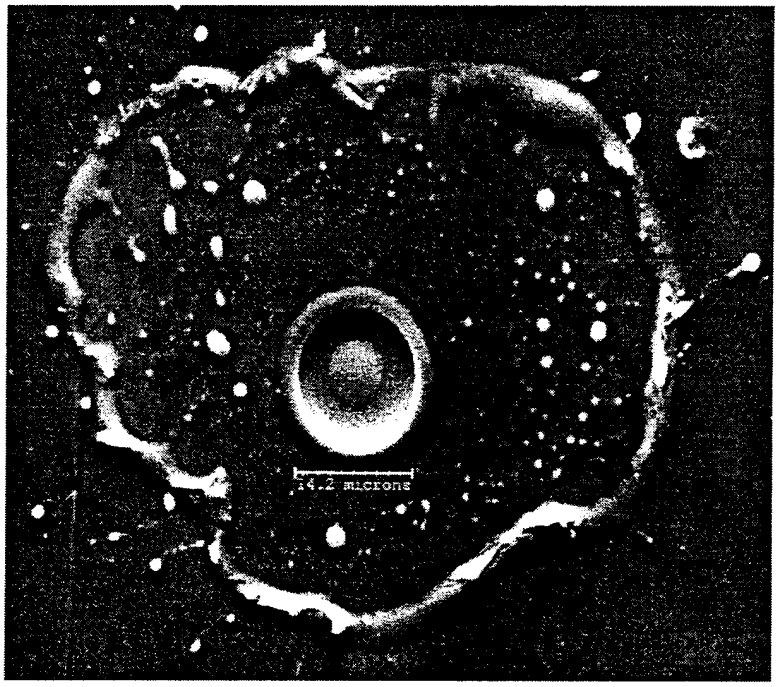

Figure 30. Micro-Particle Impact Crater. Crater Diameter Is Approximately 14.5 microns

* Miglionico C. and Robertson R., Phillips Laboratory/VT, 3550 Aberdeen Ave., SE, Kirtland AFB, NM 87117

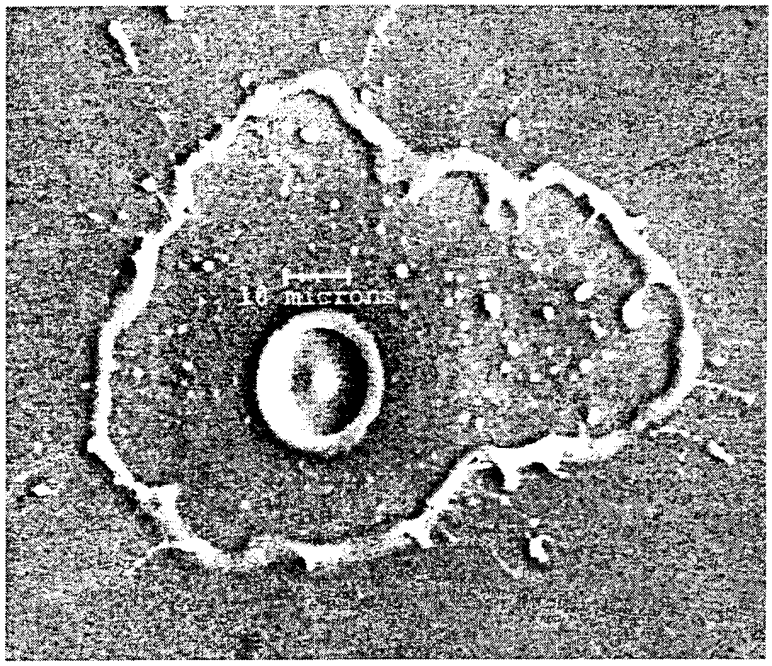

Figure 31. Micro-Particle Impact Crater. Crater Inside Diameter is Approximately 12.5 microns

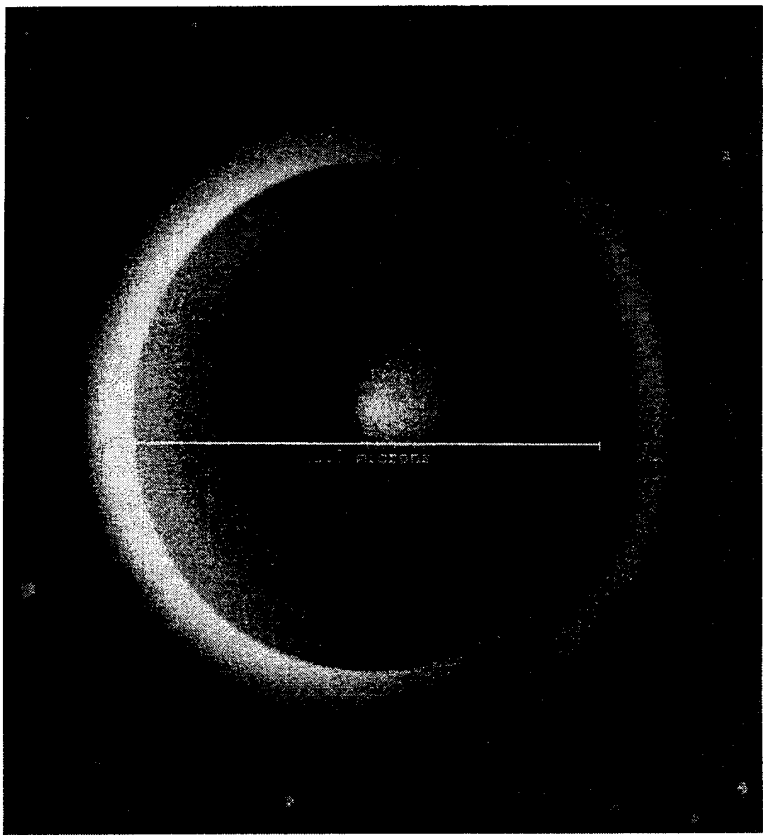

Figure 32. Enlarged Image of Figure 31

8.0 CONCLUSION

Measurements of light flash occurring during hypervelocity impacts of iron micro-particles impacting a lens and sunshade target were obtained. Favorable comparison of data obtained from this experiment with Eichhorn and McDonnell indicates that data obtained from this experiment is valid light flash data.

As stated in the introduction of this report, the purpose of this report was to only present the data obtained and discuss the validity of the data. Data obtained from this experiment will be used to supplement calculation and modeling efforts within the Phillips Laboratory and will be discussed in a separate report.

As discussed earlier, the calibration process used for the photomultiplier was relative to a blackbody source. This assumption must be stressed whenever the light flash results of this experiment are presented.

Limited MOS micro-particle detector data clearly indicates that this type of MOS micro-particle impact detector is a viable and valuable diagnostic instrument. The detectors behaved electrically and mechanically as predicted and successfully demonstrated the self-clear feature.

REFERENCES

1. Fechtig H., Gault D.E., Neukum G., and Schneider E., "Naturwiss 59", 151, 1972, Max-Plank Institut fur Kernphysik, Heidelberg, Germany

2. Wortman J.J., Kassel P.C., "Metal-Oxide-Silicon Capacitor Detectors for Measuring Micrometeoroid and Space Debris Flux", Journal of Spacecraft and Rockets, 1994, Electrical and Computer Engineering Department, North Carolina State University, Raleigh, NC 27695

3. Kassel P.C., "Characteristics of Capacitor-Type Micrometeoroid Flux Detectors When Impacted With Simulated Micrometeoroids", Langley Research Center, National Aeronautics and Space Administration, Hampton, VA 23665, NASA TN D-7359

4. International Engineering Newsletter, Space Flight Environment, Vol V., No. 4, Sept. - Oct. 1994, 14636 Silverstone Drive, Silver Spring, MD 20905, 301-236-9311

5. Engstrom R.W., "RCA Photomultiplier Handbook", RCA Handbook PMT-62, pp 145-146, 1980

6. Pedrotti F.L., Pedrotti L.S., "Modern Optics for Scientists and Engineers: A Five Day Short Course", Engineering Technology Institute, 601 Lake Air Drive, P.O. Box 8859, Waco, Texas 76714, (817) 772-0082, pg 73

7. Friichtenicht J.F., "Experiments On The Impact-Light-Flash At High Velocities", NASA Contractor Report, NASA CR-416, March 1966

8. "THORN EMI Photomultiplier Catalog", PMC/86, 1986

9. McDonnell J.A., "Investigation of Optical Damage, Energy Partitioning and Scaling Laws at Extremely High Velocities", University of Kent at Canterbury, United Kingdom, Number EOARD-93-0003, pp 64-75, 1994

10. Eichhorn G., "Analysis of the Hypervelocity Impact Process From Impact Flash Measurements", Planet Space Science, Vol. 24, pp 771-781, 1976

APPENDIX A

MICRO-PARTICLE IMPACT DETECTOR DATA

MICRO-PARTICLE DETECTOR
DATA SET D1

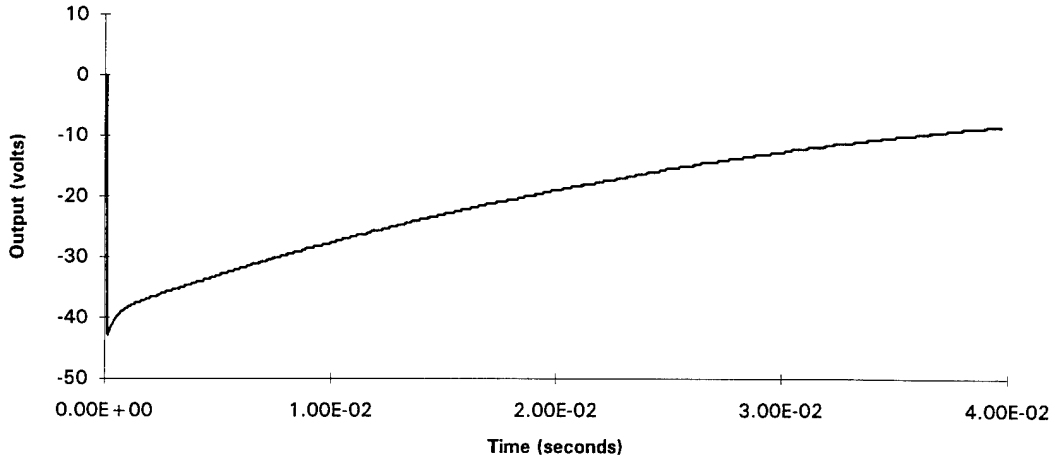

MICRO-PARTICLE DETECTOR
DATA SET D1

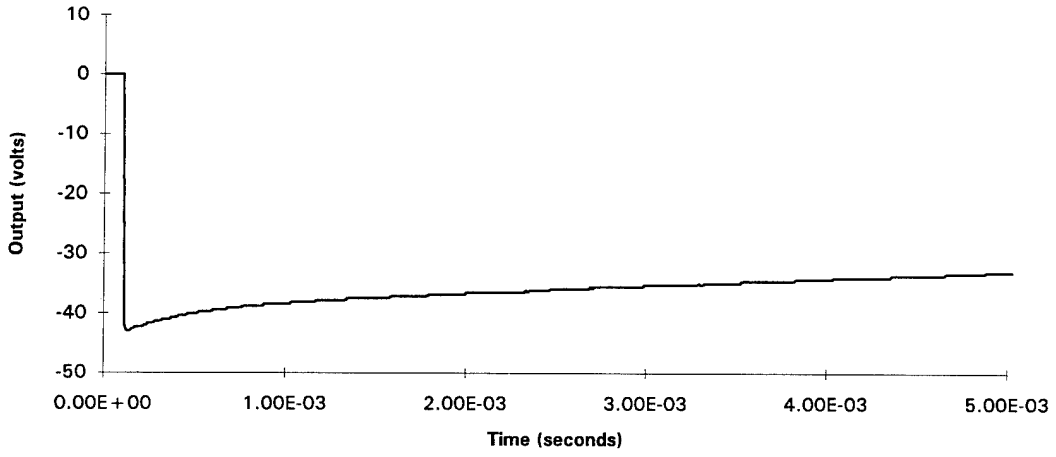

MICRO-PARTICLE DETECTOR
DATA SET D2

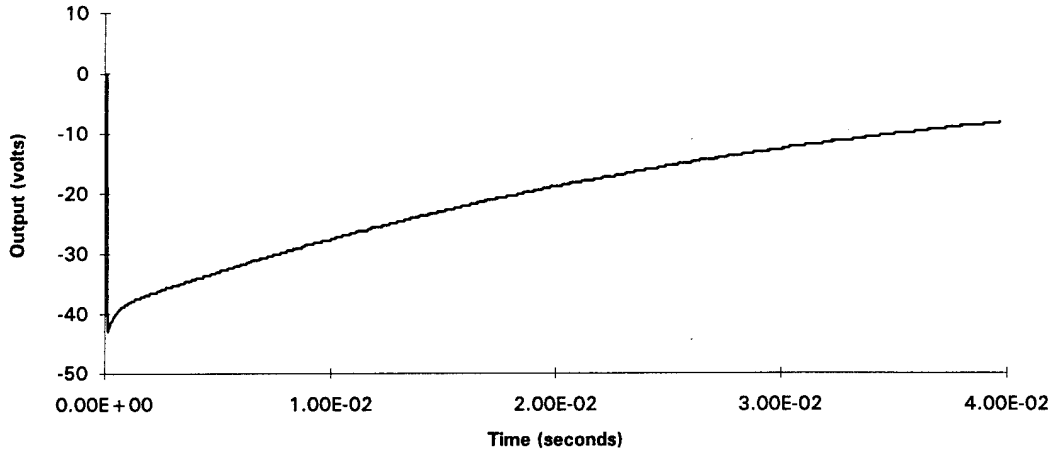

MICRO-PARTICLE DETECTOR
DATA SET D2

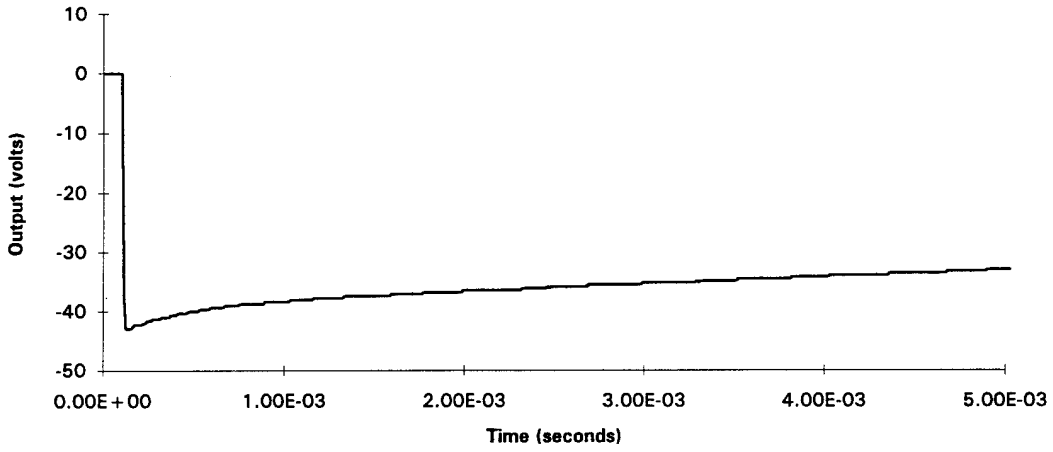

MICRO-PARTICLE
DATA SET D3

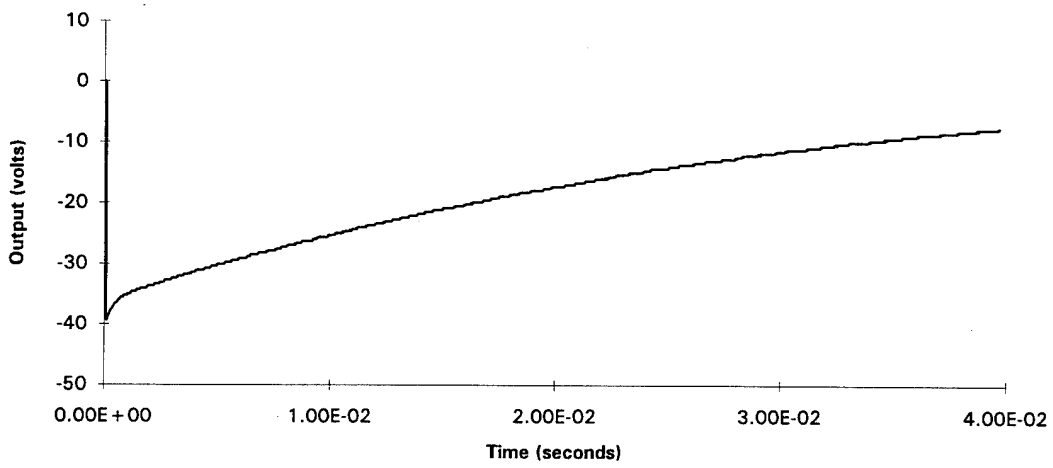

MICRO-PARTICLE
DATA SET D3

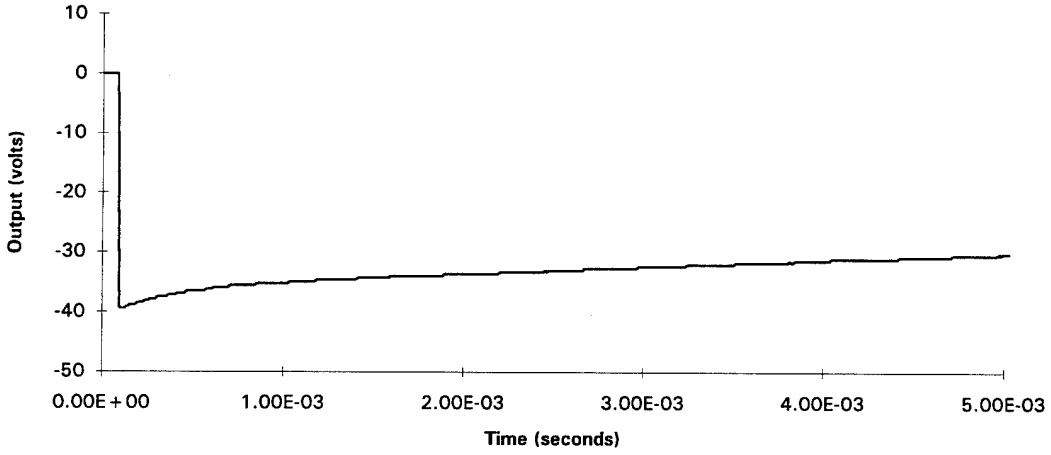

MICRO-PARTICLE DETECTOR
DATA SET D4

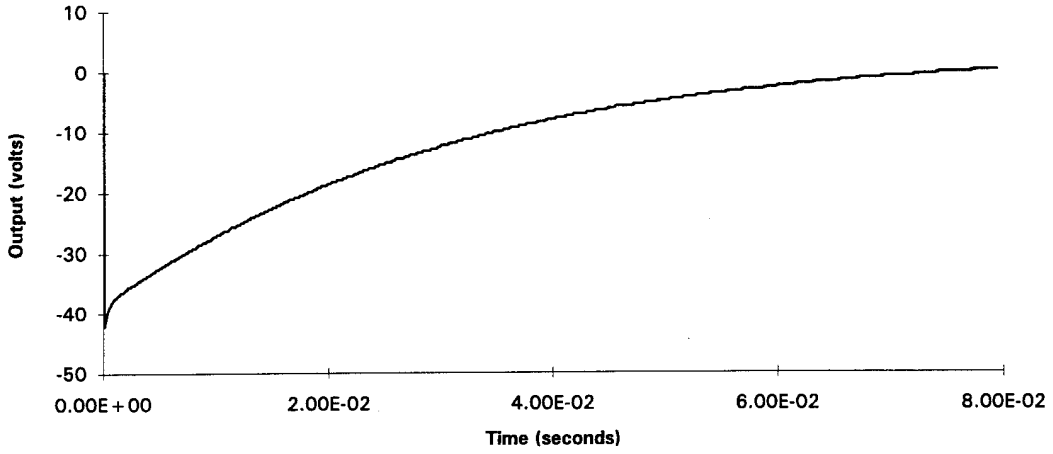

MICRO-PARTICLE DETECTOR
DATA SET D4

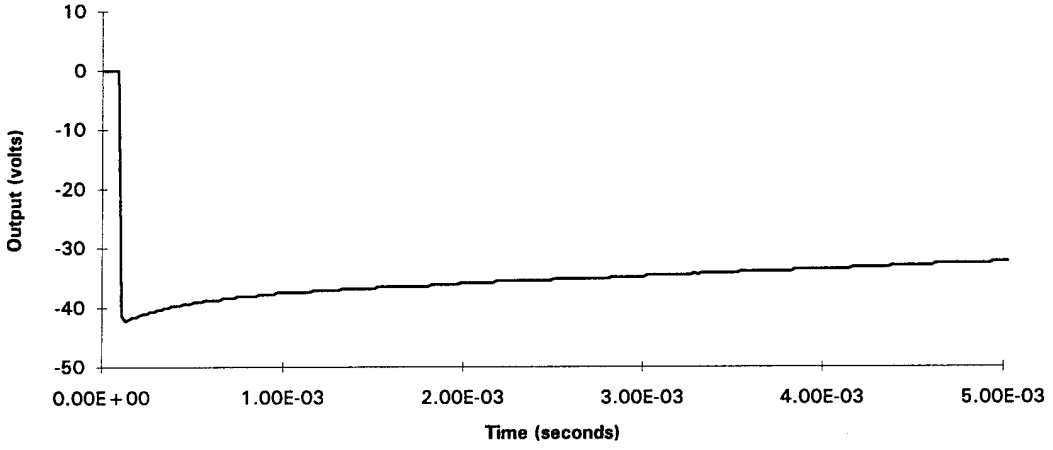

MICRO-PARTICLE DETECTOR
DATA SET D5

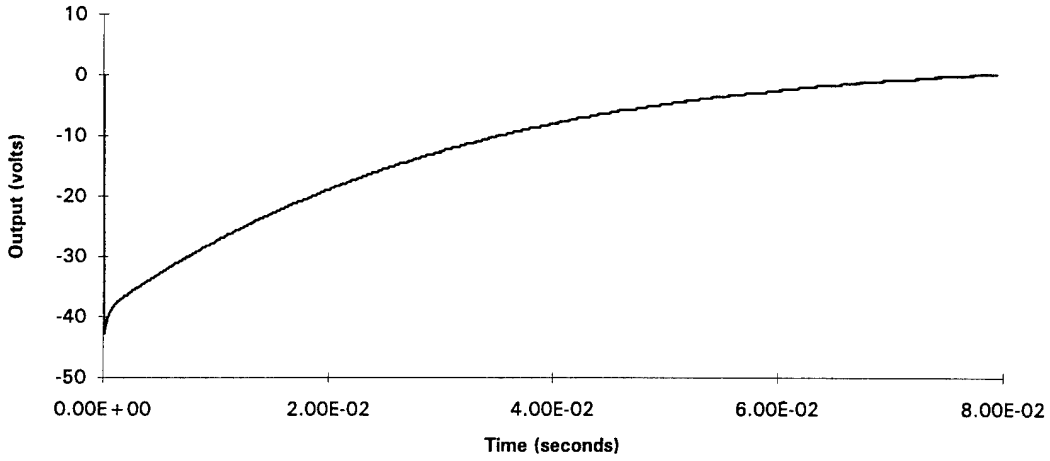

MICRO-PARTICLE DETECTOR
DATA SET D5

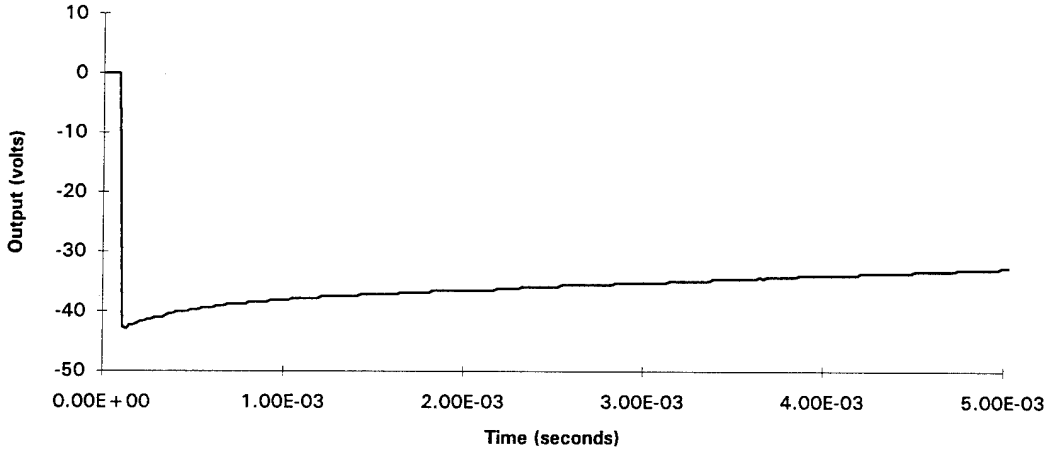

MICRO-PARTICLE DETECTOR
DATA SET D6

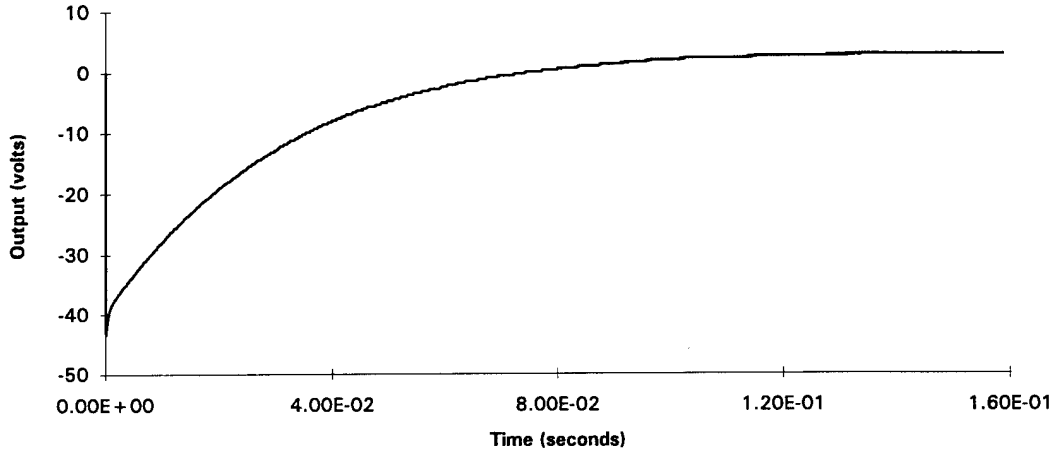

MICRO-PARTICLE DETECTOR
DATA SET D6

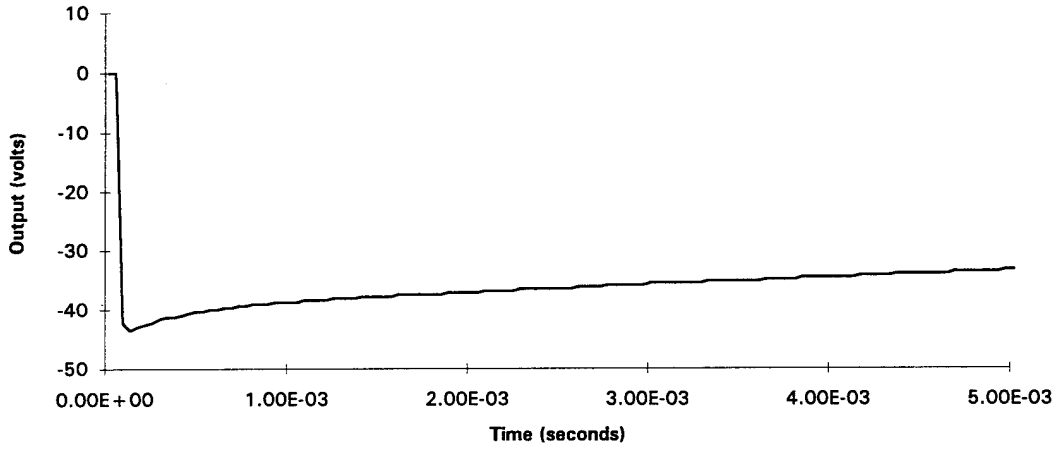

MICRO-PARTICLE DETECTOR
DATA SET D7

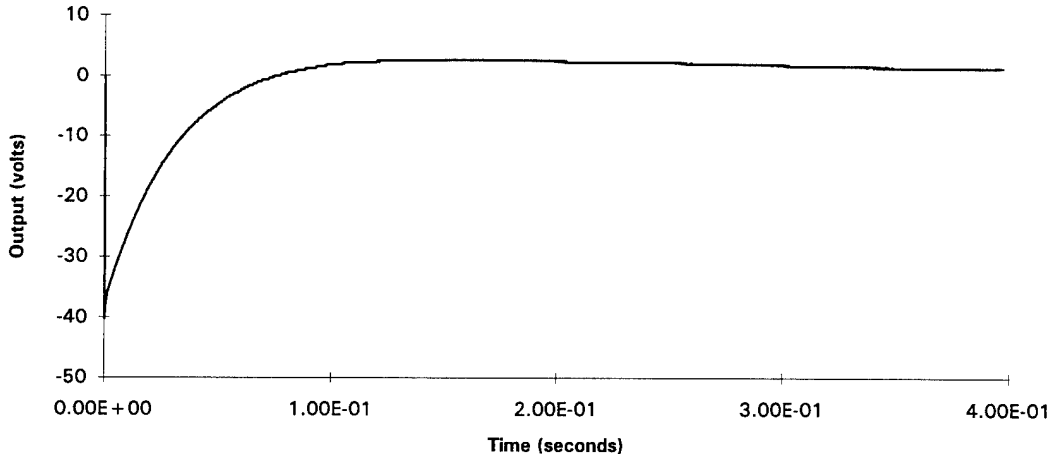

MICRO-PARTICLE DETECTOR
DATA SET D7

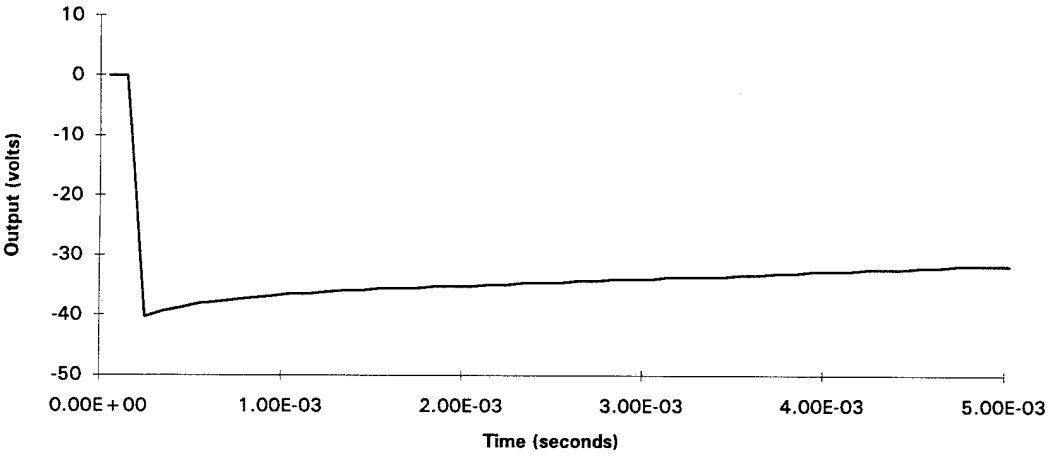

MICRO-PARTICLE DETECTOR
DATA SET D8

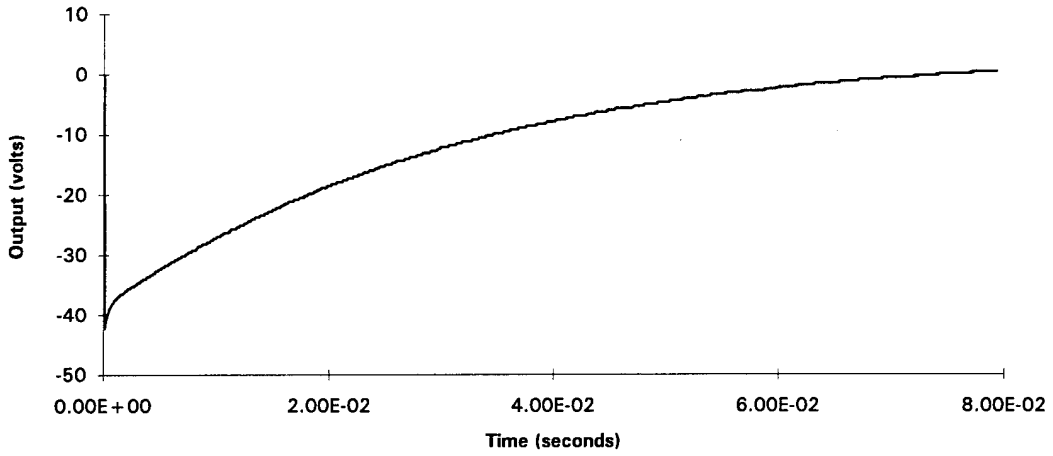

MICRO-PARTICLE DETECTOR
DATA SET D8

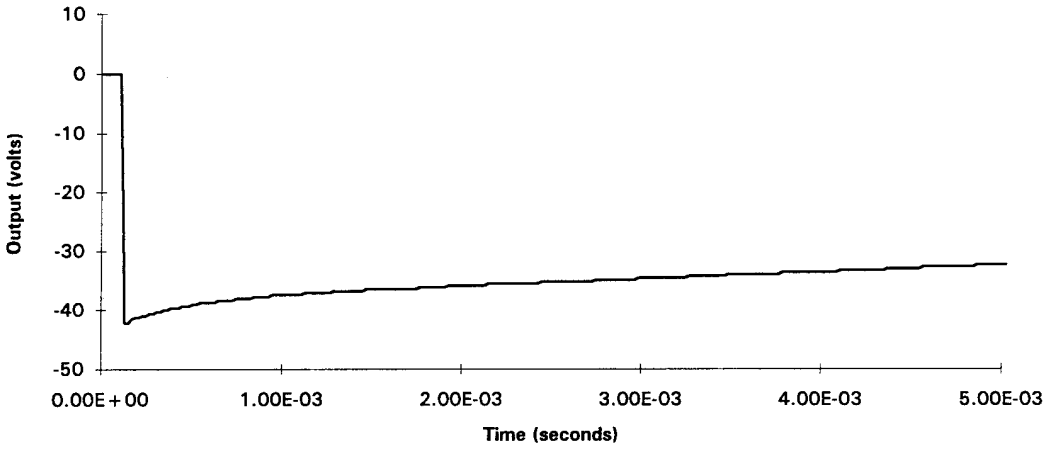

MICRO-PARTICLE DETECTOR
DATA SET D9

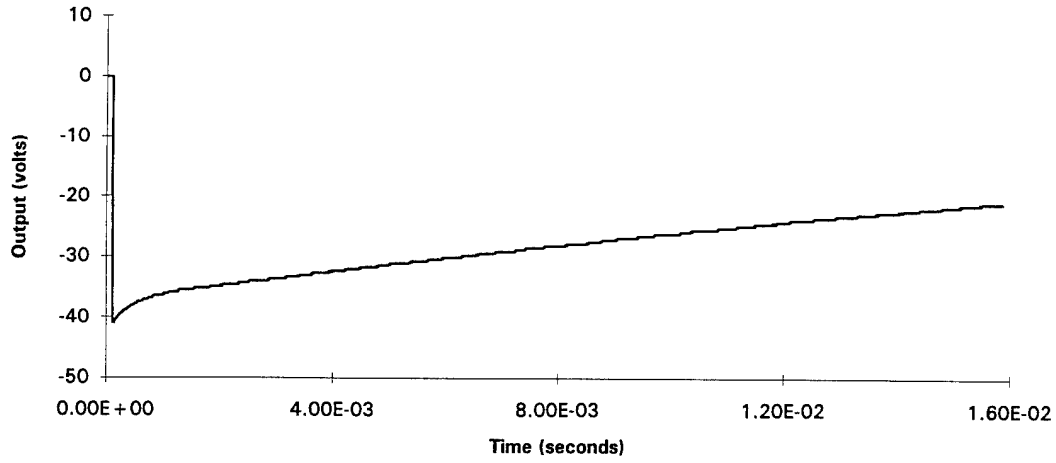

MICRO-PARTICLE DETECTOR
DATA SET D9

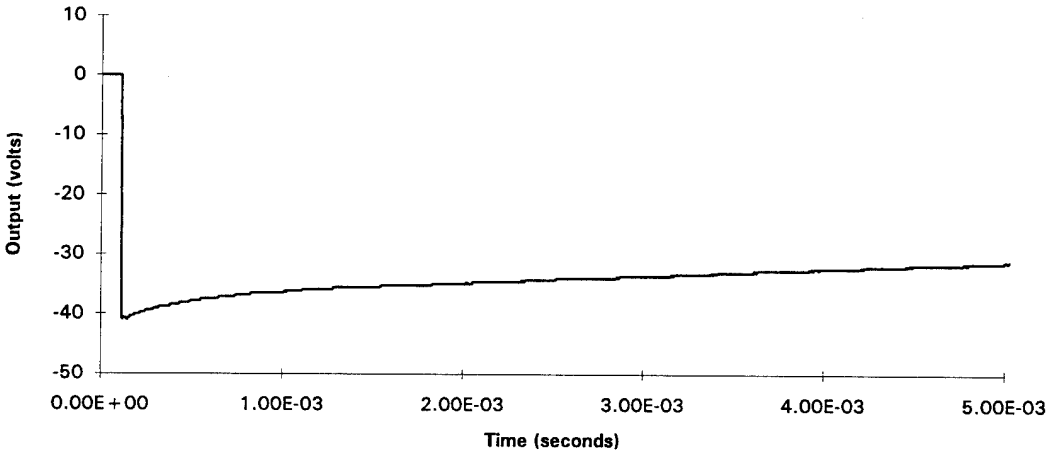

MICRO-PARTICLE DETECTOR
DATA SET D10

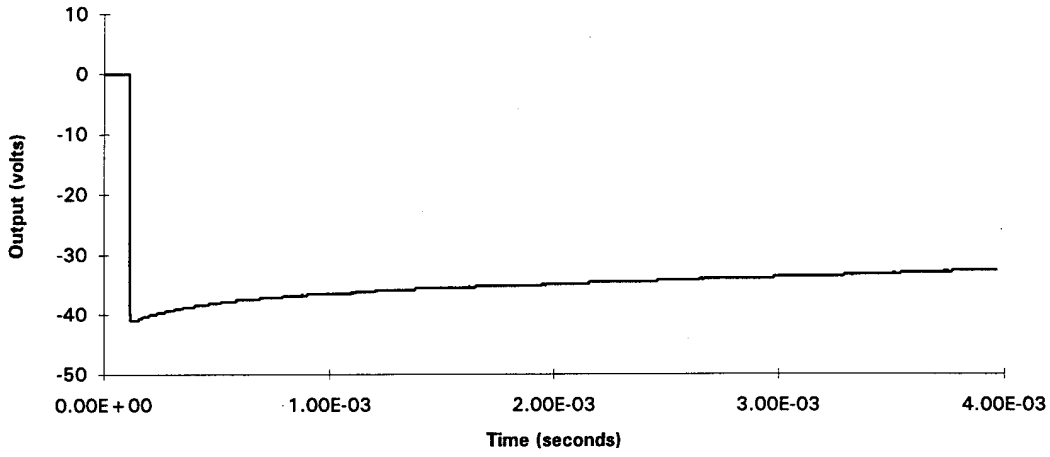

MICRO-PARTICLE DETECTOR
DATA SET D10

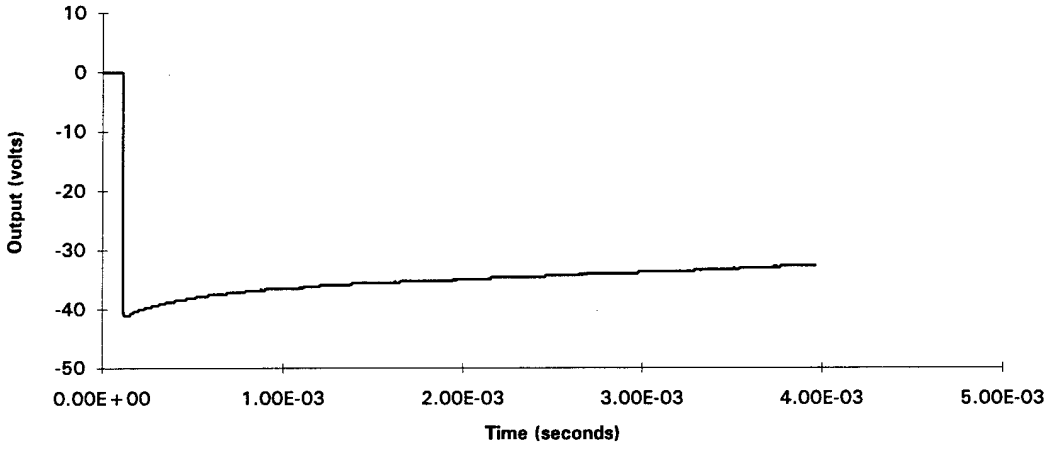

MICRO-PARTICLE DETECTOR
DATA SET D11

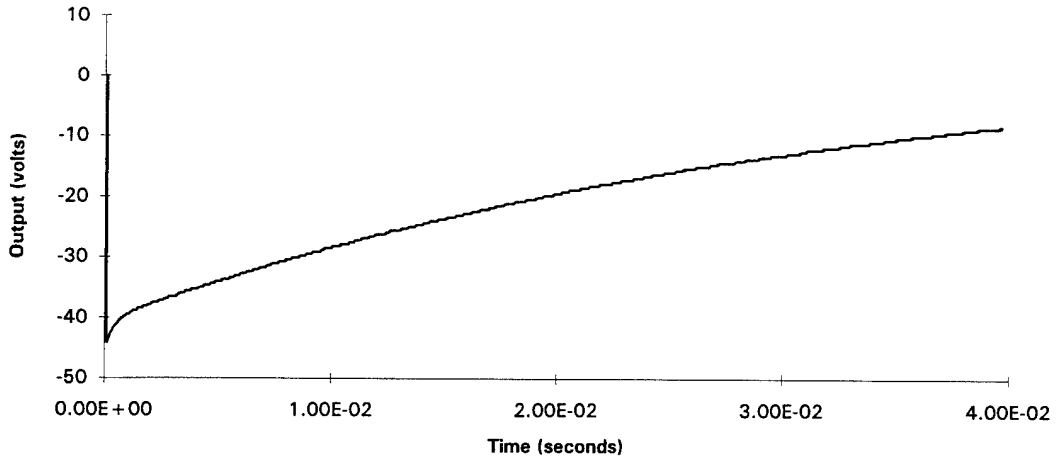

MICRO-PARTICLE DETECTOR
DATA SET D11

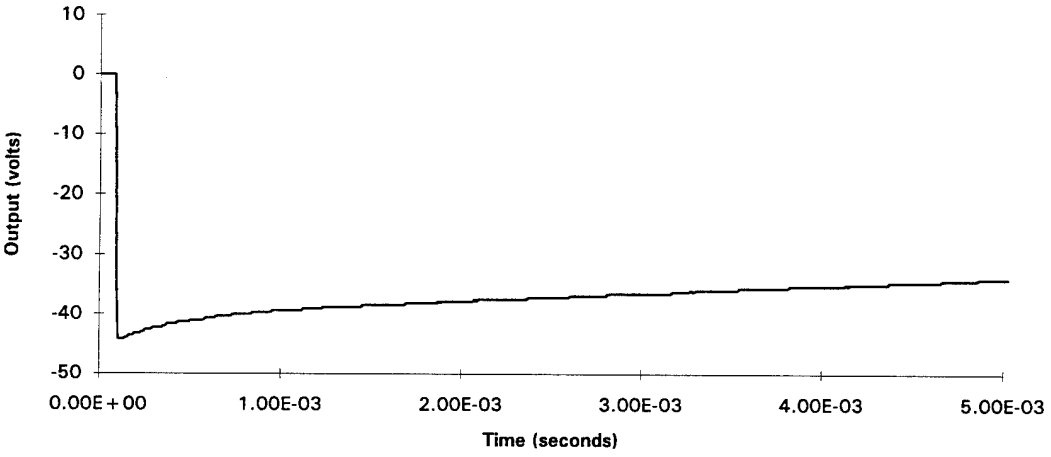

MICRO-PARTICLE DETECTOR
DATA SET D12

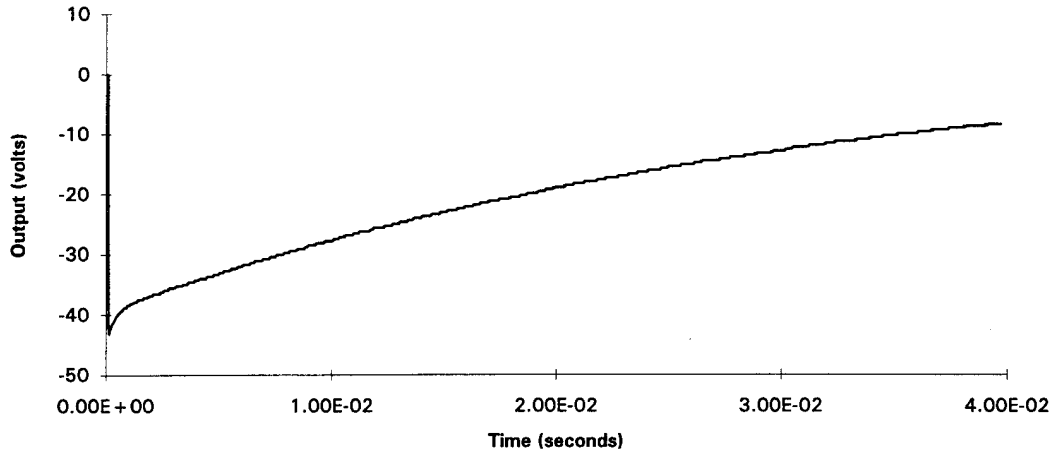

MICRO-PARTICLE DETECTOR
DATA SET D12

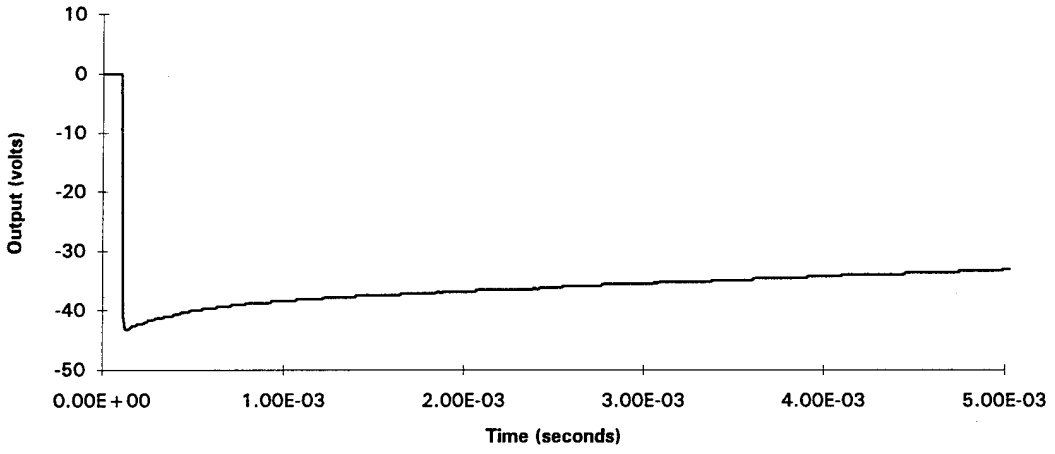

MICRO-PARTICLE DETECTOR
DATA SET D13

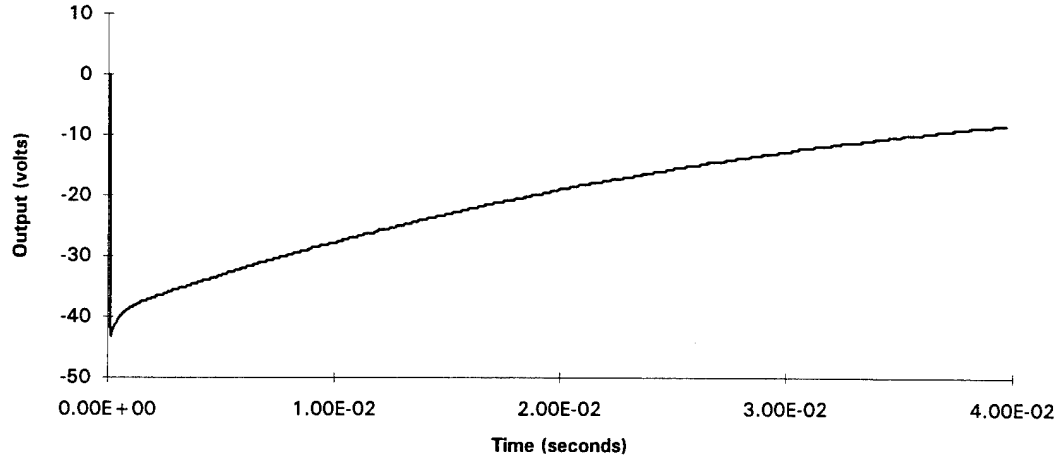

MICRO-PARTICLE DETECTOR
DATA SET D13

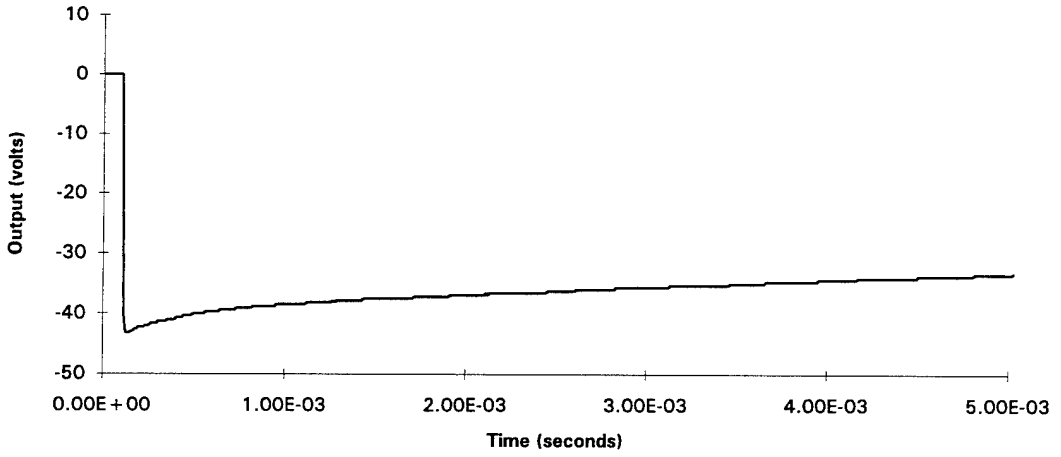

MICRO-PARTICLE DETECTOR
DATA SET D14

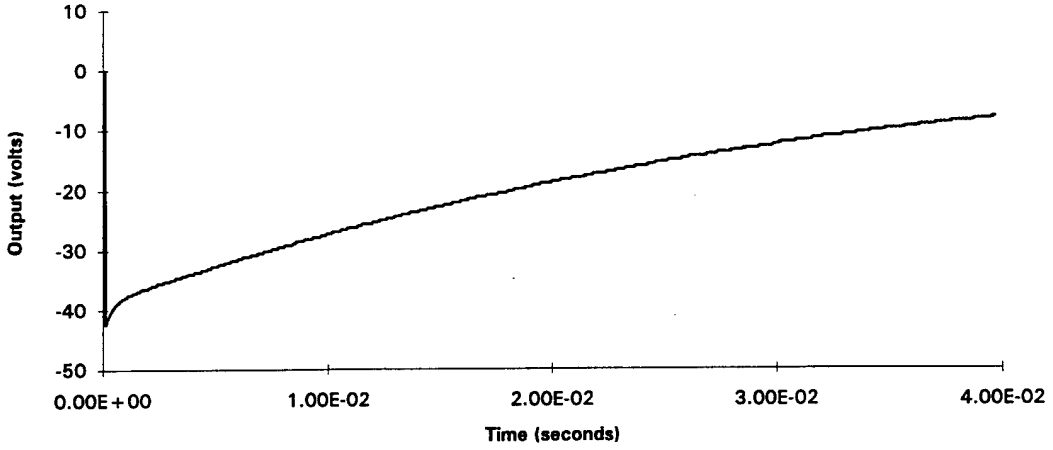

MICRO-PARTICLE DETECTOR
DATA SET D14

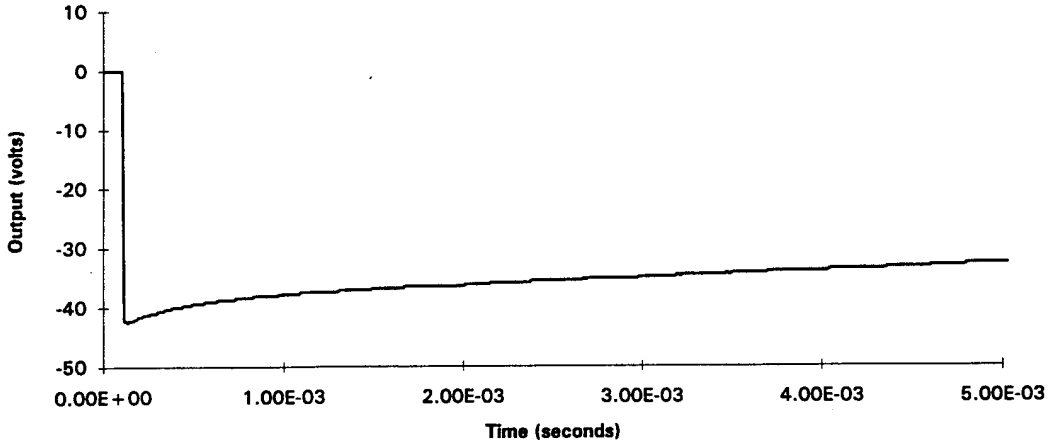

MICRO-PARTICLE DETECTOR
DATA SET D15

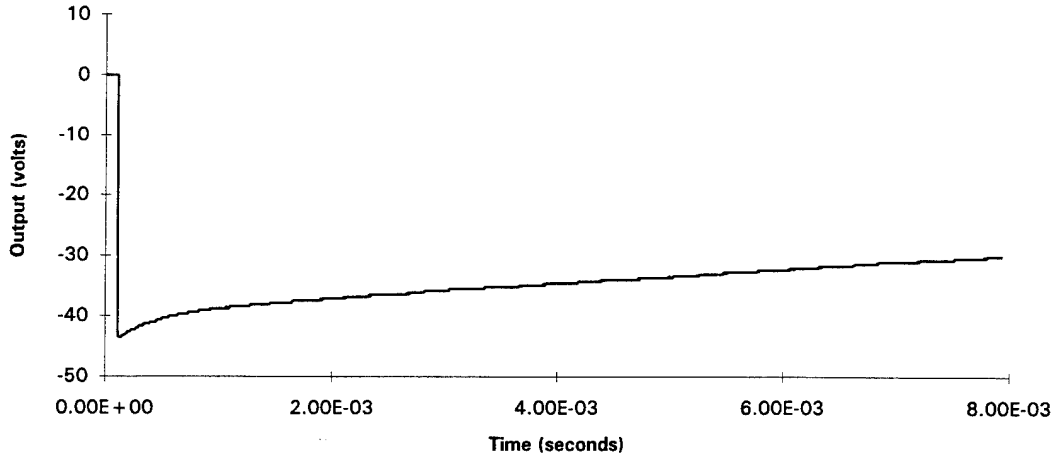

MICRO-PARTICLE DETECTOR
DATA SET D15

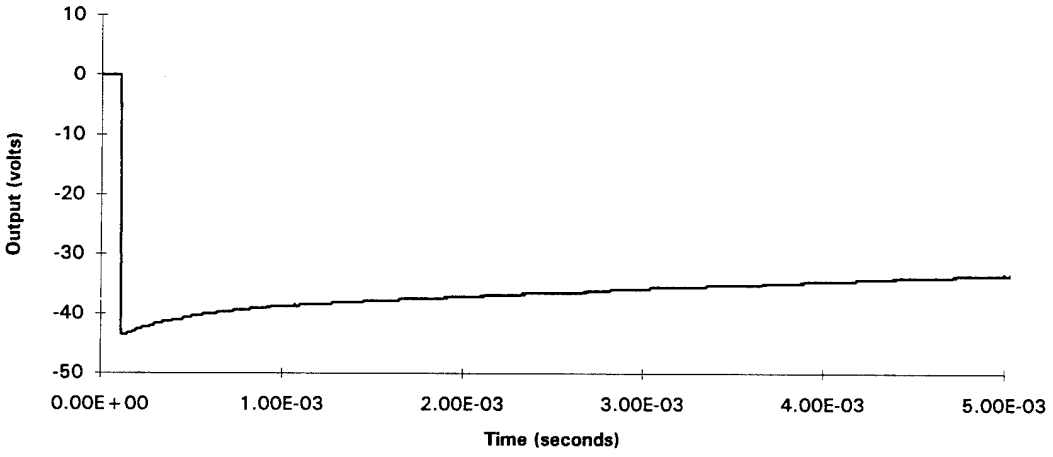

MICRO-PARTICLE DETECTOR
DATA SET D16

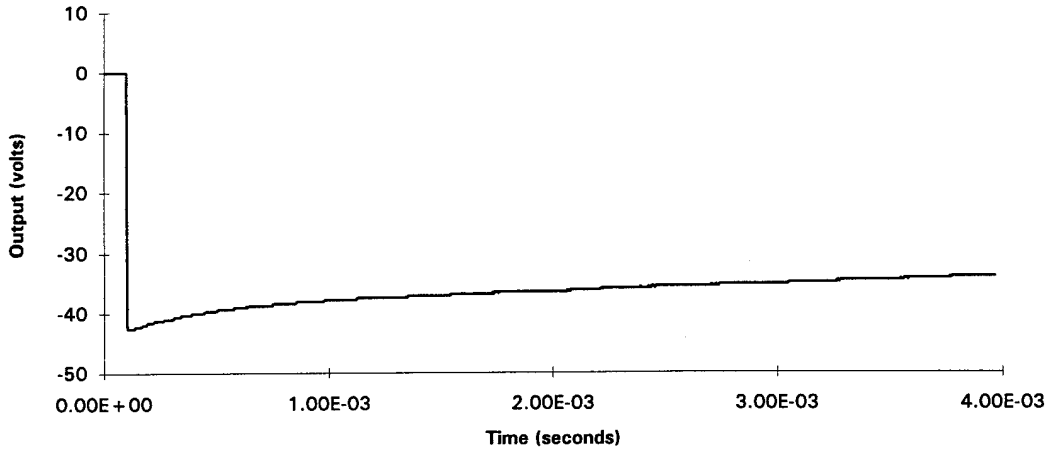

MICRO-PARTICLE DETECTOR
DATA SET D16

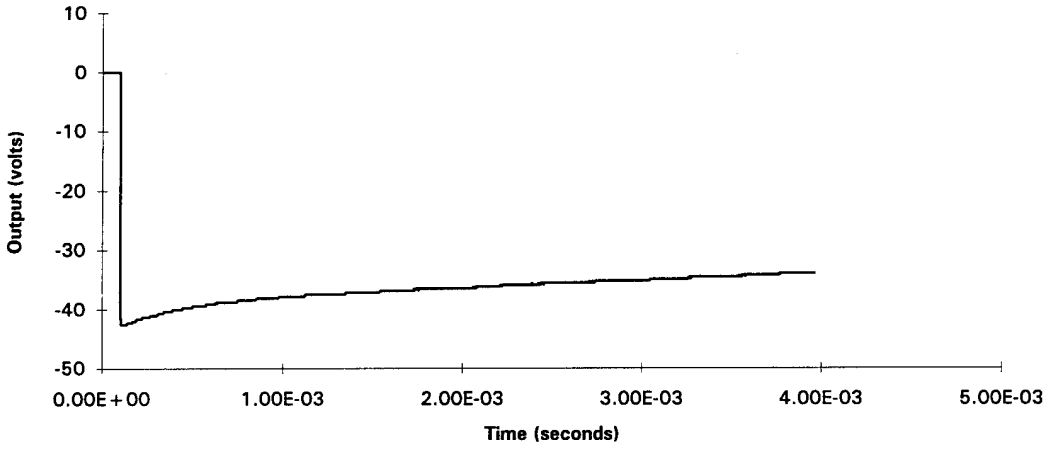

MICRO-PARTICLE DETECTOR
DATA SET D17

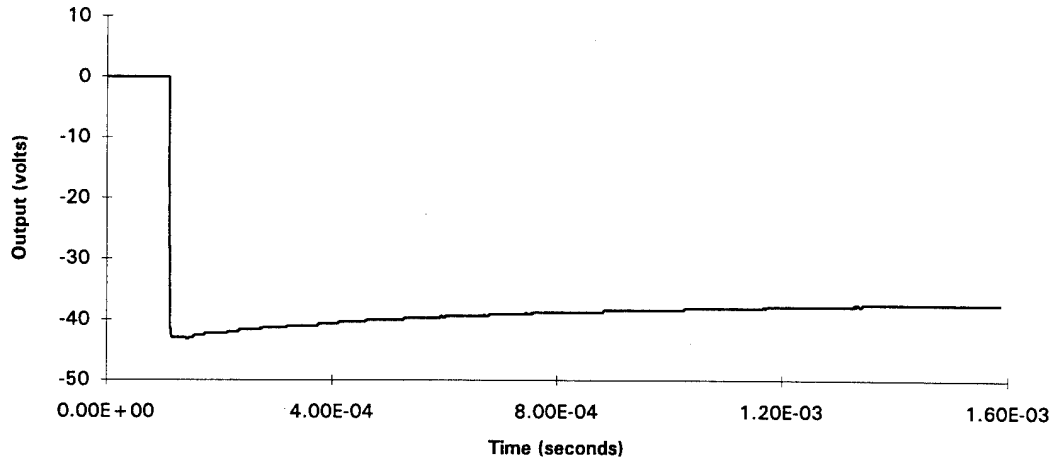

MICRO-PARTICLE DETECTOR
DATA SET D17

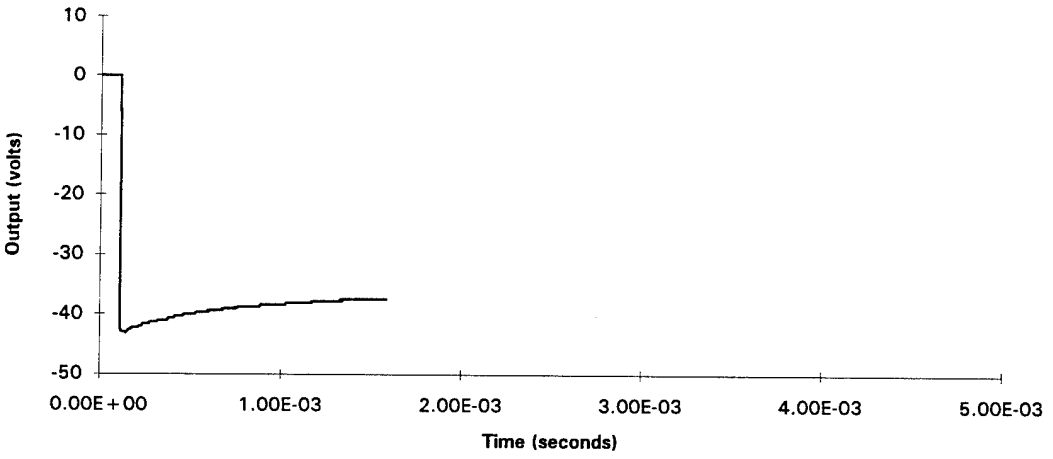

MICRO-PARTICLE DETECTOR
DATA SET D18

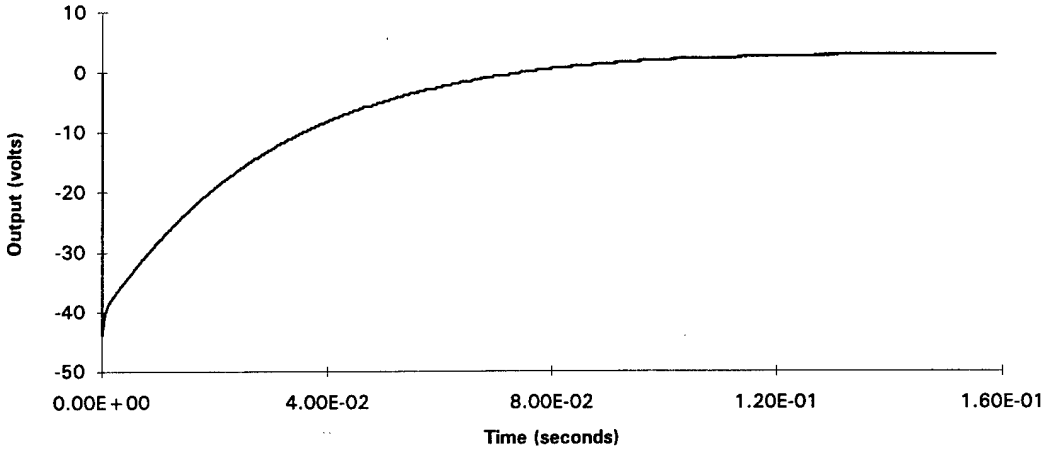

MICRO-PARTICLE DETECTOR
DATA SET D18

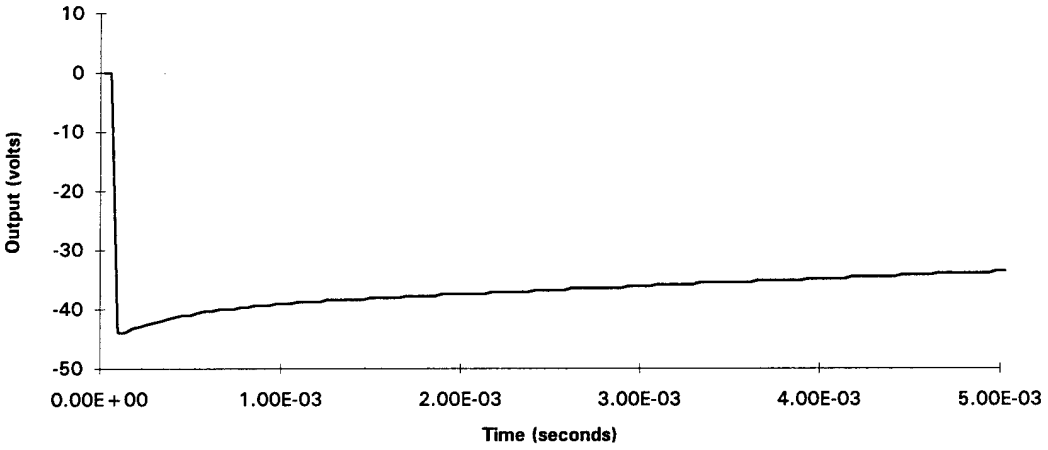

MICRO-PARTICLE DETECTOR
DATA SET D19

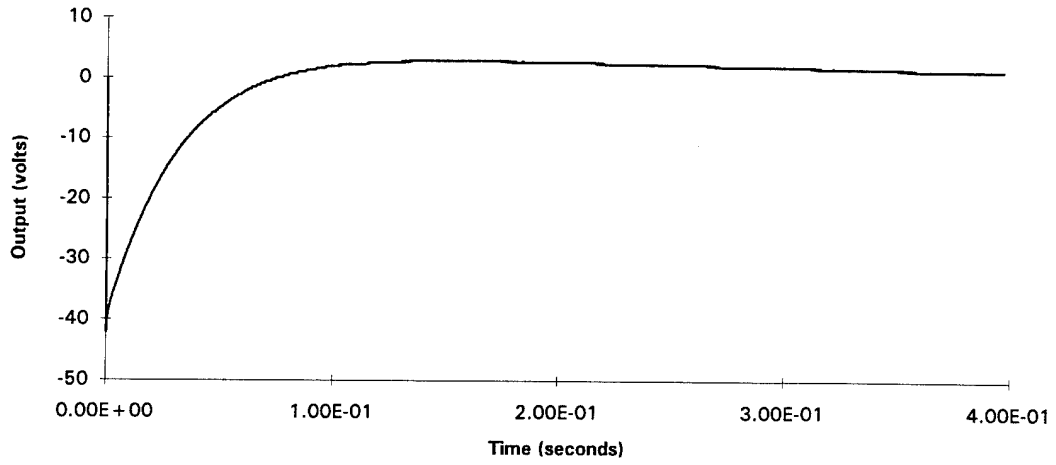

MICRO-PARTICLE DETECTOR
DATA SET D19

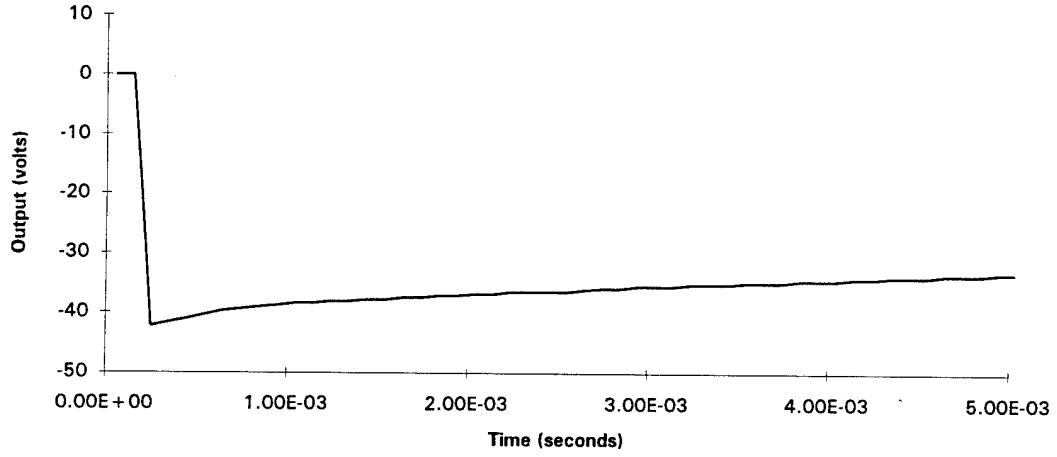

MICRO-PARTICLE DETECTOR
DATA SET D20

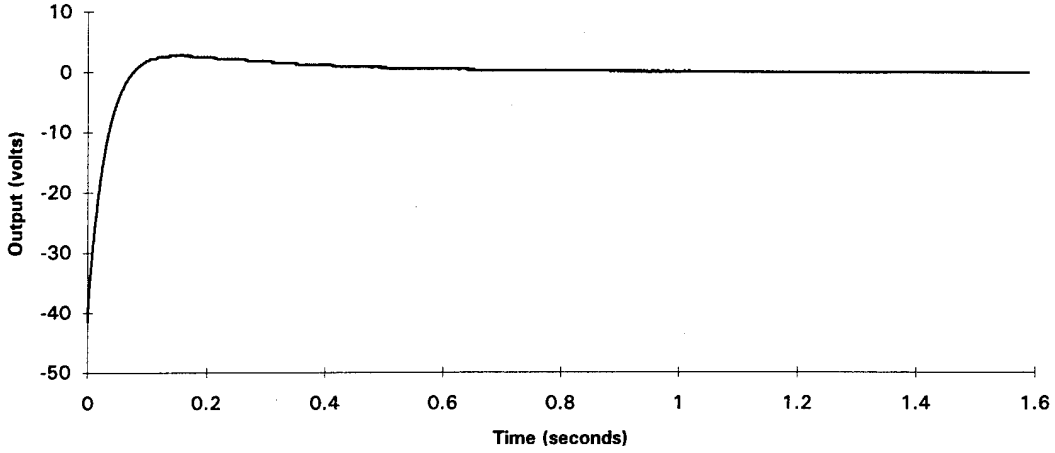

MICRO-PARTICLE DETECTOR
DATA SET D20

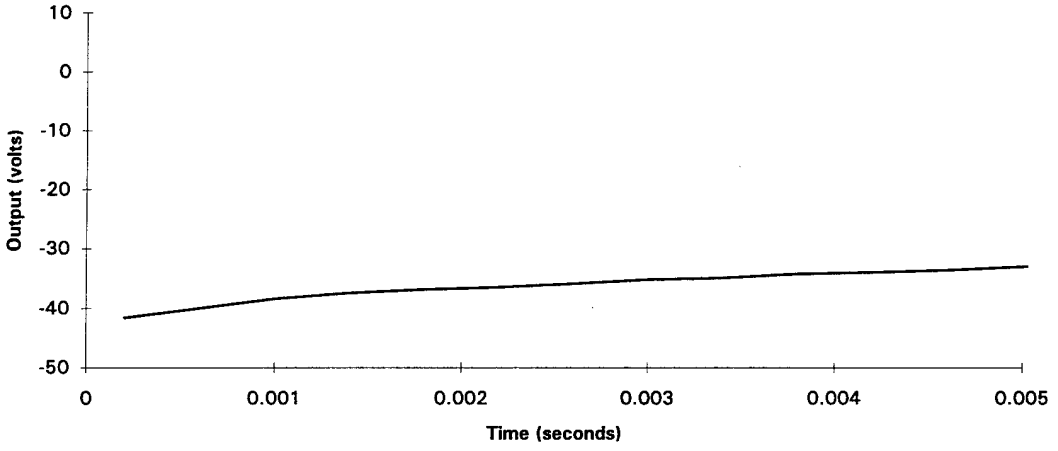

APPENDIX B

LENS DATA, 700 VOLT APPLIED

LENS - NORMAL IMPACT
DATA SET A6, 700 VOLT APPLIED

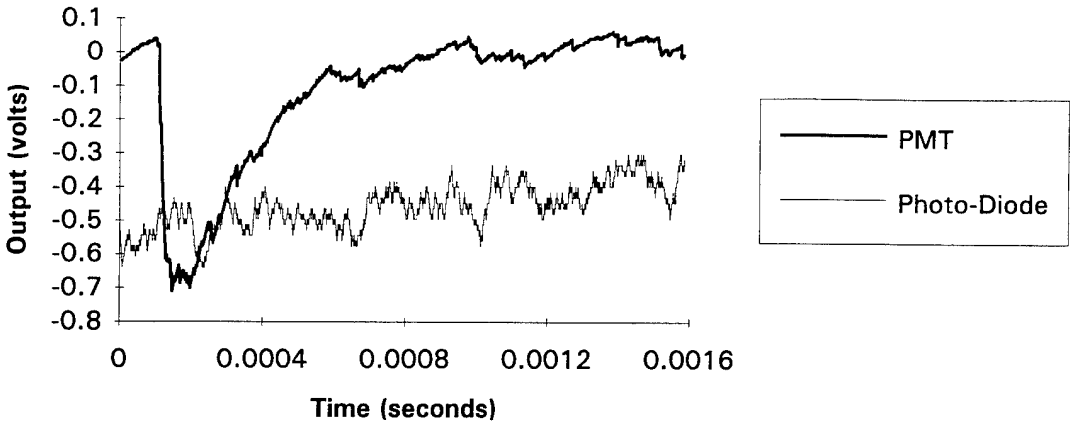

LENS - NORMAL IMPACT
DATA SET A7, 700 VOLT APPLIED

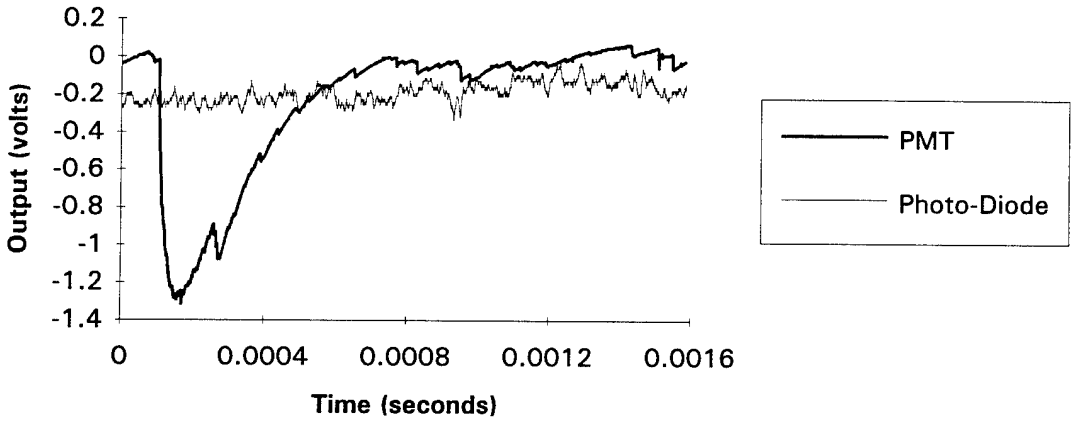

LENS - NORMAL IMPACT
DATA SET A8, 700 VOLT APPLIED

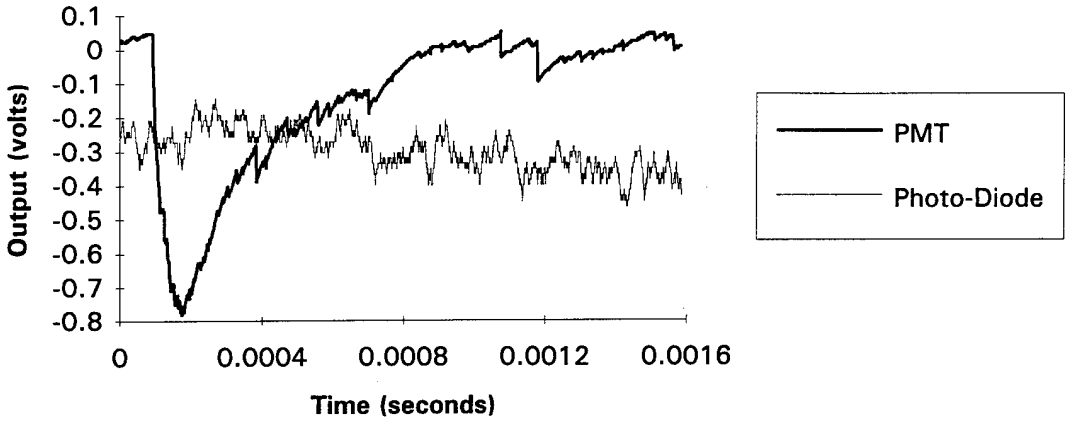

LENS - NORMAL IMPACT
DATA SET A9, 700 VOLT APPLIED

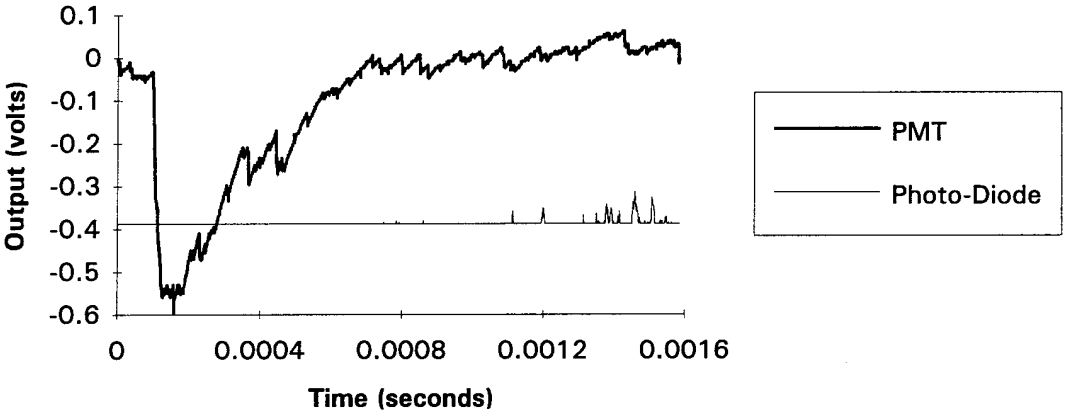

LENS - NORMAL IMPACT
DATA SET A10, 700 VOLT APPLIED

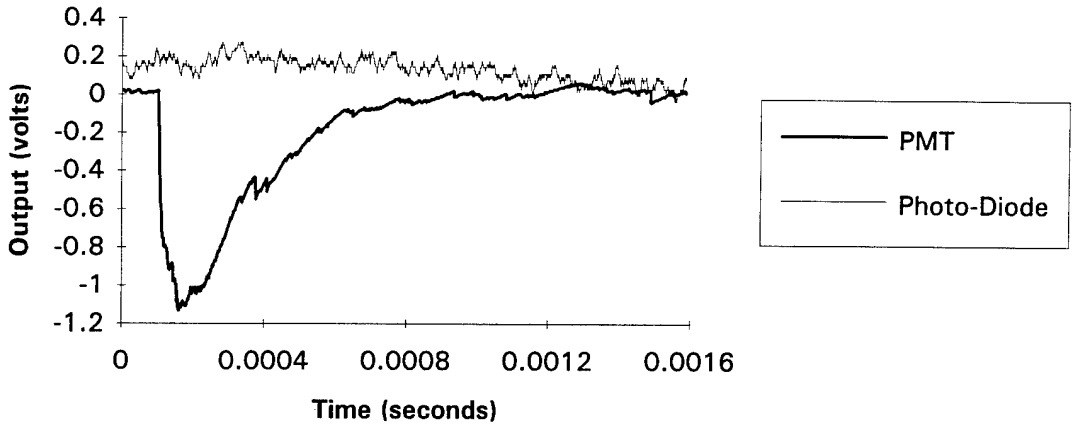

LENS - NORMAL IMPACT
DATA SET A11, 700 VOLT APPLIED

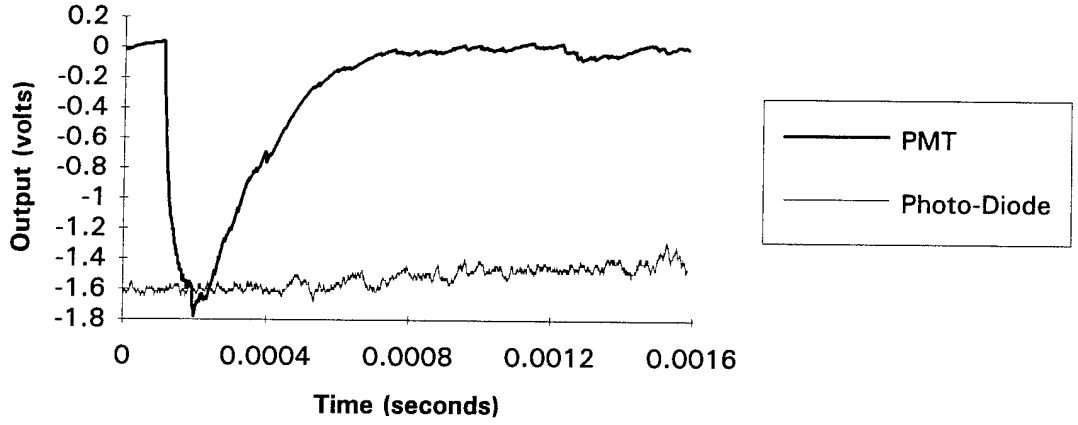

LENS - NORMAL IMPACT
DATA SET A12, 700 VOLT APPLIED

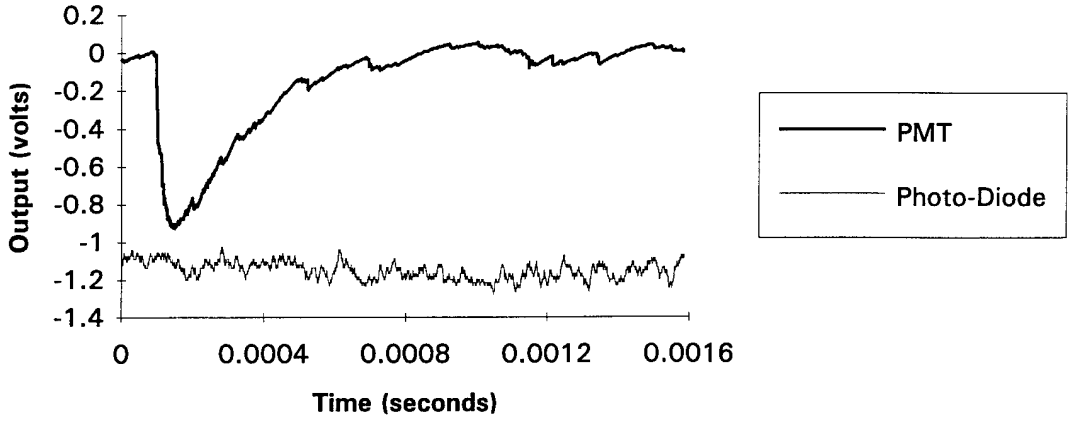

LENS - NORMAL IMPACT
DATA SET A13, 700 VOLT APPLIED

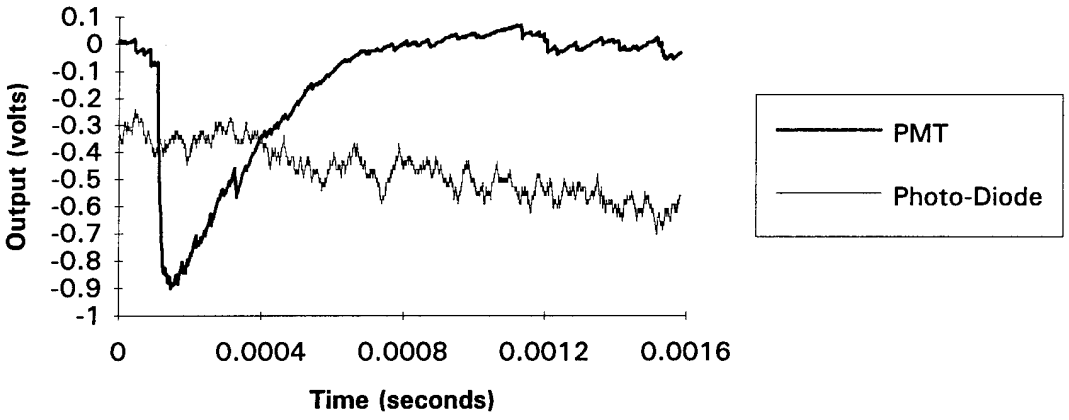

LENS - NORMAL IMPACT
DATA SET A14, 700 VOLT APPLIED

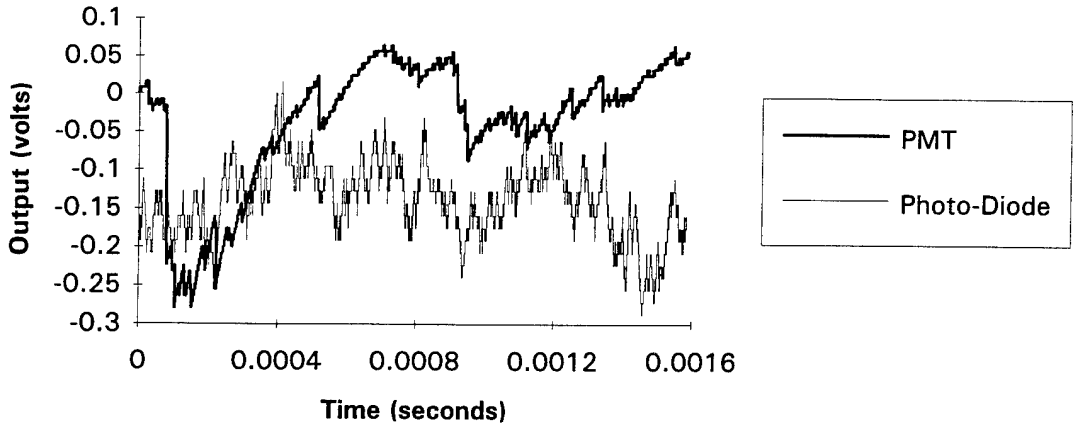

LENS - NORMAL IMPACT
DATA SET A15, 700 VOLT APPLIED

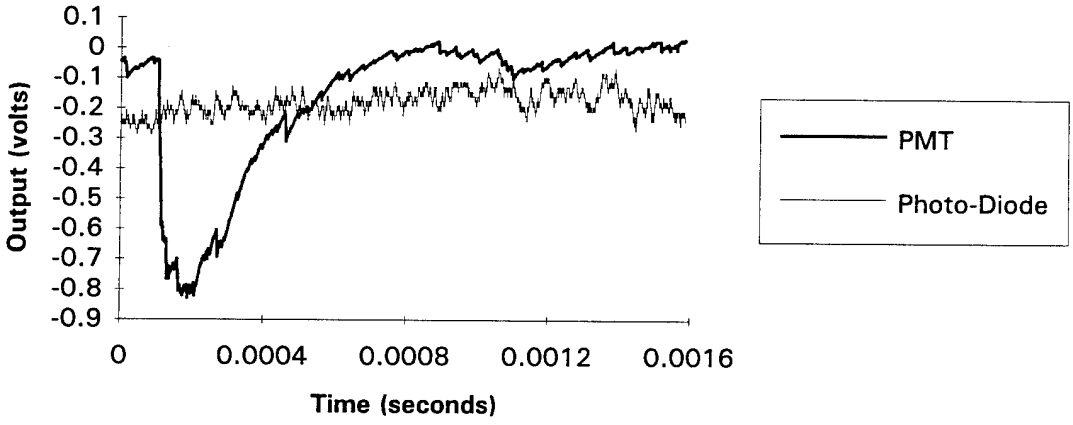

LENS - NORMAL IMPACT
DATA SET A16, 700 VOLT APPLIED

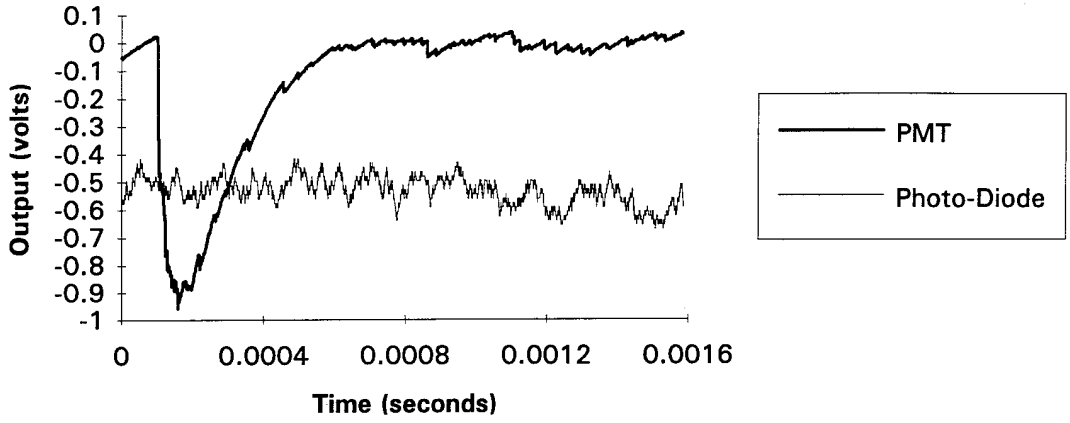

LENS - NORMAL IMPACT
DATA SET A17, 700 VOLT APPLIED

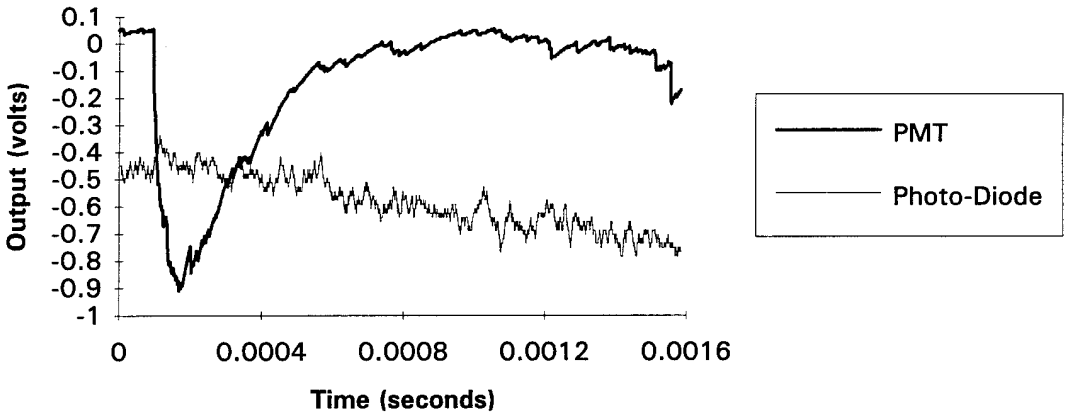

LENS - NORMAL IMPACT
DATA SET A18, 700 VOLT APPLIED

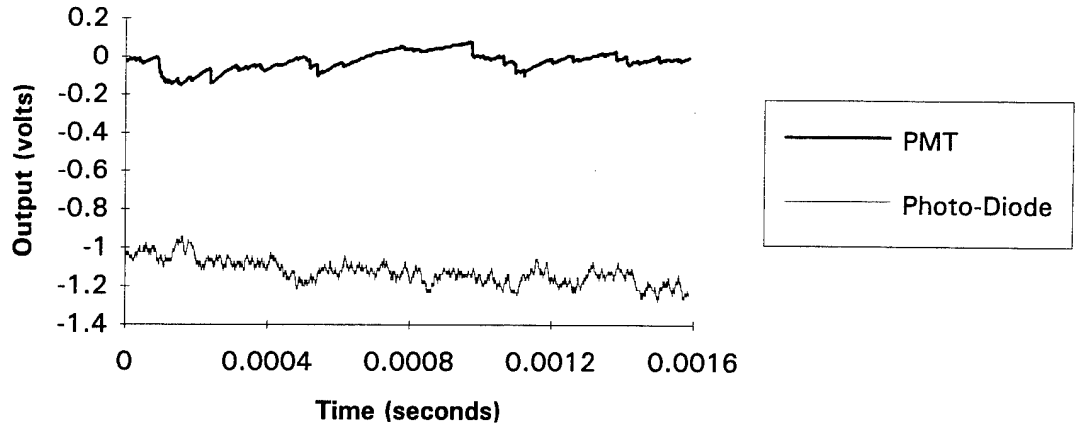

LENS - NORMAL IMPACT
DATA SET A19, 700 VOLT APPLIED

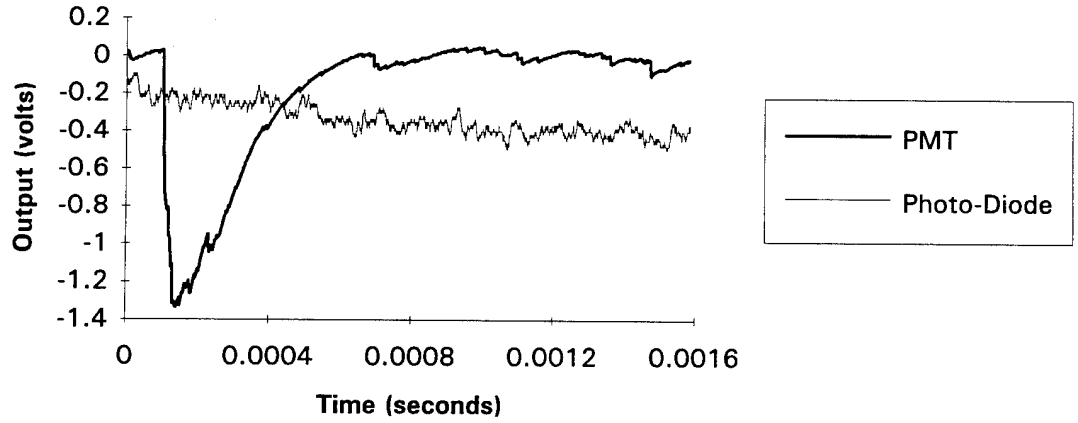

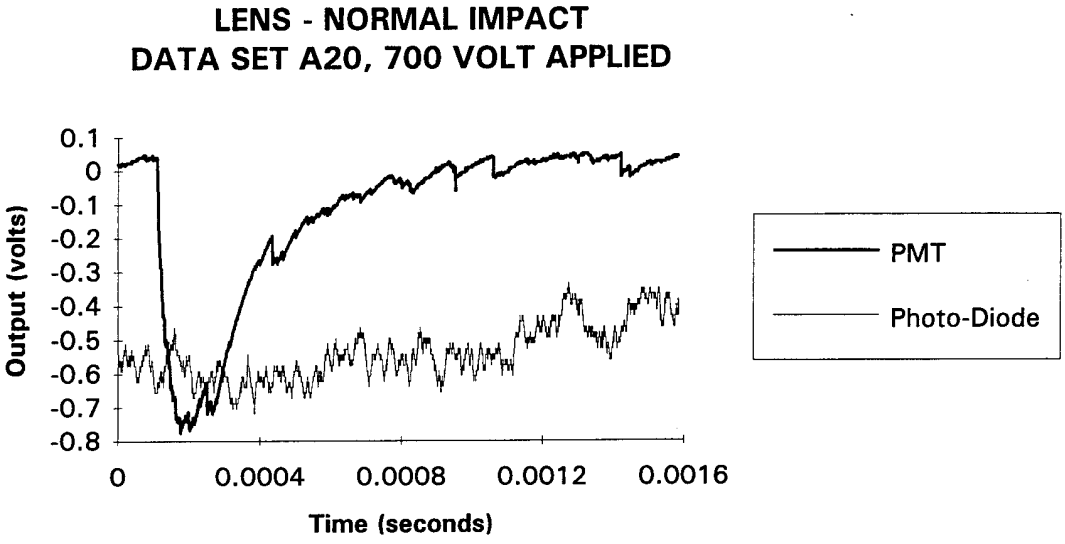
LENS - NORMAL IMPACT
DATA SET A20, 700 VOLT APPLIED
Output (volts)
0.1
0
-0.1
-0.2
-0.3
-0.4
-0.5
-0.6
-0.7
-0.8
0
0.0004
0.0008
0.0012
0.0016
Time (seconds)
PMT
Photo-Diode

APPENDIX C

LENS DATA, 700 VOLT REMOVED

LENS - NORMAL IMPACT
DATA SET A1, 700 VOLT REMOVED

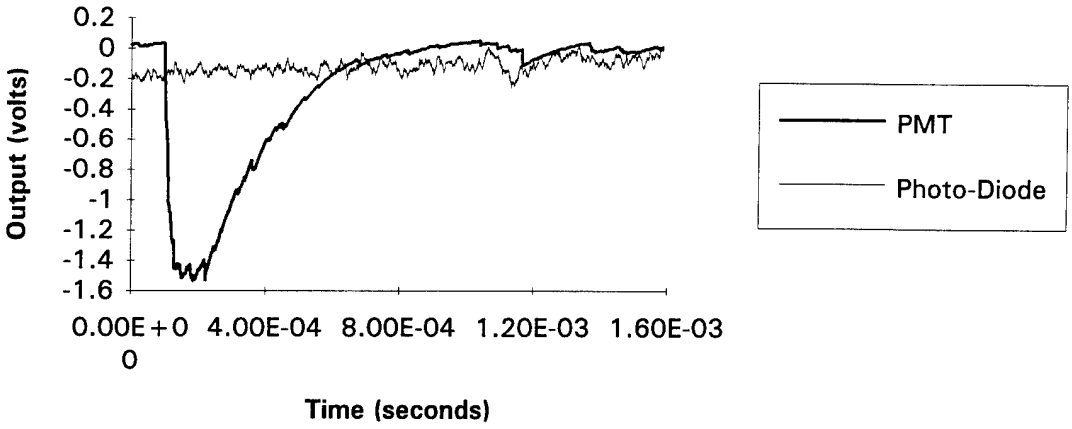

LENS - NORMAL IMPACT
DATA SET A2, 700 VOLT REMOVED

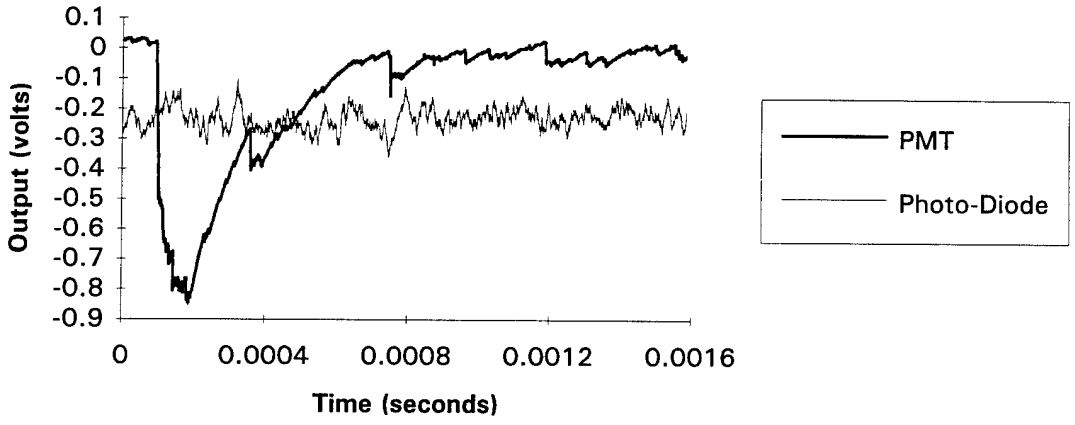

LENS - NORMAL IMPACT
DATA SET A3, 700 VOLT REMOVED

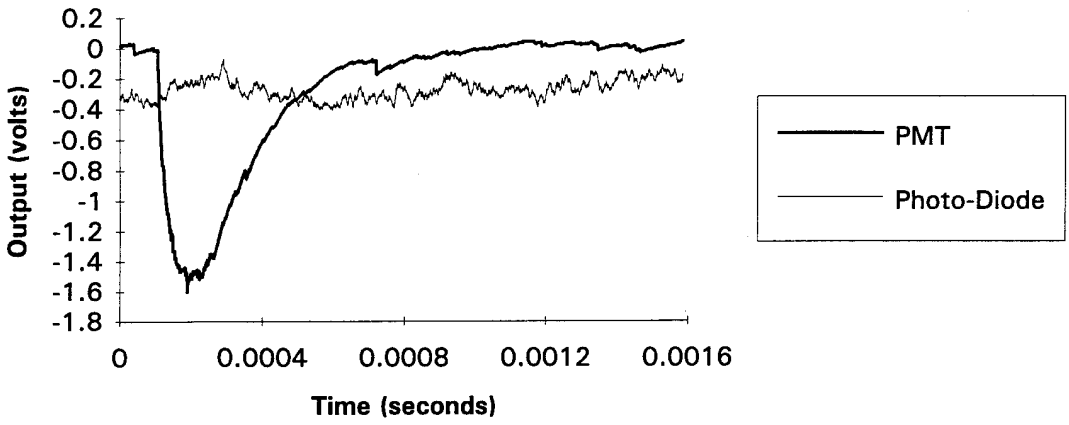

LENS - NORMAL IMPACT
DATA SET A4, 700 VOLT REMOVED

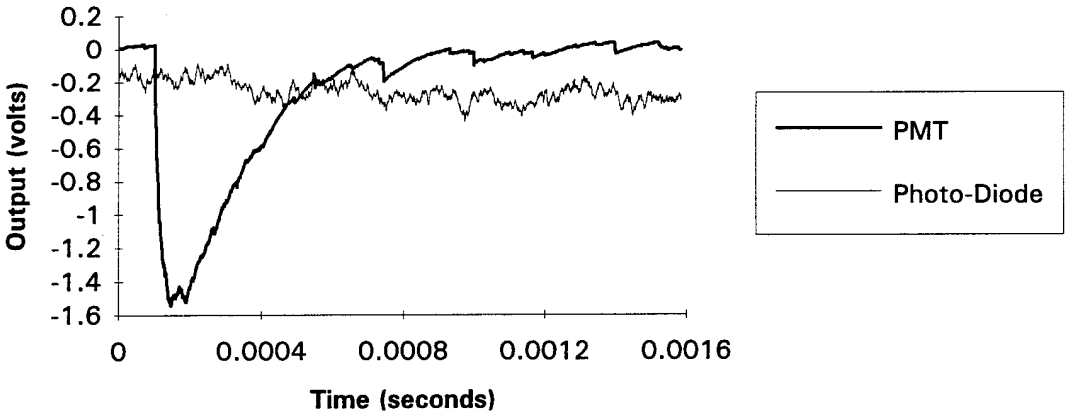

LENS - NORMAL IMPACT
DATA SET A5, 700 VOLT REMOVED

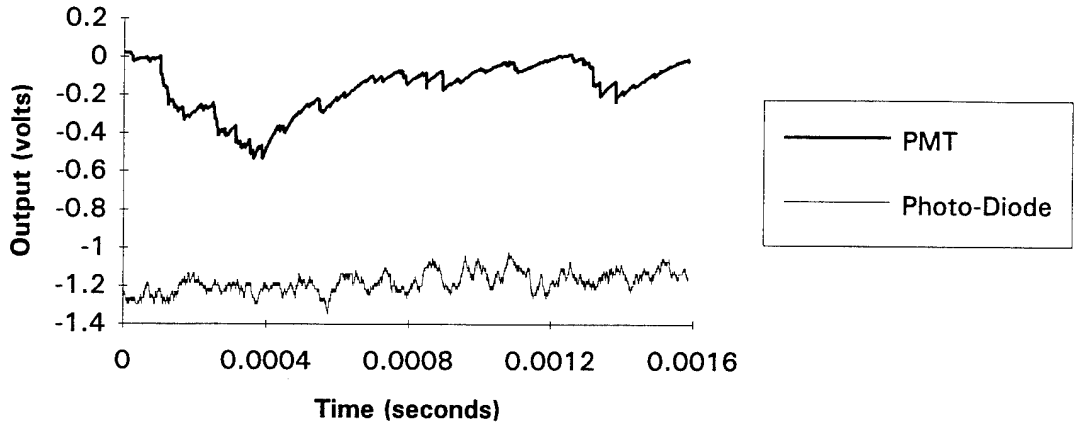

LENS - NORMAL IMPACT
DATA SET B3, 700 VOLT REMOVED

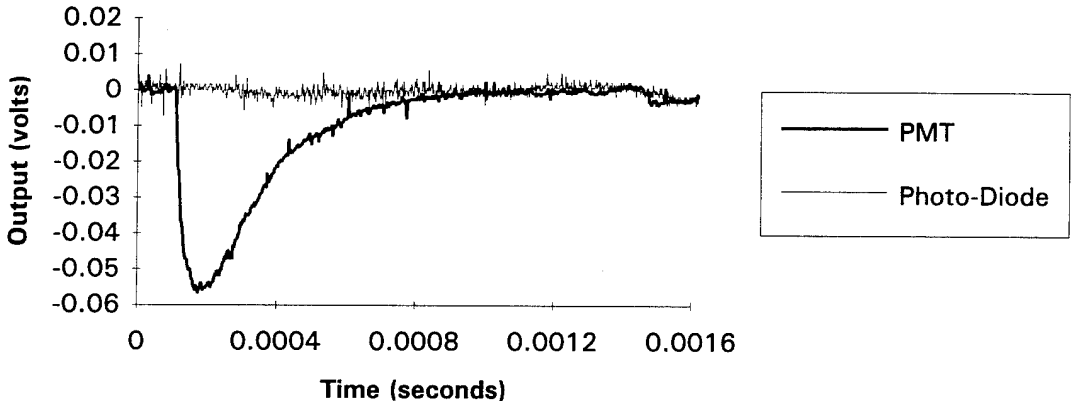

LENS - NORMAL IMPACT
DATA SET B4, 700 VOLT REMOVED

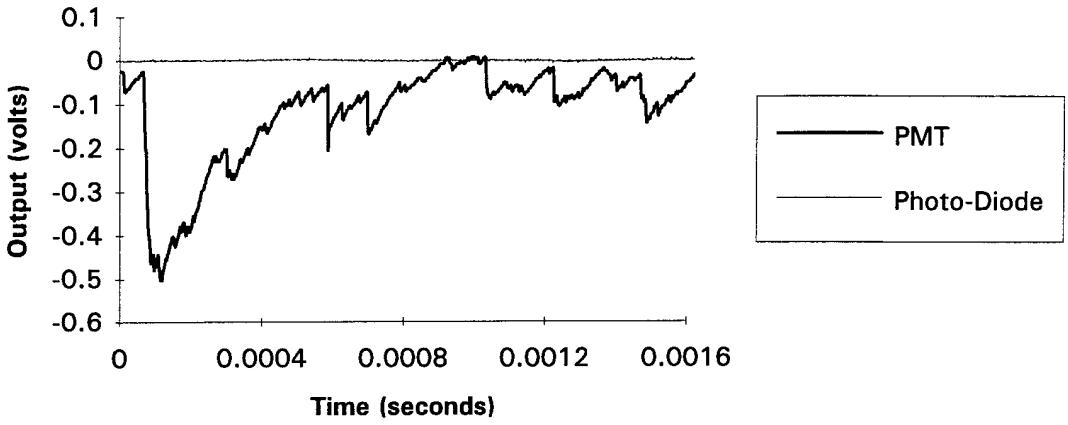

LENS - NORMAL IMPACT
DATA SET B5, 700 VOLT REMOVED

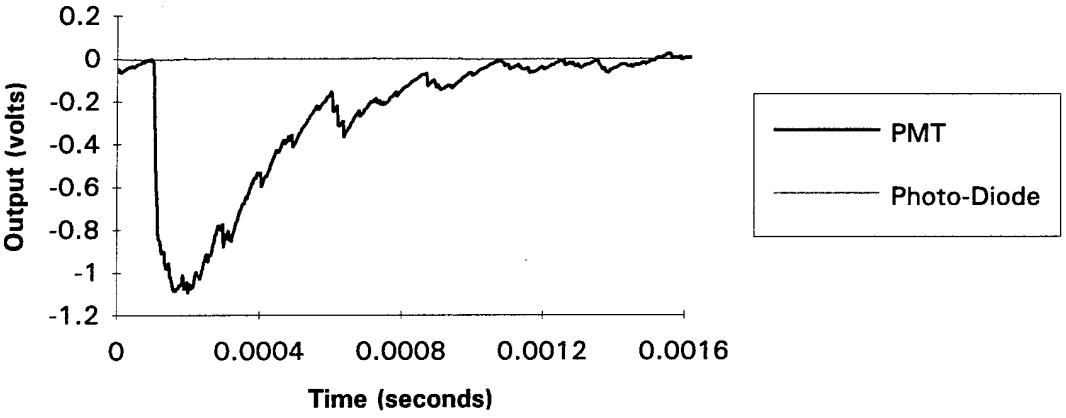

LENS - NORMAL IMPACT
DATA SET B6, 700 VOLT REMOVED

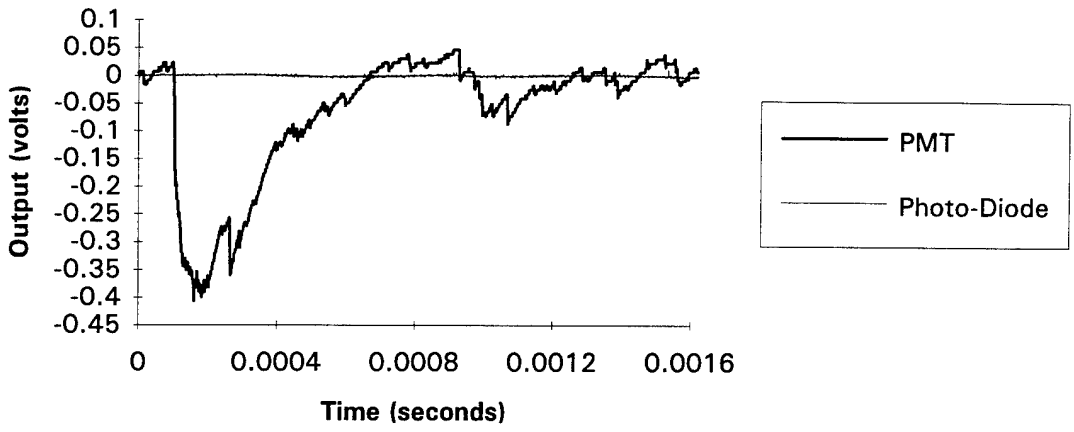

LENS - NORMAL IMPACT
DATA SET B7, 700 VOLT REMOVED

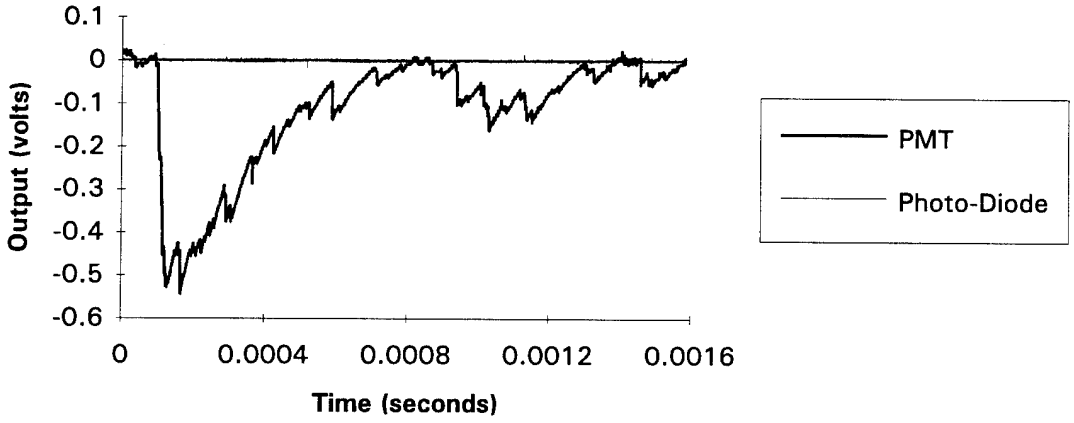

LENS - NORMAL IMPACT
DATA SET B8, 700 VOLT REMOVED

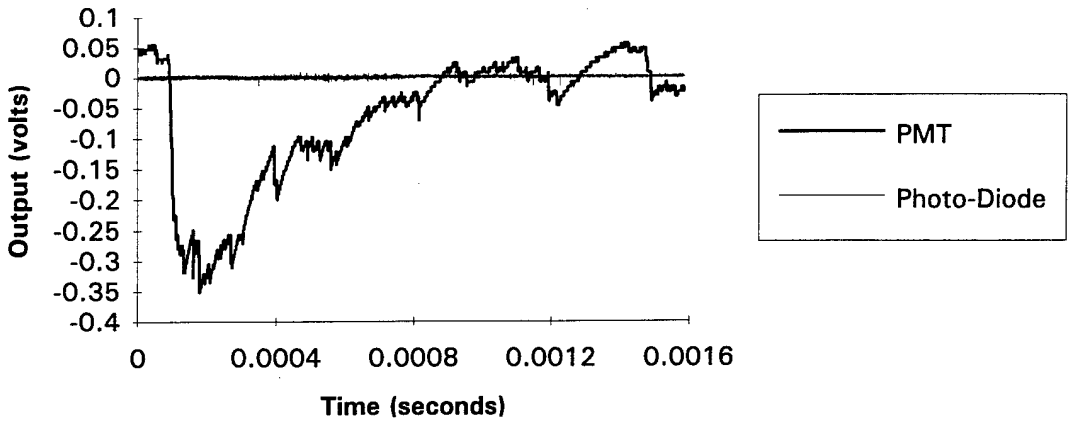

LENS - NORMAL IMPACT
DATA SET B9, 700 VOLT REMOVED

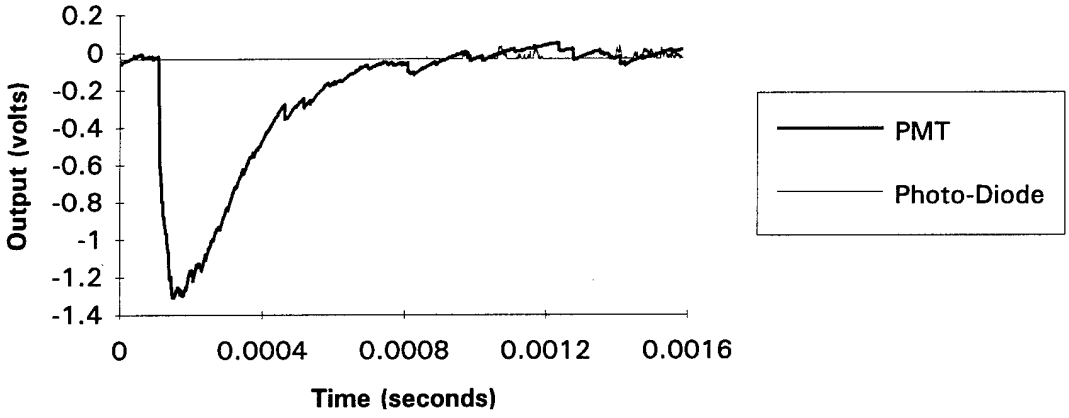

LENS - NORMAL IMPACT
DATA SET B10, 700 VOLT REMOVED

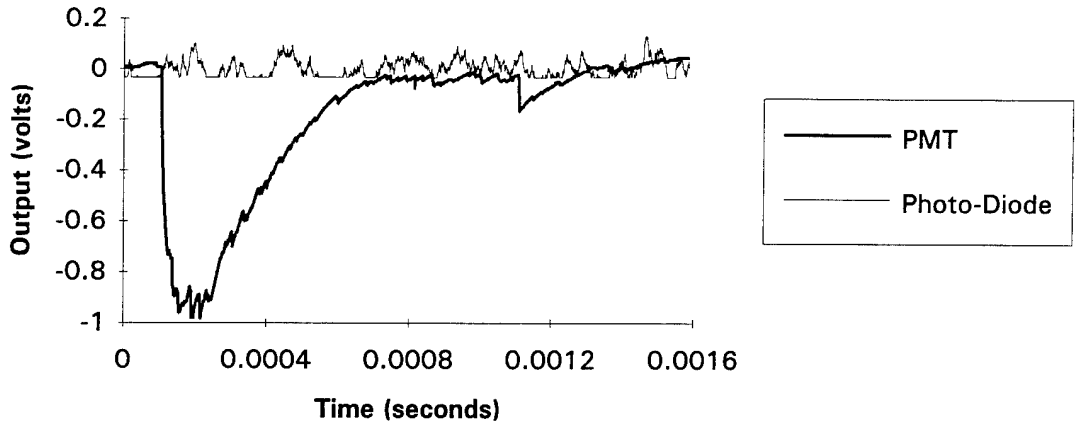

LENS - NORMAL IMPACT
DATA SET B11, 700 VOLT REMOVED

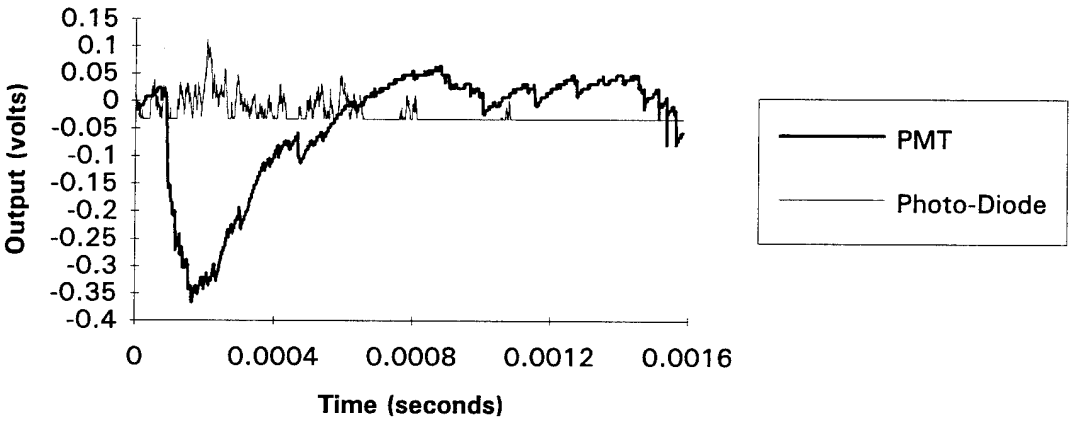

LENS - NORMAL IMPACT
DATA SET B12, 700 VOLT REMOVED

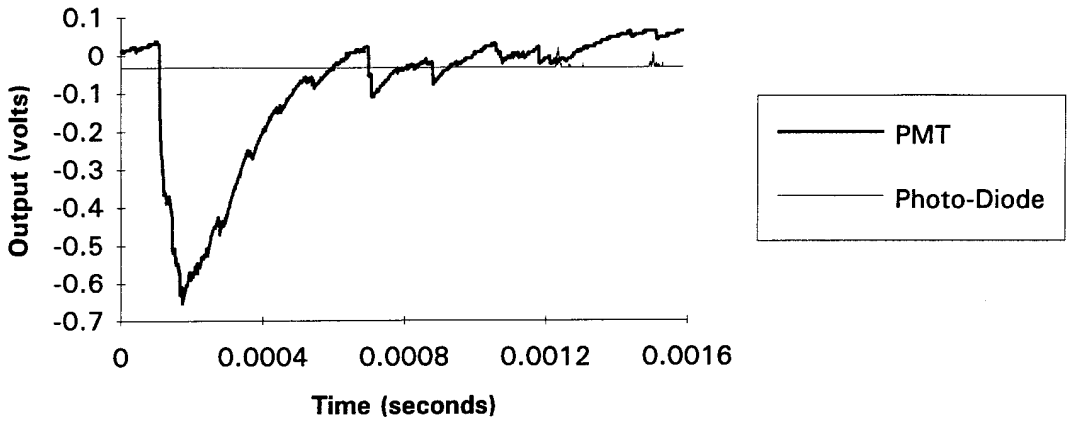

LENS - NORMAL IMPACT
DATA SET B13, 700 VOLT REMOVED

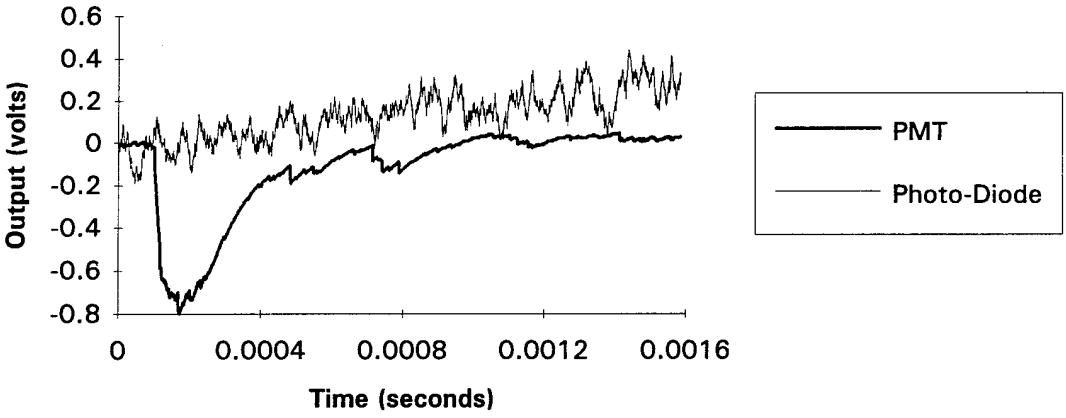

LENS - NORMAL IMPACT
DATA SET B14, 700 VOLT REMOVED

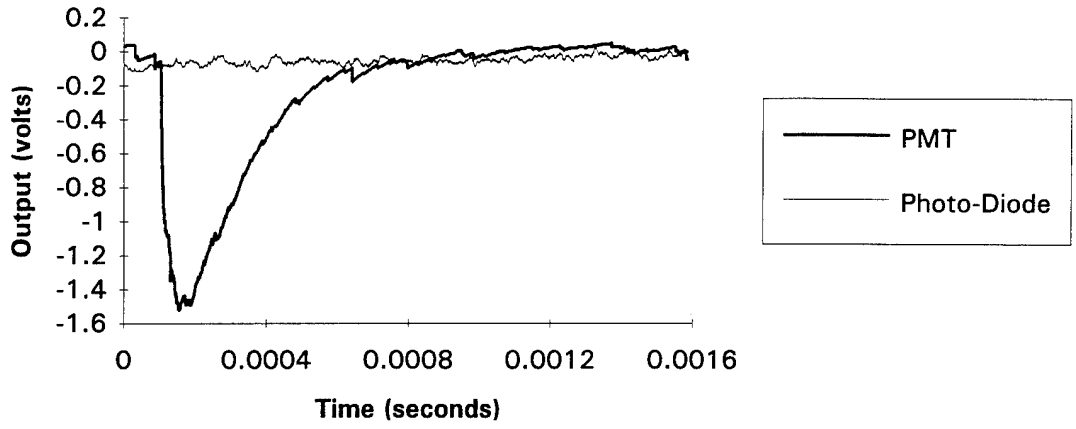

LENS - NORMAL IMPACT
DATA SET B15, 700 VOLT REMOVED

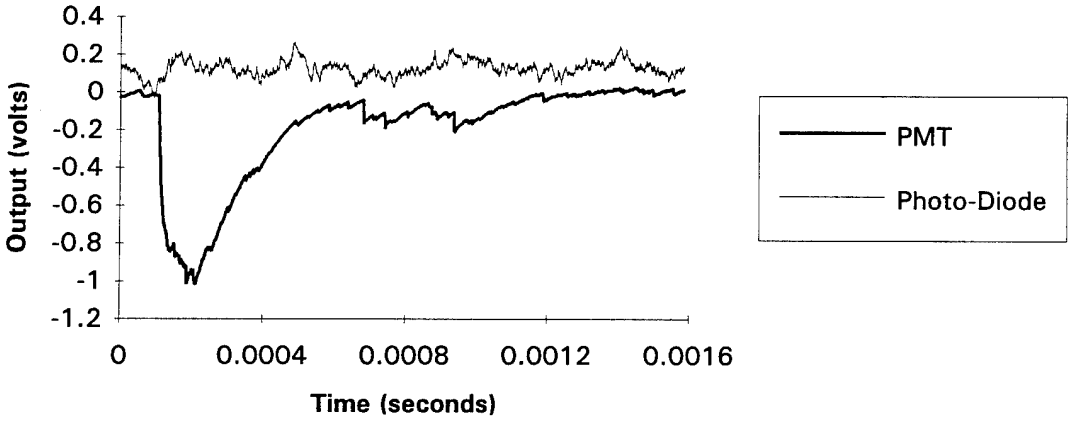

LENS - NORMAL IMPACT
DATA SET B16, 700 VOLT REMOVED

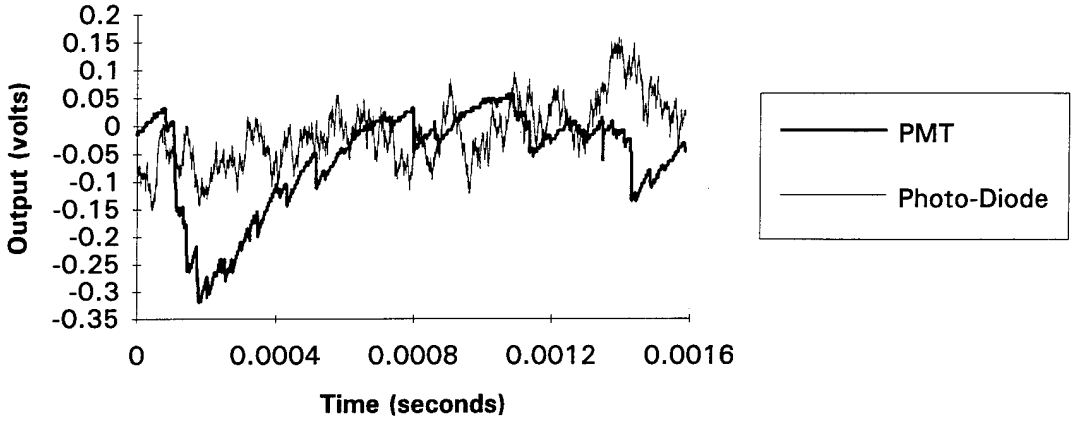

LENS - NORMAL IMPACT
DATA SET B17, 700 VOLT REMOVED

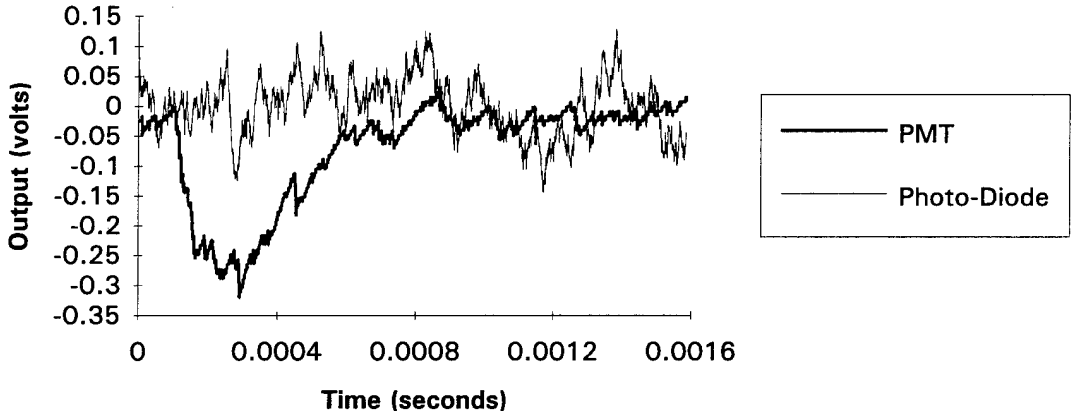

LENS - NORMAL IMPACT
DATA SET B18, 700 VOLT REMOVED

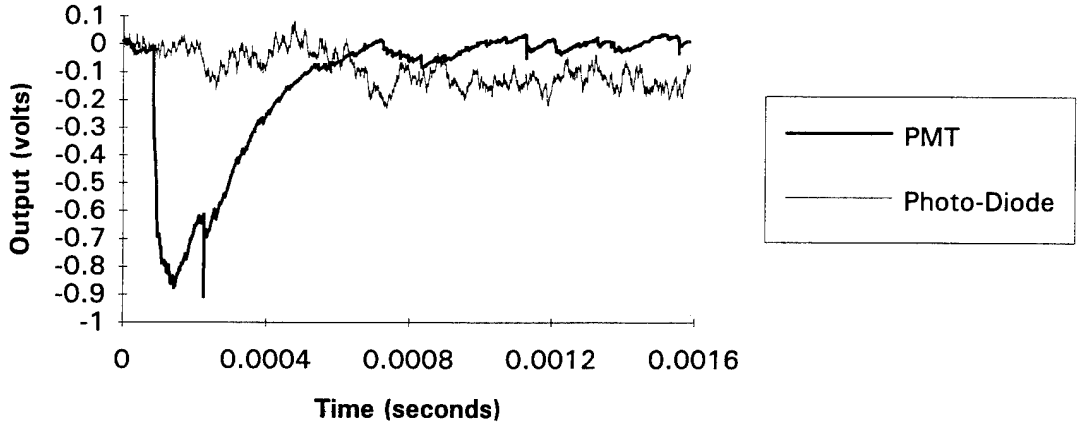

LENS - NORMAL IMPACT
DATA SET B19, 700 VOLT REMOVED

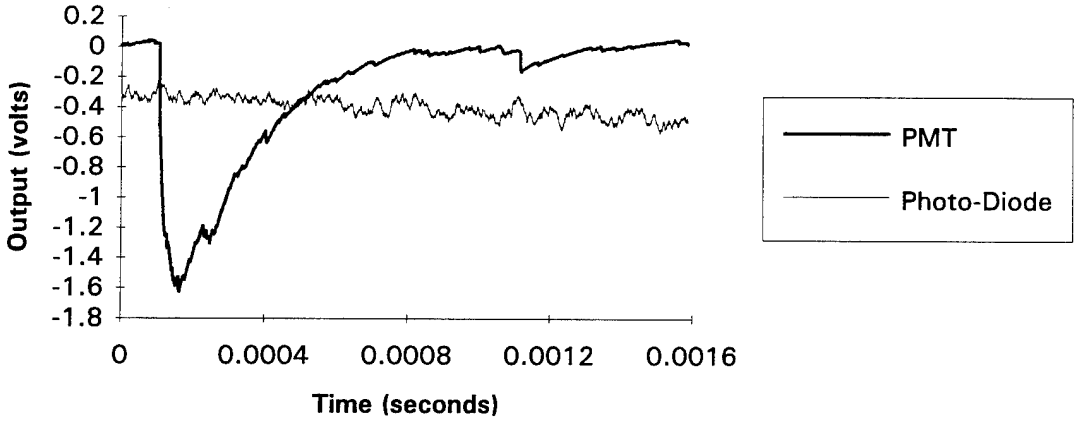

LENS - NORMAL IMPACT
DATA SET B20, 700 VOLT REMOVED

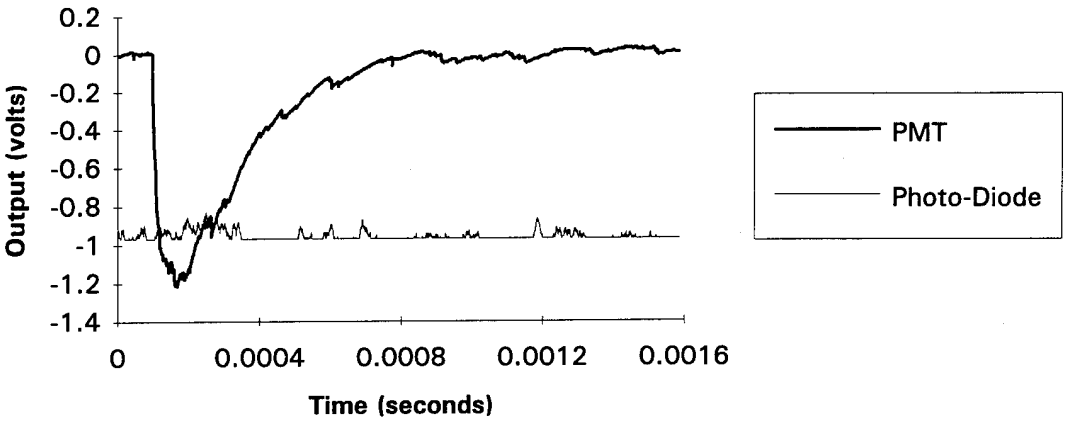

APPENDIX D

SUNSHADE DATA, 700 VOLT APPLIED

SUNSHADE - 25 DEGREE IMPACT
DATA SET F7, 700 VOLT APPLIED

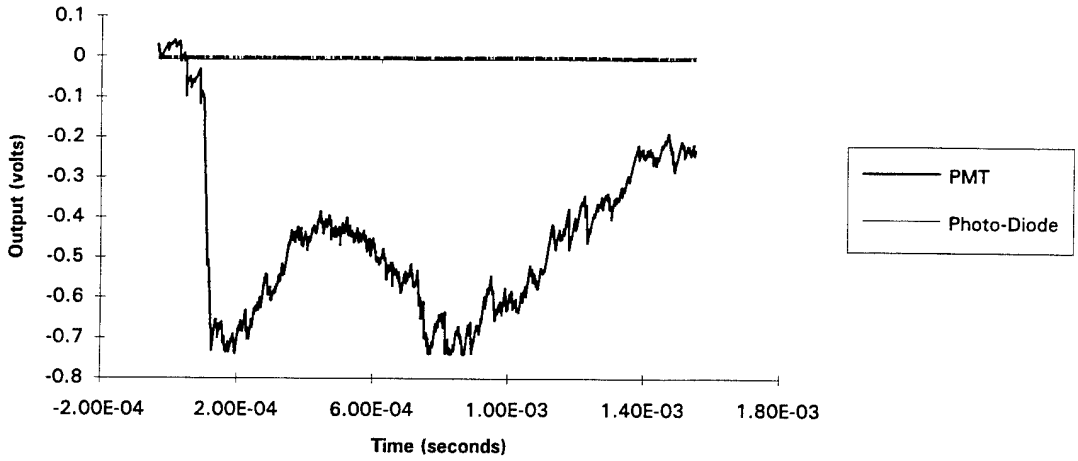

SUNSHADE - 25 DEGREE IMPACT
DATA SET F8, 700 VOLT APPLIED

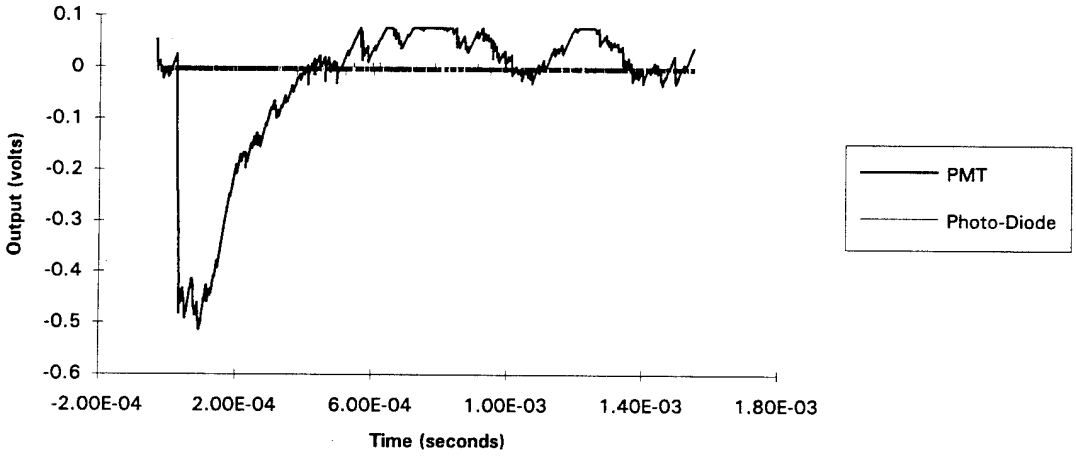

SUNSHADE - 25 DEGREE IMPACT
DATA SET F9, 700 VOLT APPLIED

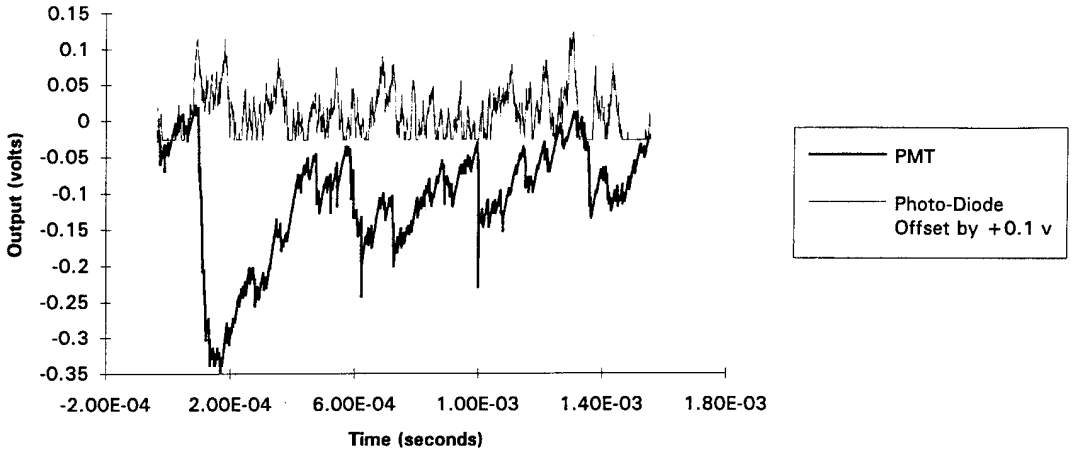

SUNSHADE - 25 DEGREE IMPACT
DATA SET F10, 700 VOLT APPLIED

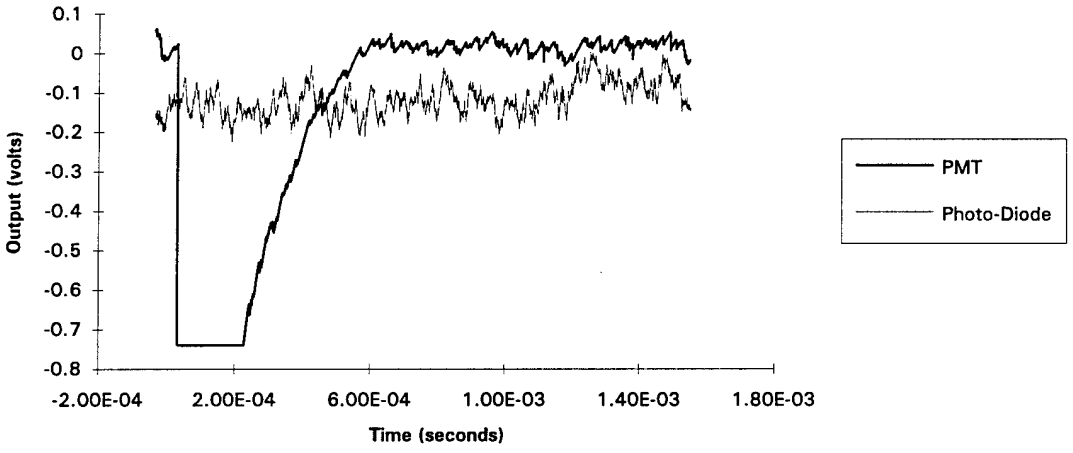

SUNSHADE - 25 DEGREE IMPACT
DATA SET F11, 700 VOLT APPLIED

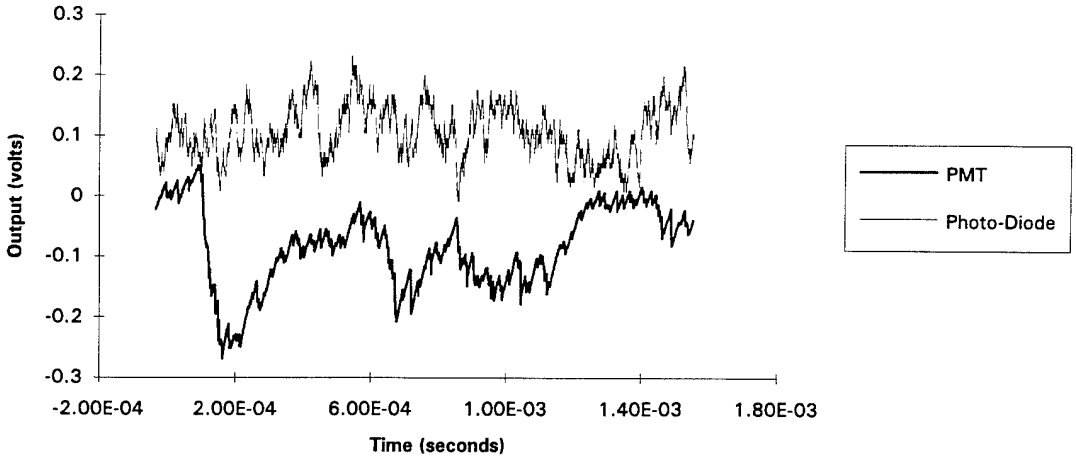

SUNSHADE - 25 DEGREE IMPACT
DATA SET F12, 700 VOLT APPLIED

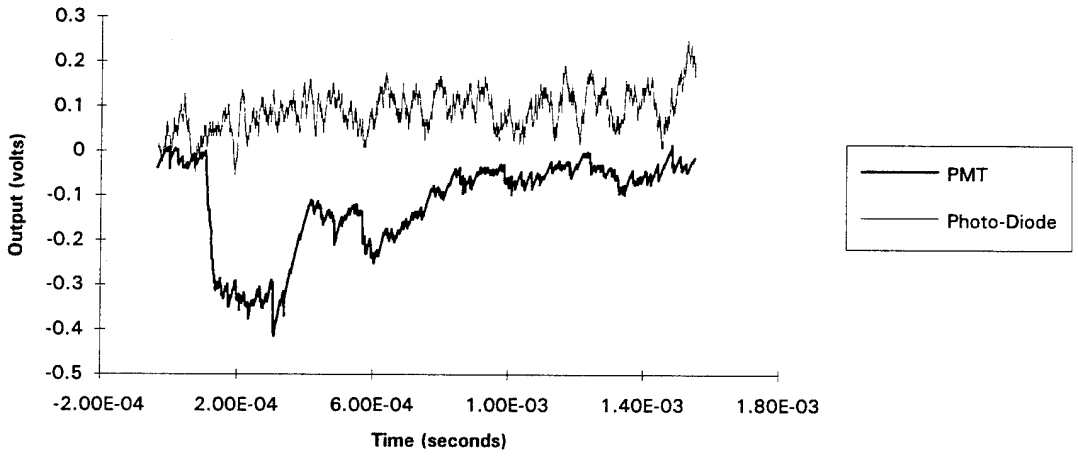

SUNSHADE - 25 DEGREE IMPACT
DATA SET F13, 700 VOLT APPLIED

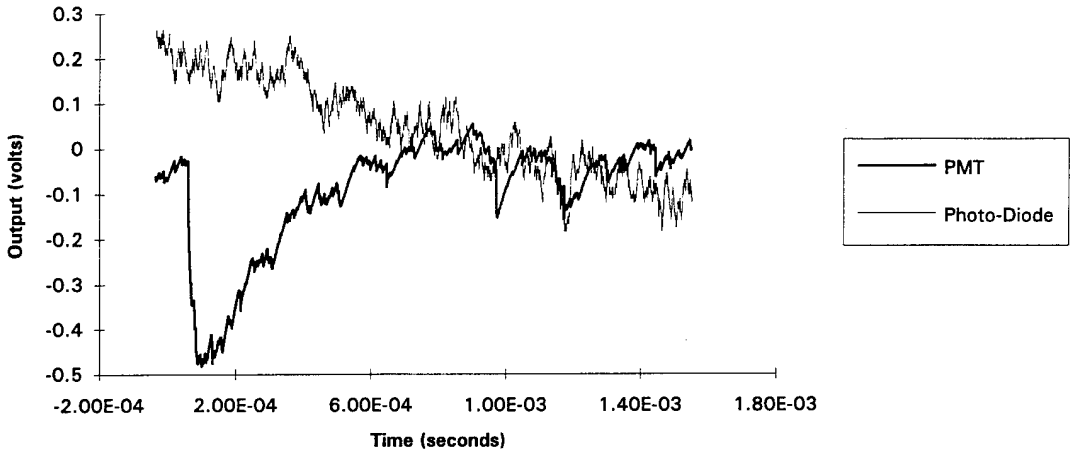

SUNSHADE - 25 DEGREE IMPACT
DATA SET F14, 700 VOLT APPLIED

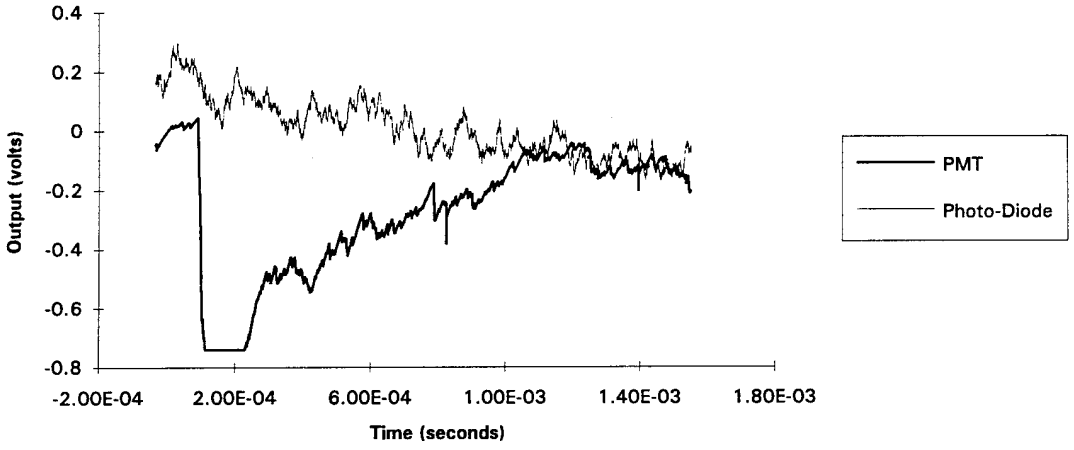

SUNSHADE - 25 DEGREE IMPACT
DATA SET F15, 700 VOLT APPLIED

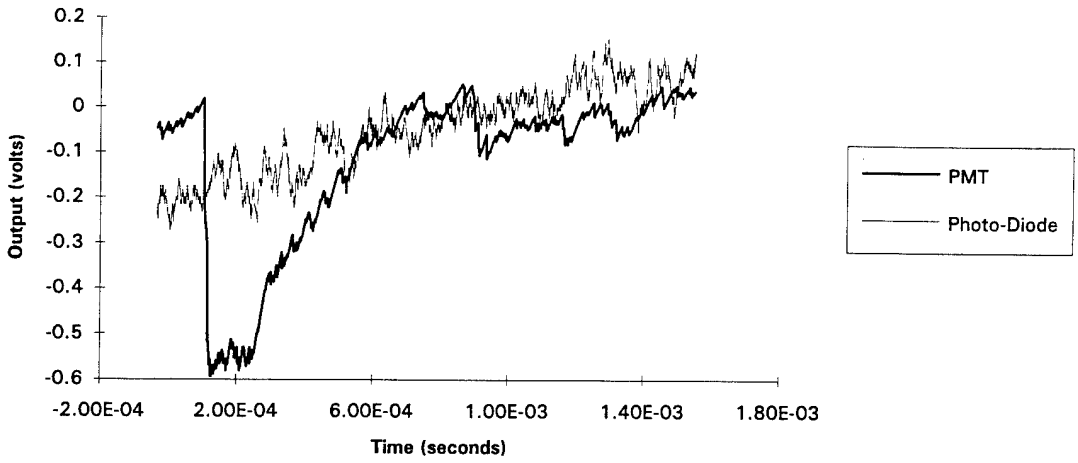

SUNSHADE - 25 DEGREE IMPACT
DATA SET F16, 700 VOLT APPLIED

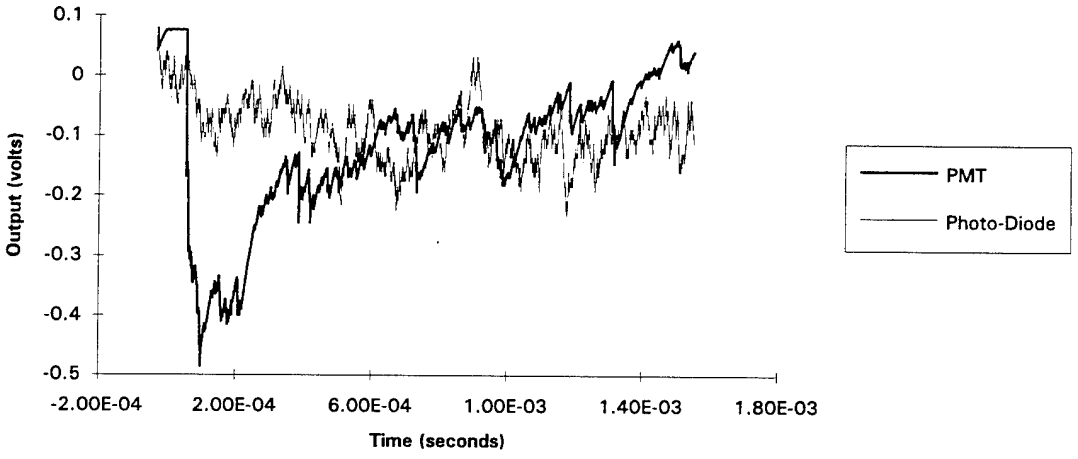

SUNSHADE - 25 DEGREE IMPACT
DATA SET F17, 700 VOLT APPLIED

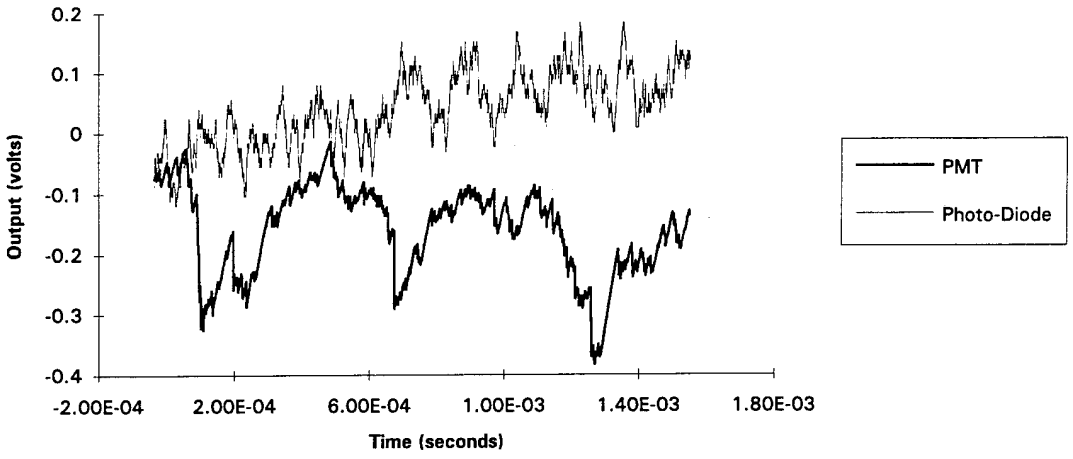

SUNSHADE - 25 DEGREE IMPACT
DATA SET F18, 700 VOLT APPLIED

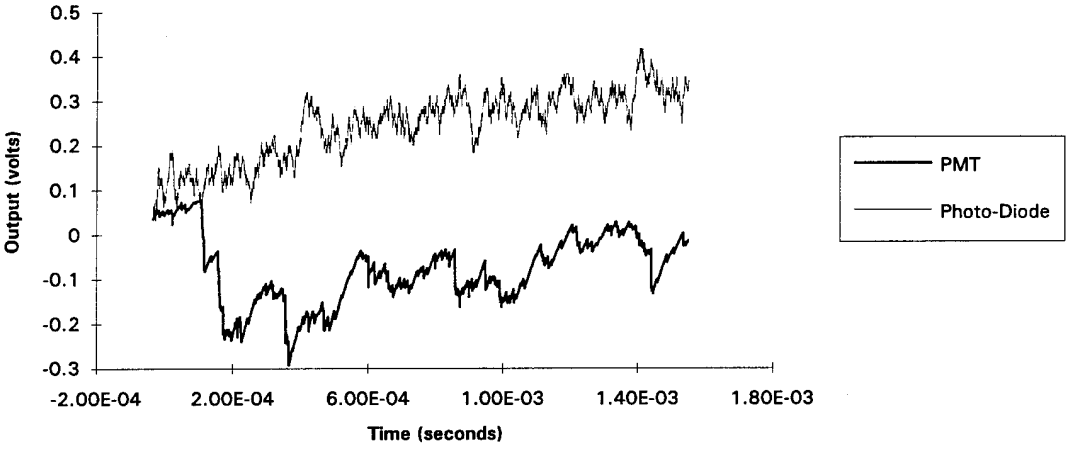

SUNSHADE - 25 DEGREE IMPACT
DATA SET F19, 700 VOLT APPLIED

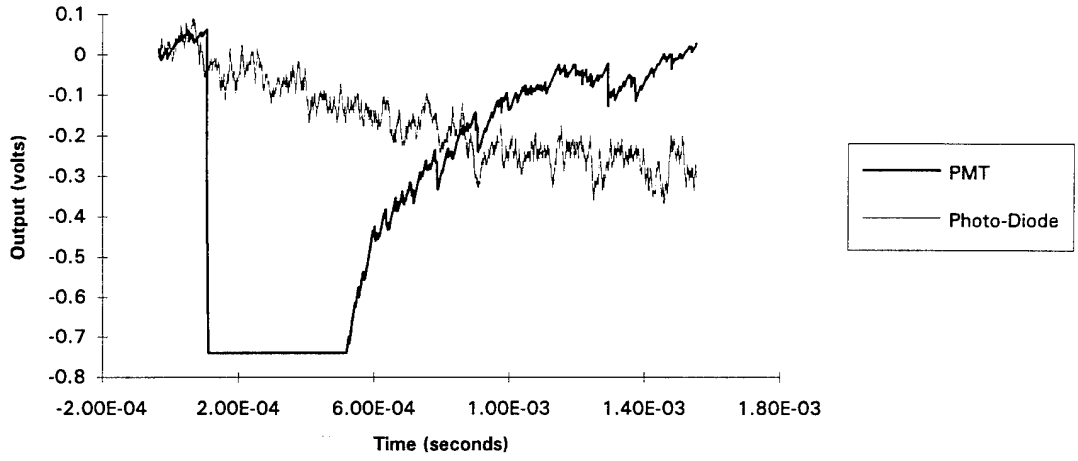

SUNSHADE - 25 DEGREE IMPACT
DATA SET F20, 700 VOLT APPLIED

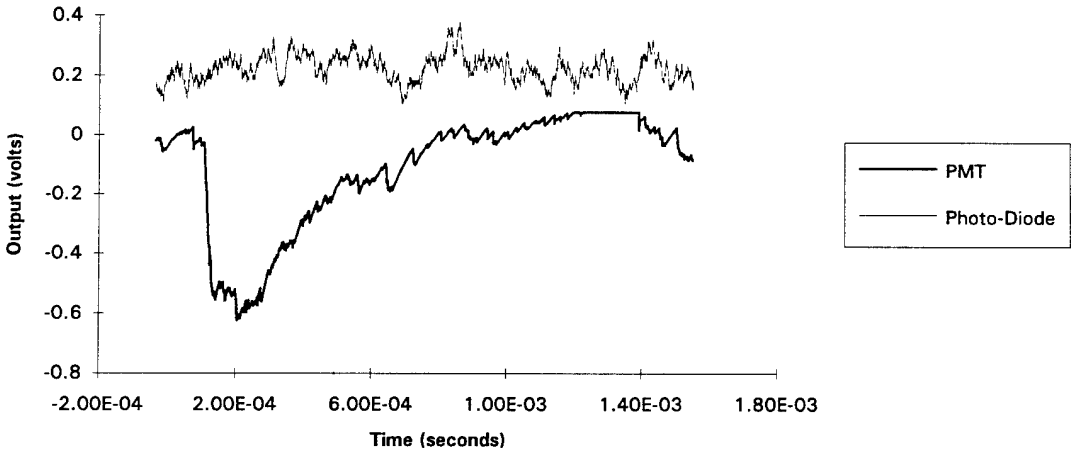

SUNSHADE - 25 DEGREE IMPACT
DATA SET G1, 700 VOLT APPLIED

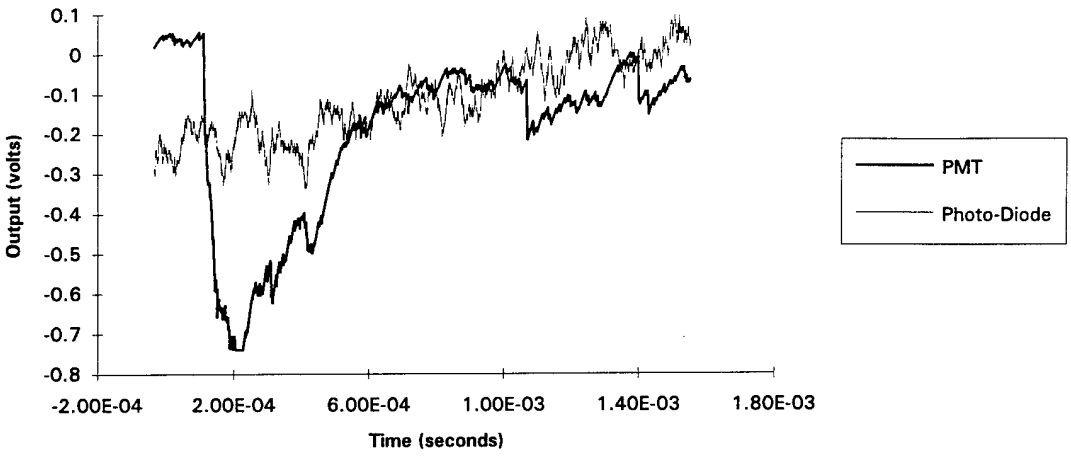

SUNSHADE - 25 DEGREE IMPACT
DATA SET G2, 700 VOLT APPLIED

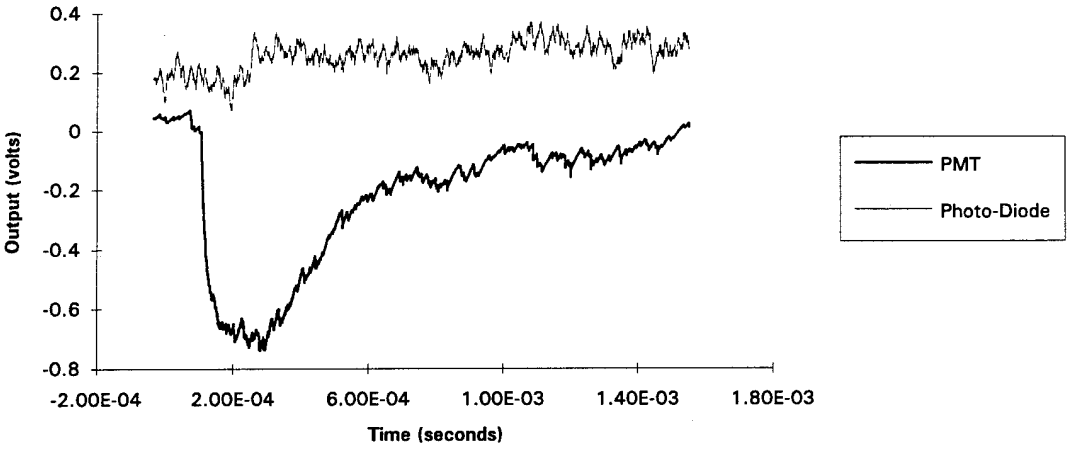

SUNSHADE - 25 DEGREE IMPACT
DATA SET G3, 700 VOLT APPLIED

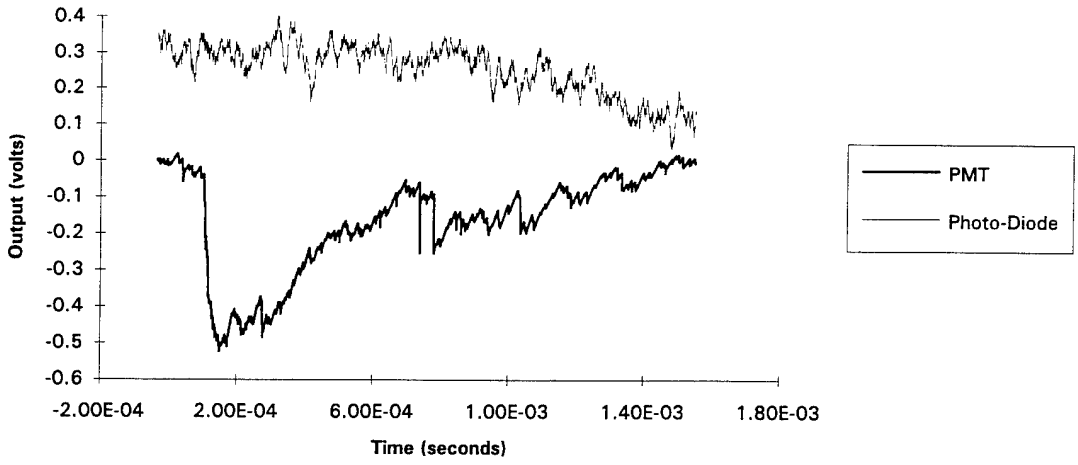

SUNSHADE - 25 DEGREE IMPACT
DATA SET G4, 700 VOLT APPLIED

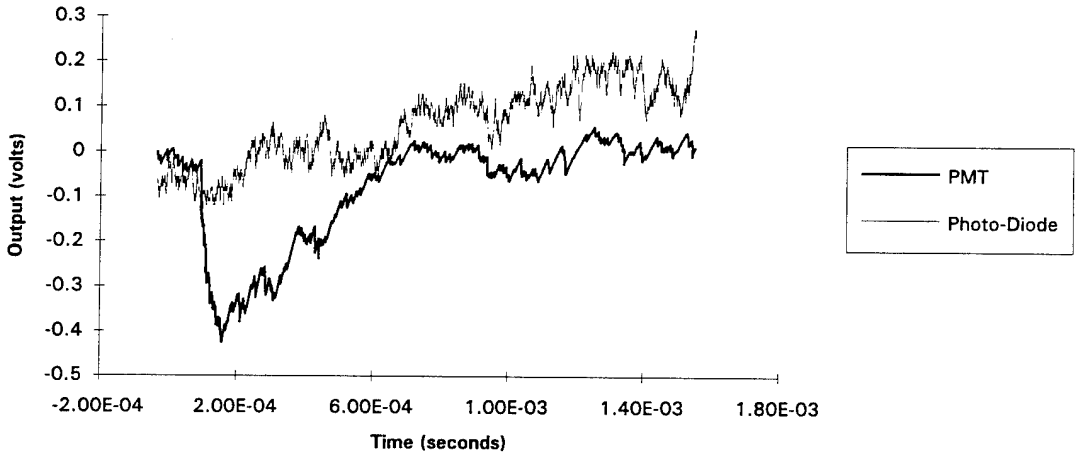

SUNSHADE - 25 DEGREE IMPACT
DATA SET G5, 700 VOLT APPLIED

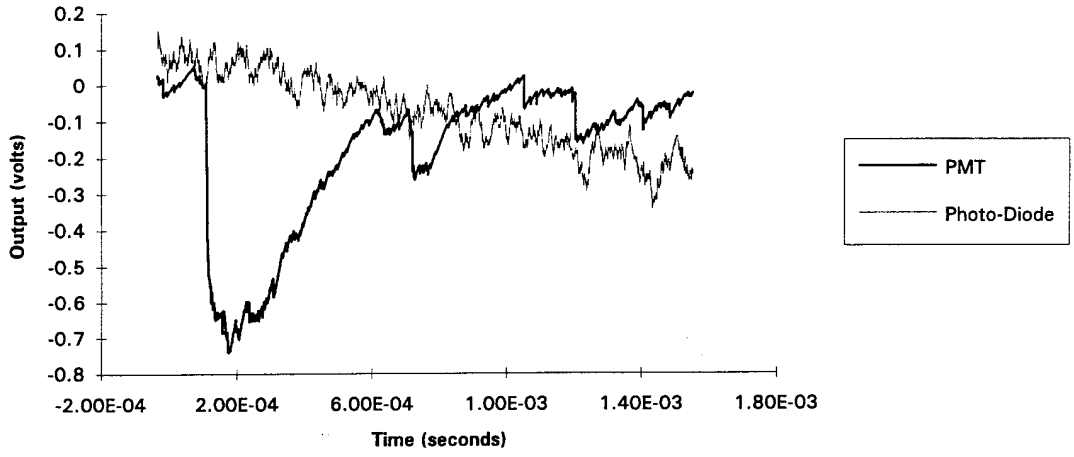

SUNSHADE - 25 DEGREE IMPACT
DATA SET G6, 700 VOLT APPLIED

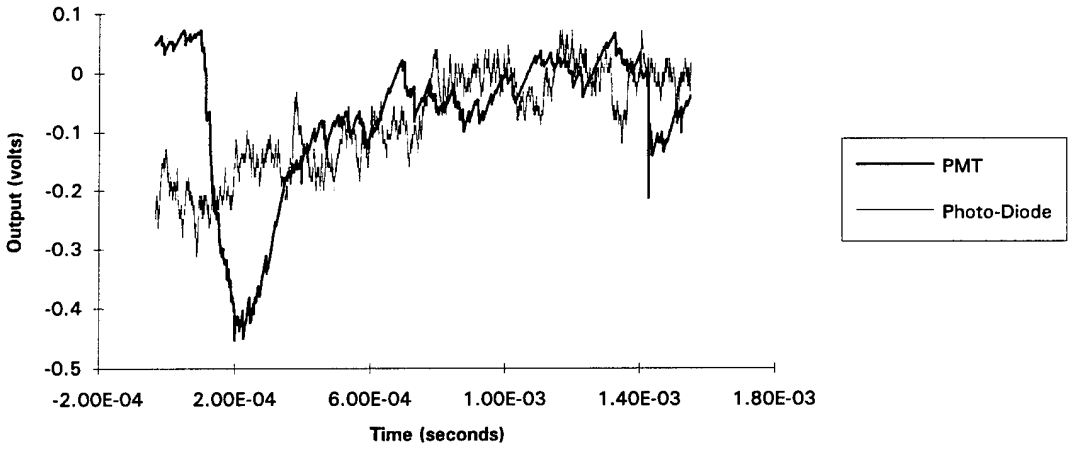

SUNSHADE - 25 DEGREE IMPACT
DATA SET G7, 700 VOLT APPLIED

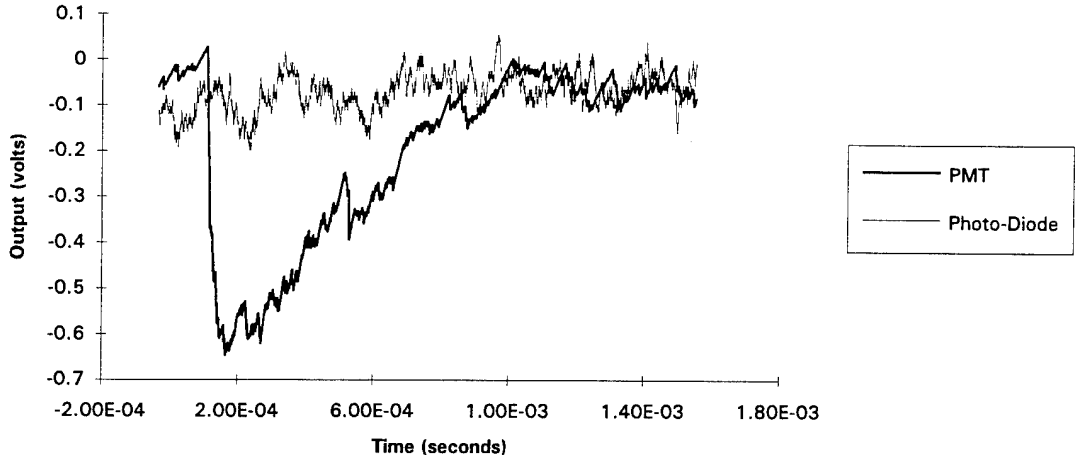

SUNSHADE - 25 DEGREE IMPACT
DATA SET G8, 700 VOLT APPLIED

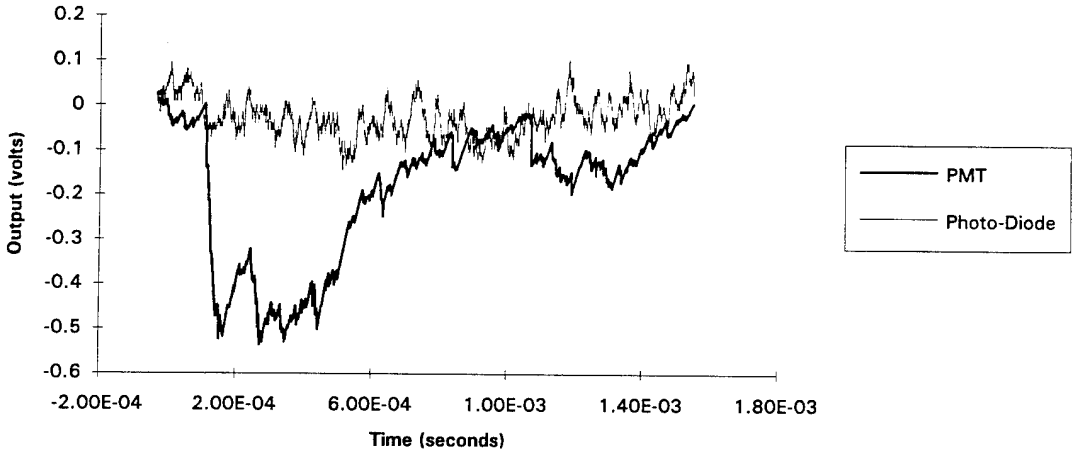

SUNSHADE - 25 DEGREE IMPACT
DATA SET G9, 700 VOLT APPLIED

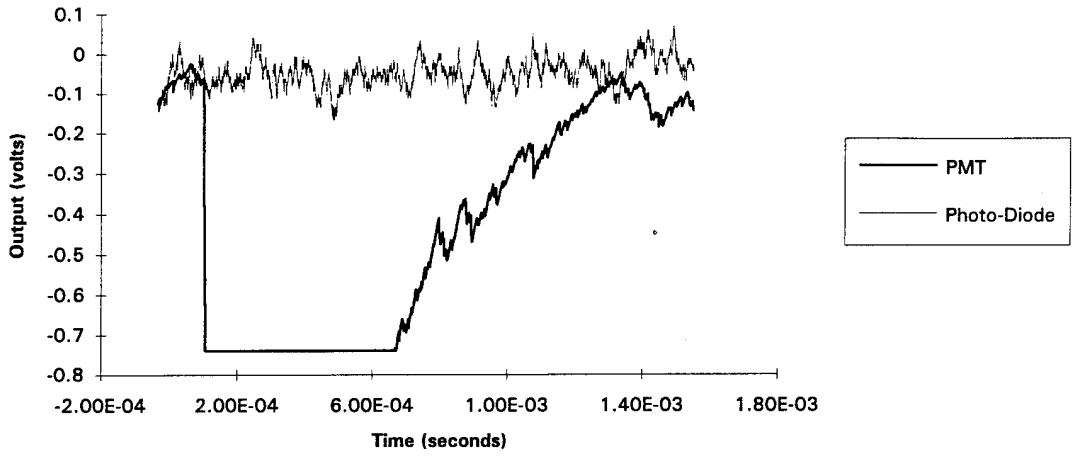

SUNSHADE - 25 DEGREE IMPACT
DATA SET G10, 700 VOLT APPLIED

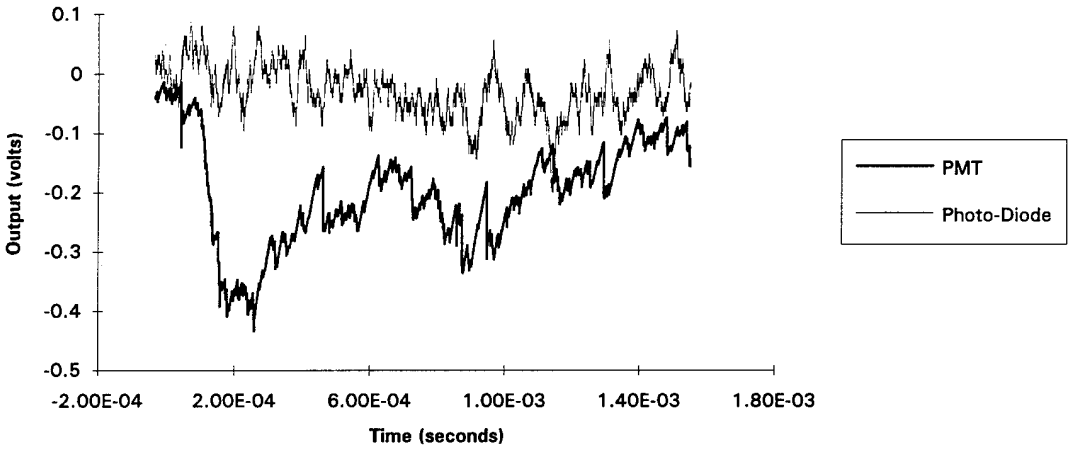

SUNSHADE - 25 DEGREE IMPACT
DATA SET G11, 700 VOLT APPLIED

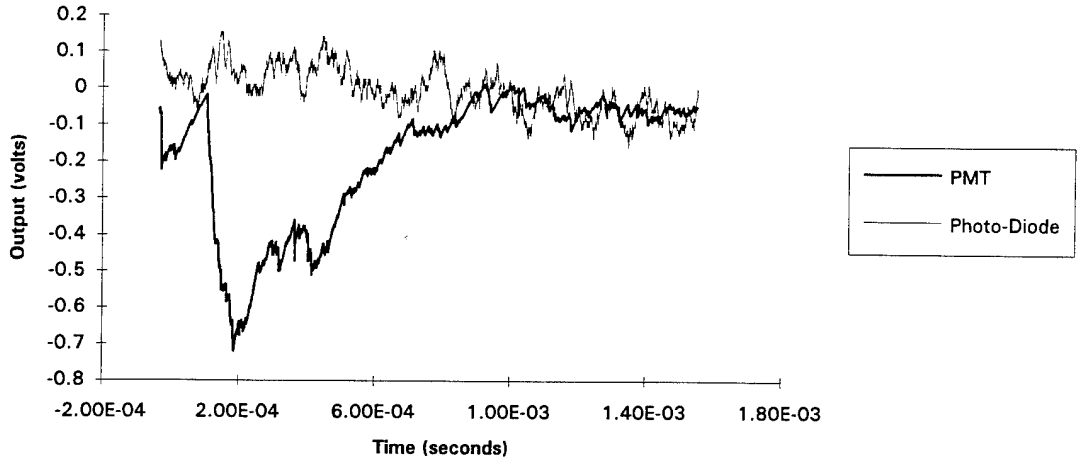

SUNSHADE - 25 DEGREE IMPACT
DATA SET G12, 700 VOLT APPLIED

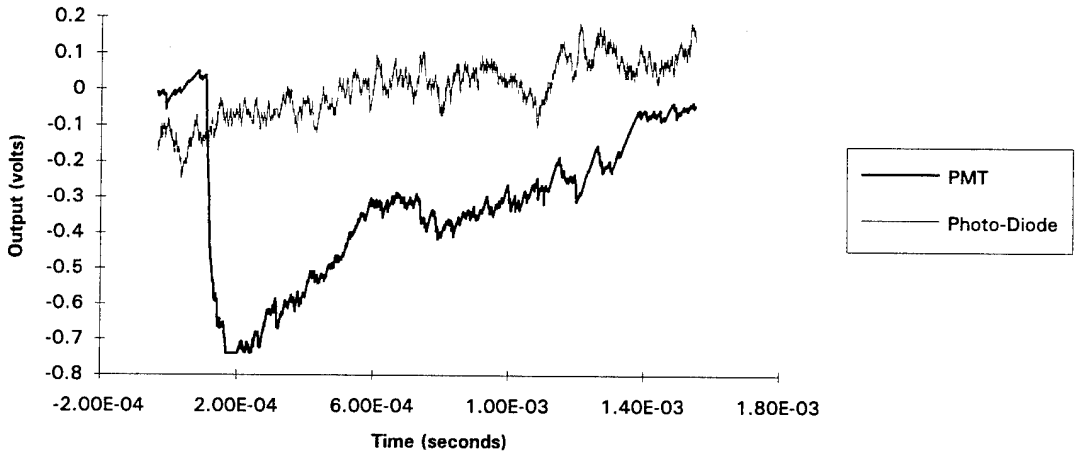

SUNSHADE - 25 DEGREE IMPACT
DATA SET G13, 700 VOLT APPLIED

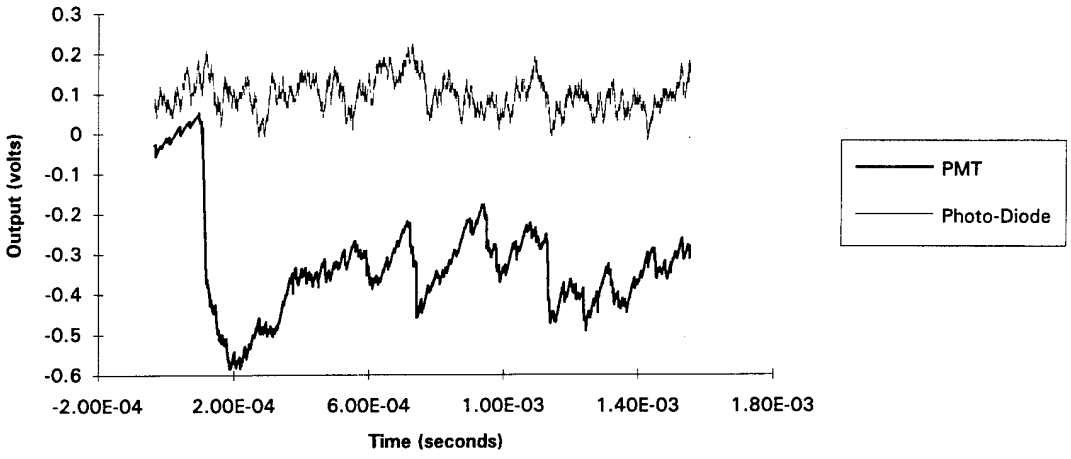

SUNSHADE - 25 DEGREE IMPACT
DATA SET G14, 700 VOLT APPLIED

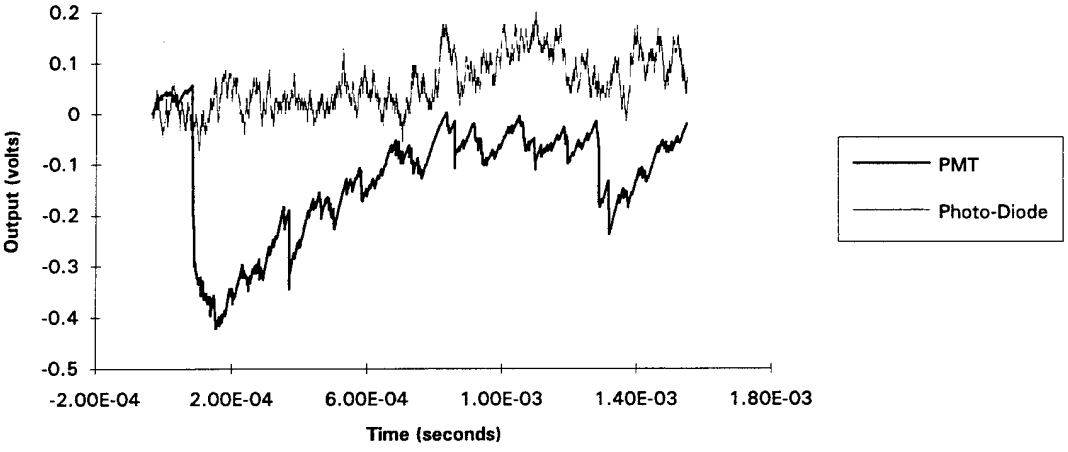

APPENDIX E

SUNSHADE DATA, 700 VOLT REMOVED

SUNSHADE - 25 DEGREE IMPACT
DATA SET C1, 700 VOLT REMOVED

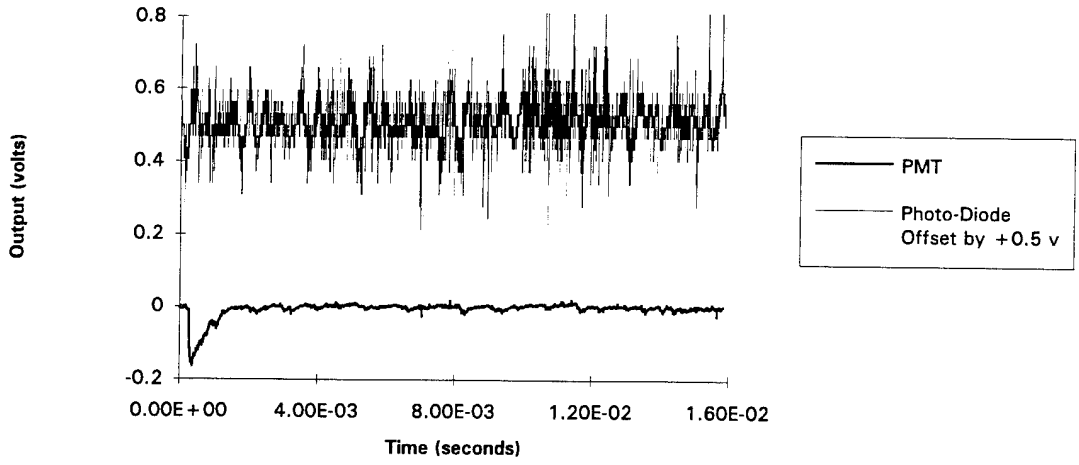

SUNSHADE - 25 DEGREE IMPACT
DATA SET C2, 700 VOLT REMOVED

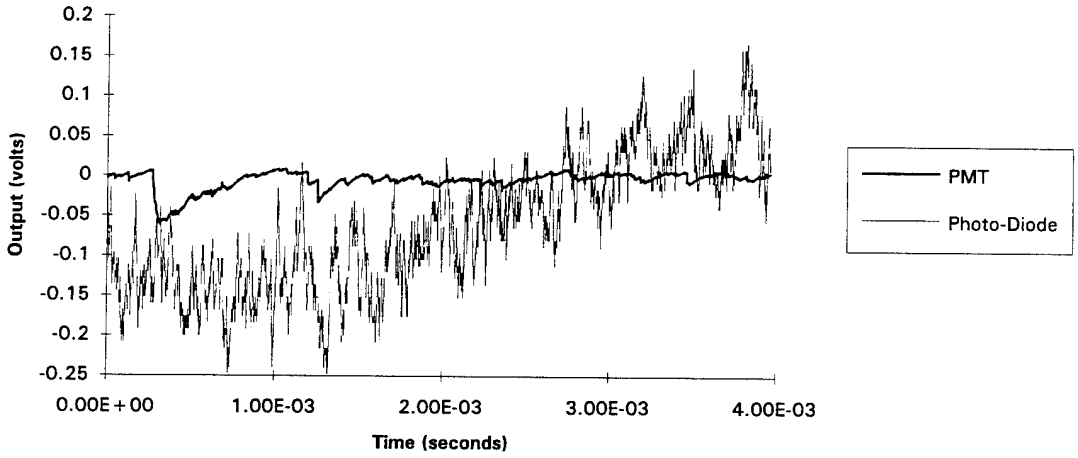

SUNSHADE - 25 DEGREE IMPACT
DATA SET C3, 700 VOLT REMOVED

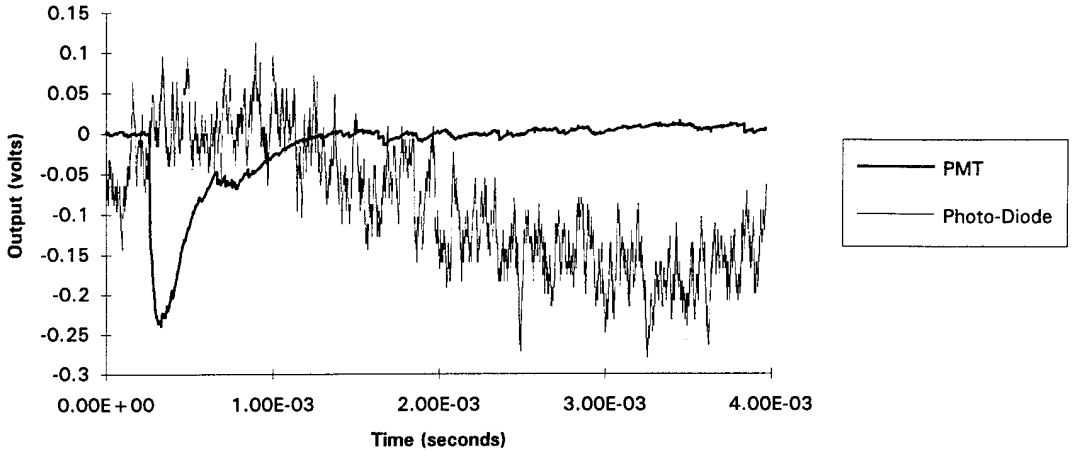

SUNSHADE - 25 DEGREE IMPACT
DATA SET C5, 700 VOLT REMOVED

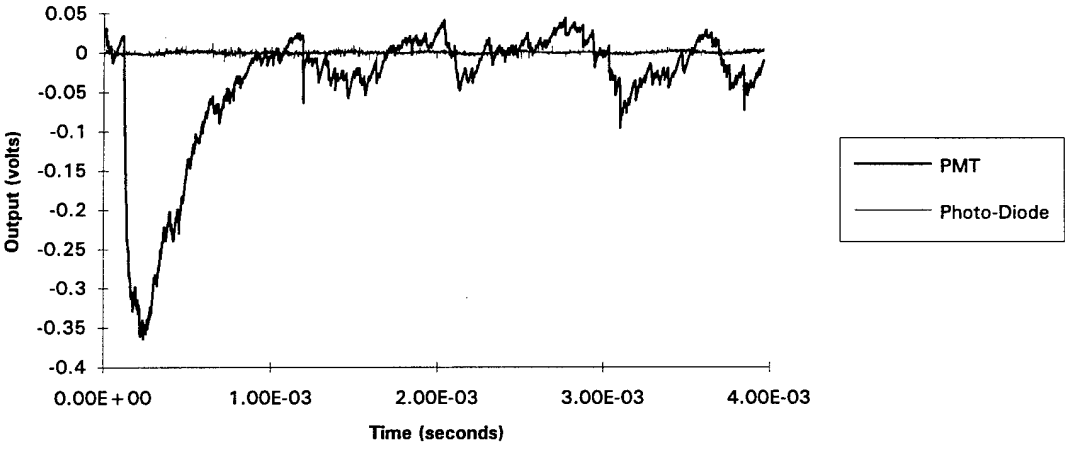

SUNSHADE - 25 DEGREE IMPACT
DATA SET C6, 700 VOLT REMOVED

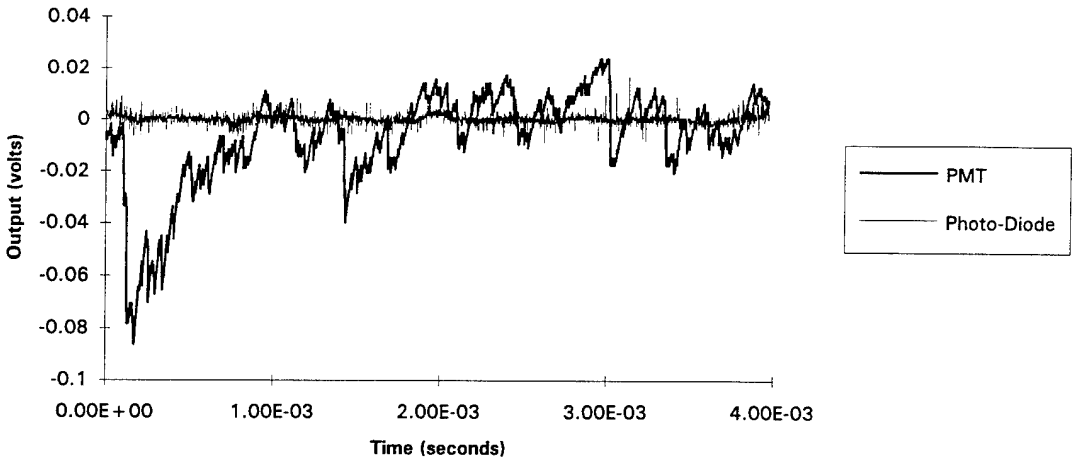

SUNSHADE - 25 DEGREE IMPACT
DATA SET C7, 700 VOLT REMOVED

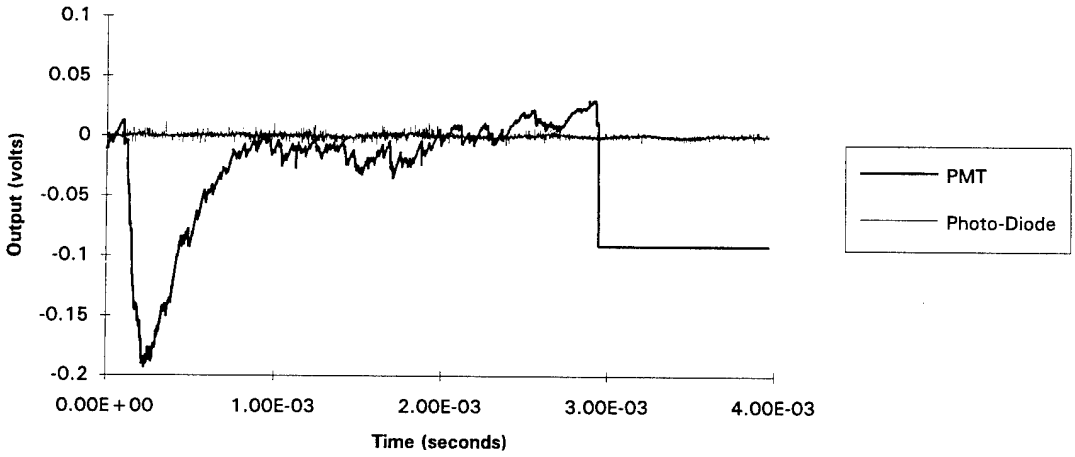

SUNSHADE - 25 DEGREE IMPACT
DATA SET C8, 700 VOLT REMOVED

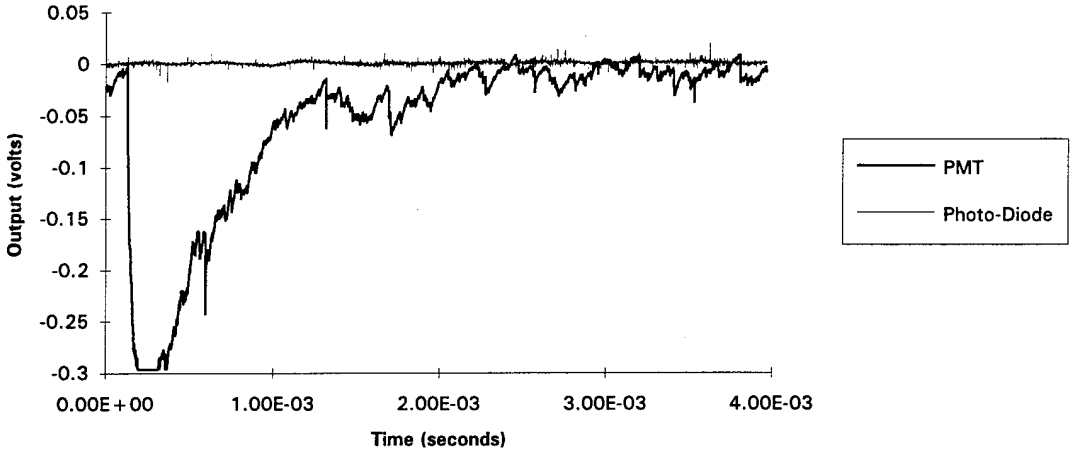

SUNSHADE - 25 DEGREE IMPACT
DATA SET C9, 700 VOLT REMOVED

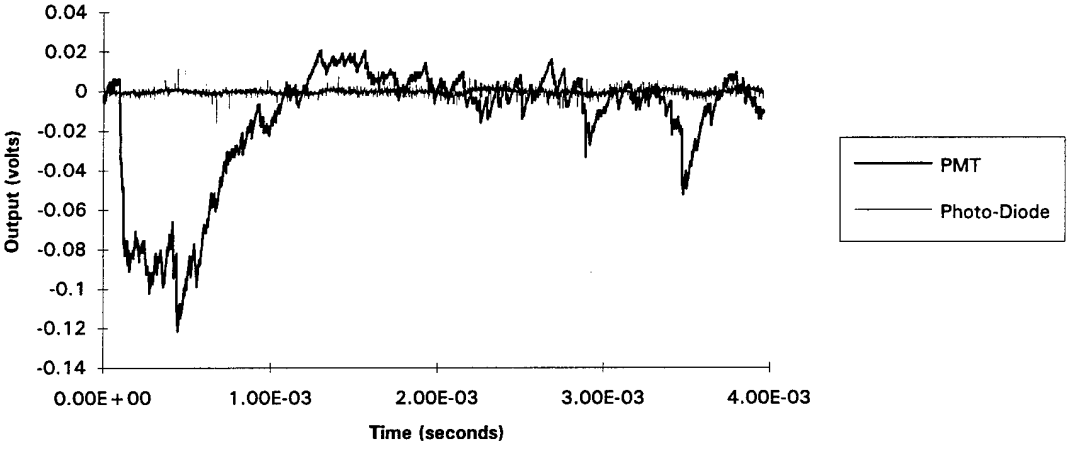

SUNSHADE - 25 DEGREE IMPACT
DATA SET C10, 700 VOLT REMOVED

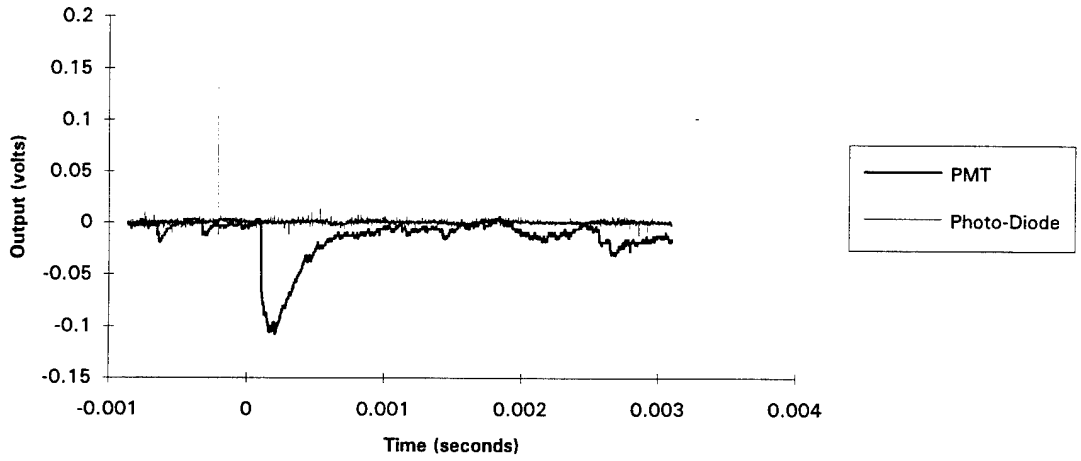

SUNSHADE - 25 DEGREE IMPACT
DATA SET C11, 700 VOLT REMOVED

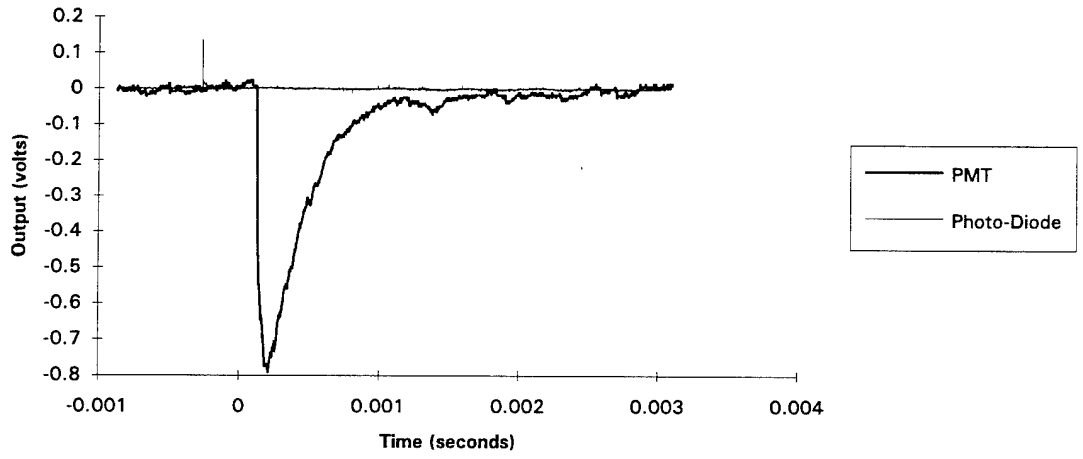

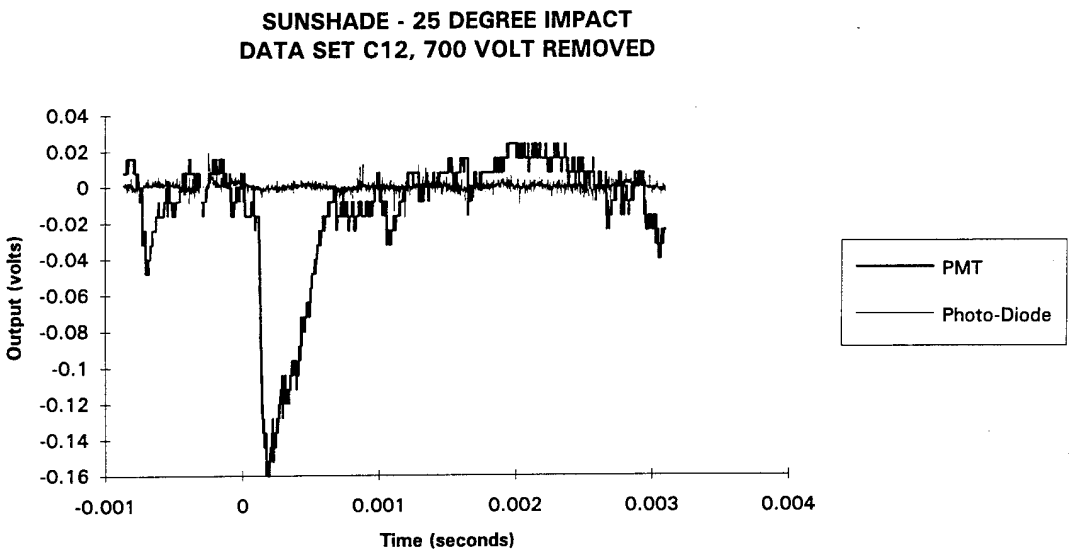
SUNSHADE - 25 DEGREE IMPACT
DATA SET C12, 700 VOLT REMOVED
0.04
0.02
0
-0.02
-0.04
-0.06
-0.08
-0.1
-0.12
-0.14
-0.16
Output (volts)
-0.001
0
0.001
0.002
0.003
0.004
Time (seconds)
PMT
Photo-Diode

SUNSHADE - 25 DEGREE IMPACT
DATA SET C13, 700 VOLT REMOVED

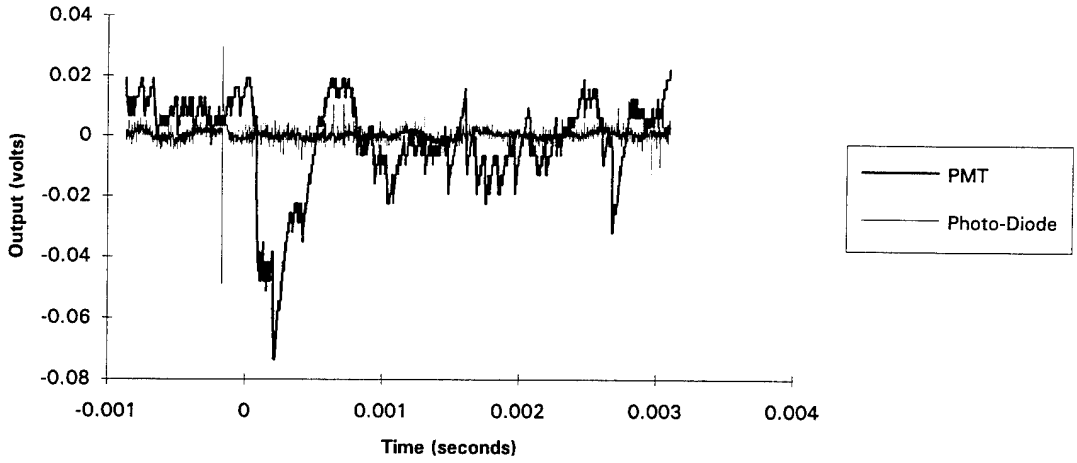

SUNSHADE - 25 DEGREE IMPACT
DATA SET C14, 700 VOLT REMOVED

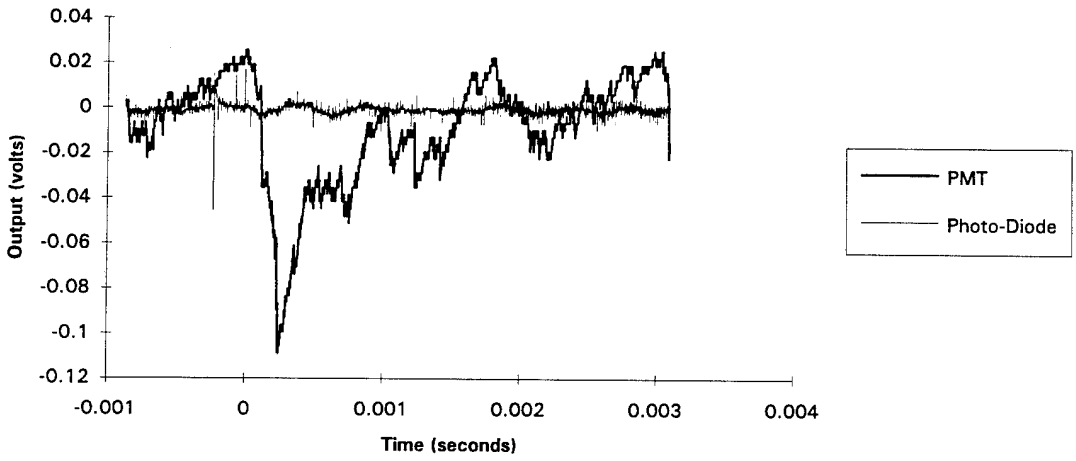

SUNSHADE - 25 DEGREE IMPACT
DATA SET C15, 700 VOLT REMOVED

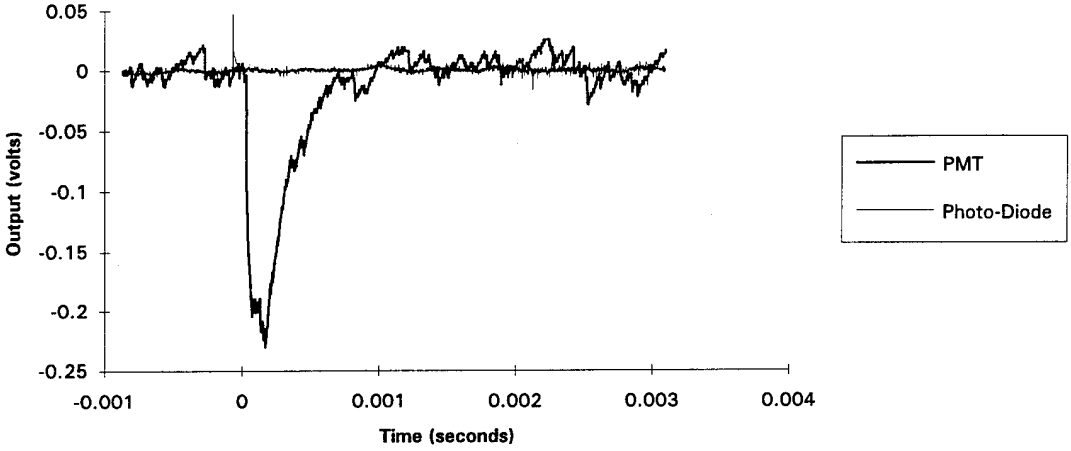

SUNSHADE - 25 DEGREE IMPACT
DATA SET C16, 700 VOLT REMOVED

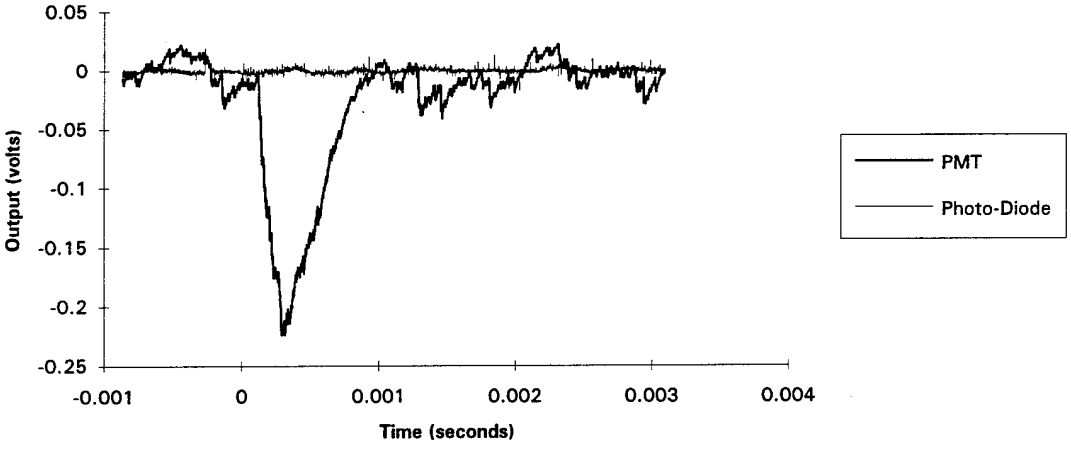

SUNSHADE - 25 DEGREE IMPACT
DATA SET C17, 700 VOLT REMOVED

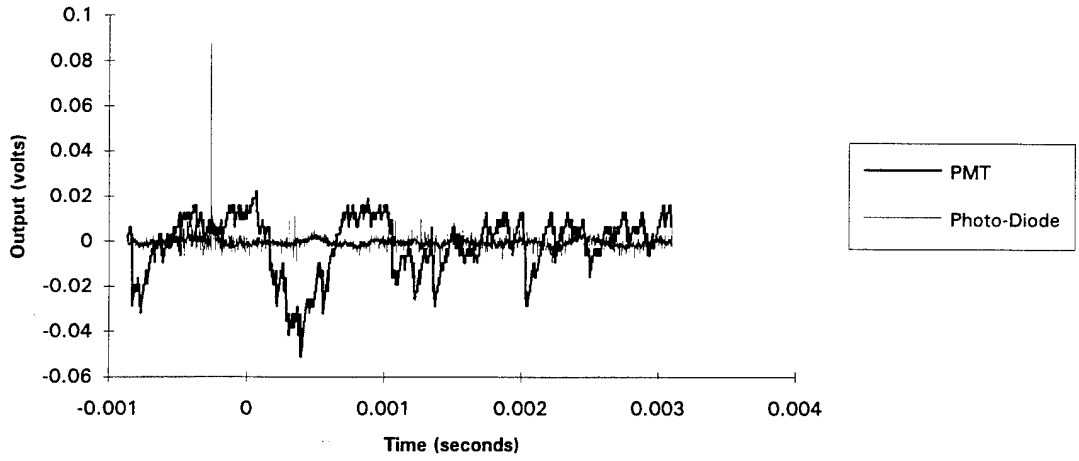

SUNSHADE - 25 DEGREE IMPACT
DATA SET C18, 700 VOLT REMOVED

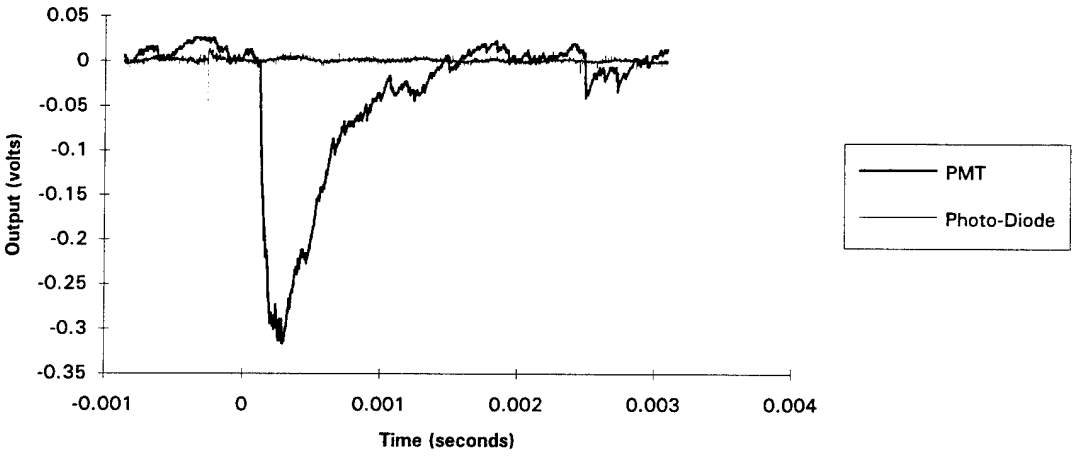

SUNSHADE - 25 DEGREE IMPACT
DATA SET C19, 700 VOLT REMOVED

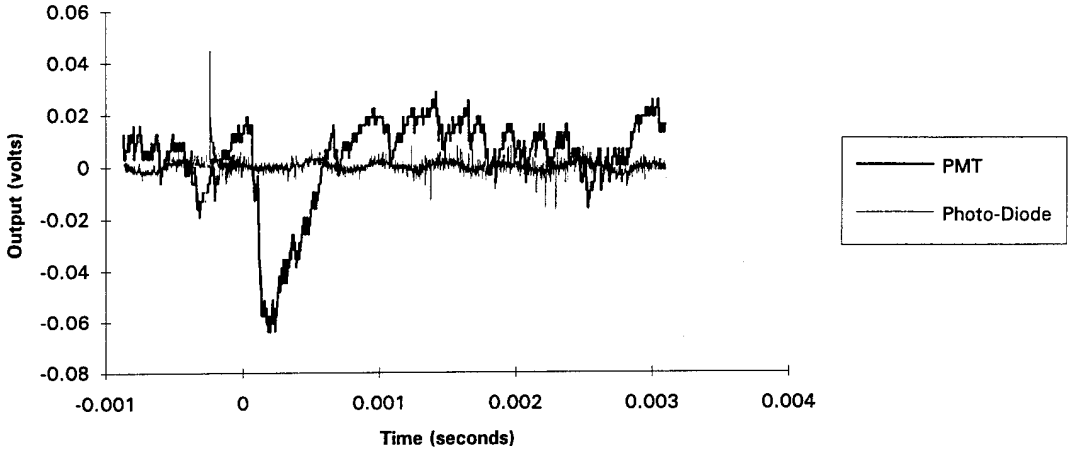

SUNSHADE - 25 DEGREE IMPACT
DATA SET C20, 700 VOLT REMOVED

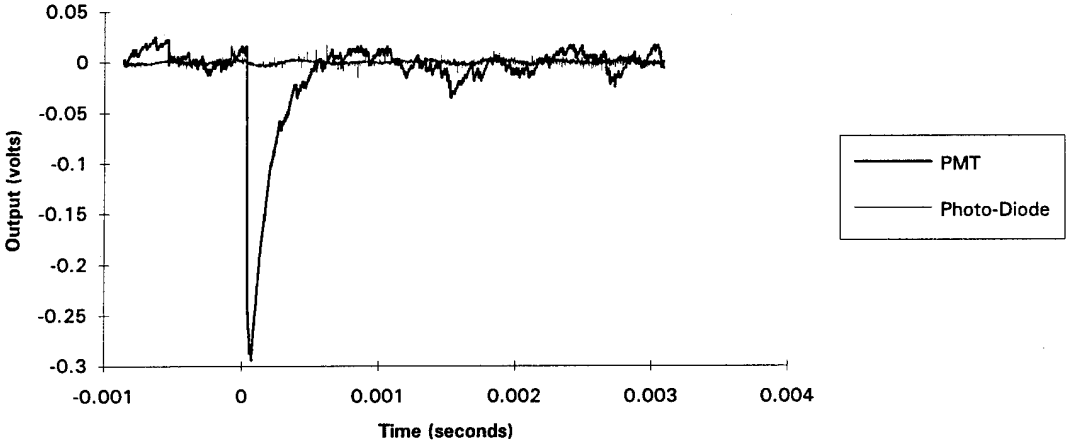

SUNSHADE - 25 DEGREE IMPACT
DATA SET E10, 700 VOLT REMOVED

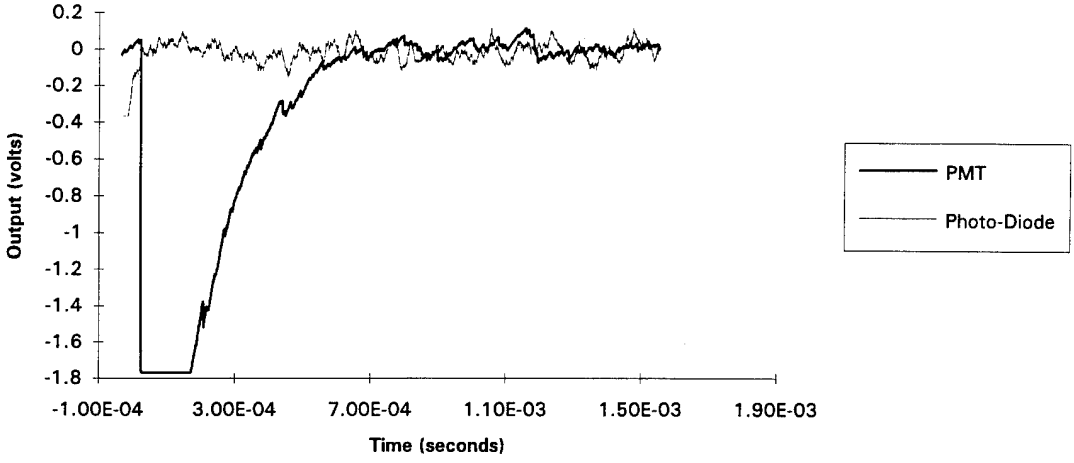

SUNSHADE - 25 DEGREE IMPACT
DATA SET E11, 700 VOLT REMOVED

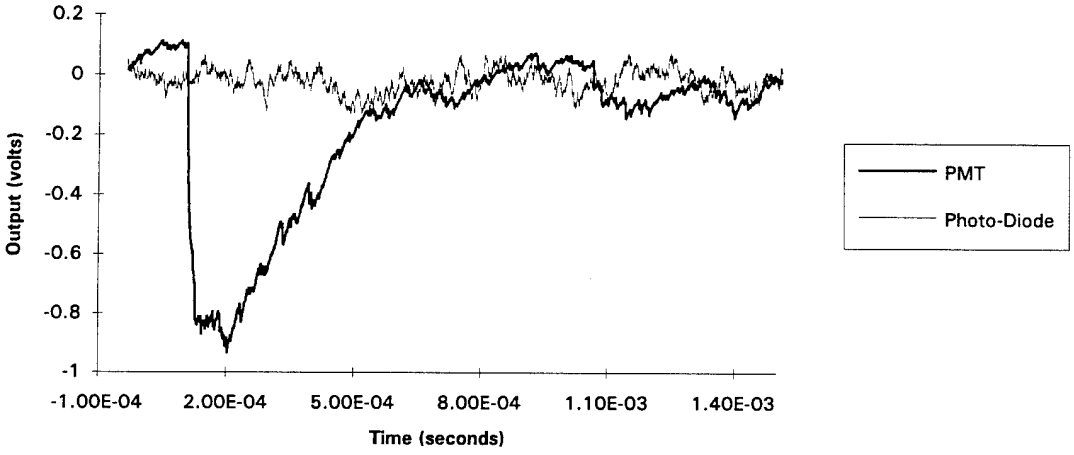

SUNSHADE - 25 DEGREE IMPACT
DATA SET E12, 700 VOLT REMOVED

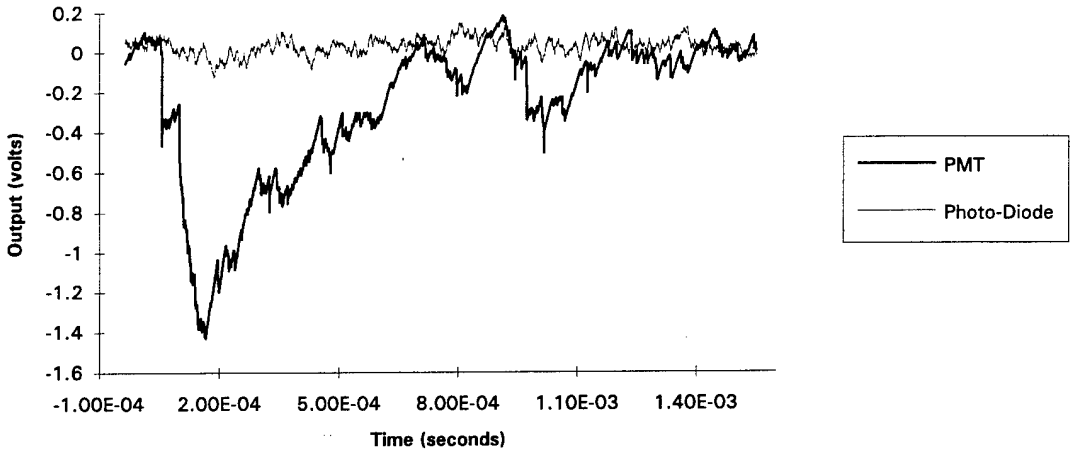

SUNSHADE - 25 DEGREE IMPACT
DATA SET E13, 700 VOLT REMOVED

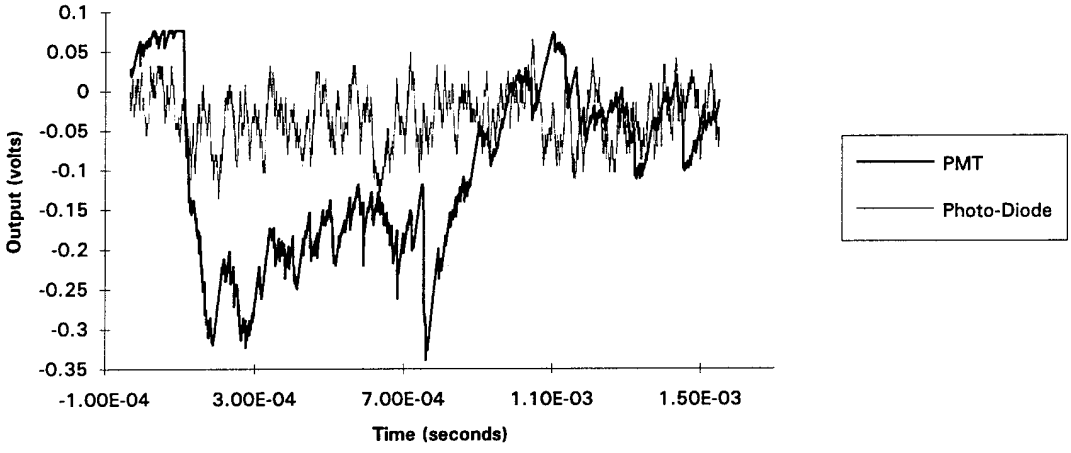

SUNSHADE - 25 DEGREE IMPACT
DATA SET E14, 700 VOLT REMOVED

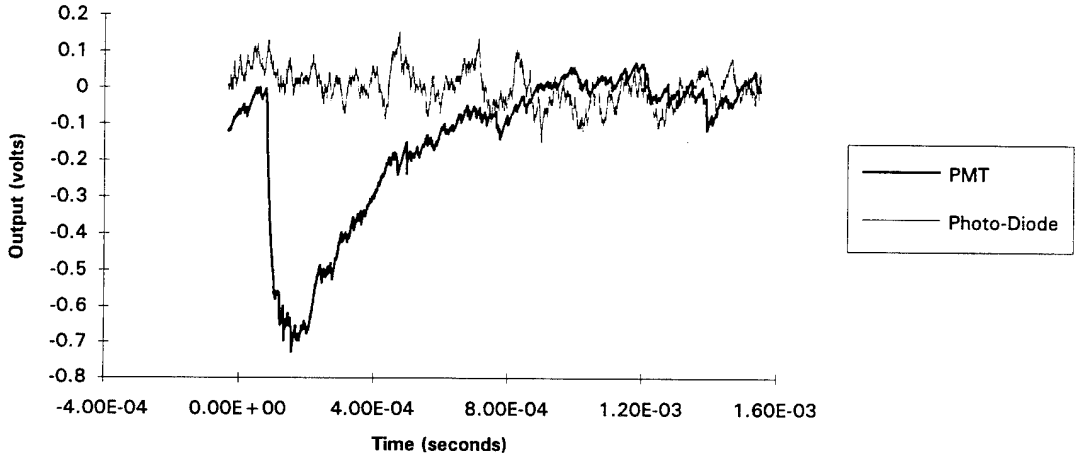

SUNSHADE - 25 DEGREE IMPACT
DATA SET E15, 700 VOLT REMOVED

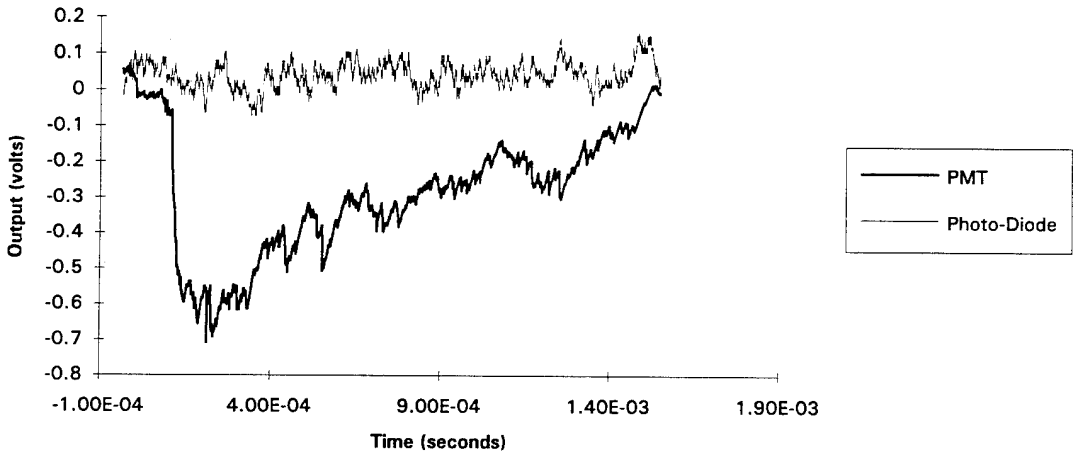

SUNSHADE - 25 DEGREE IMPACT
DATA SET E16, 700 VOLT REMOVED

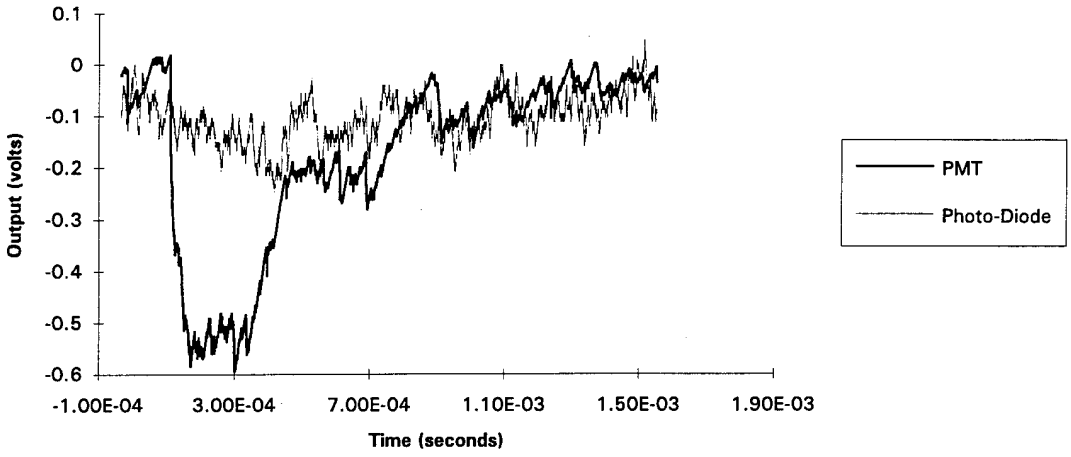

SUNSHADE - 25 DEGREE IMPACT
DATA SET E17, 700 VOLT REMOVED

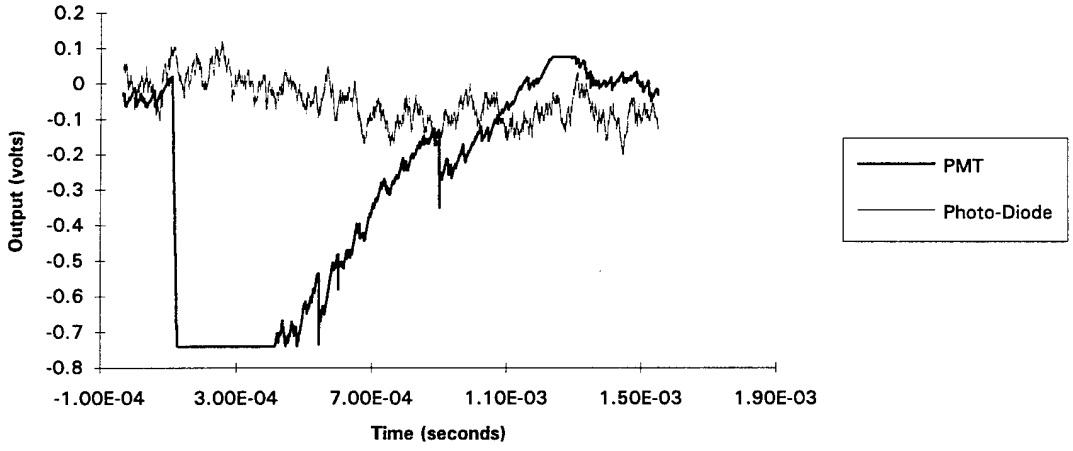

SUNSHADE - 25 DEGREE IMPACT
DATA SET E18, 700 VOLT REMOVED

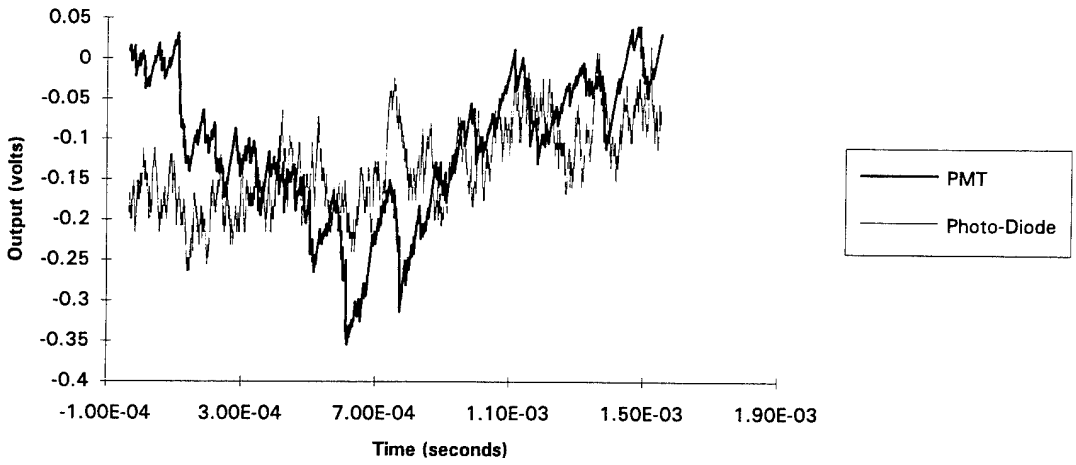

SUNSHADE - 25 DEGREE IMPACT
DATA SET E19, 700 VOLT REMOVED

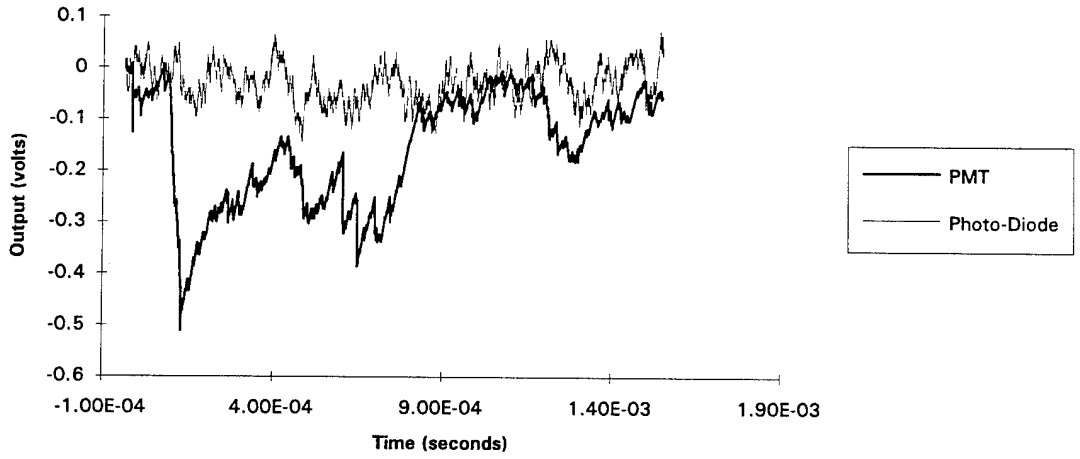

SUNSHADE - 25 DEGREE IMPACT
DATA SET E20, 700 VOLT REMOVED

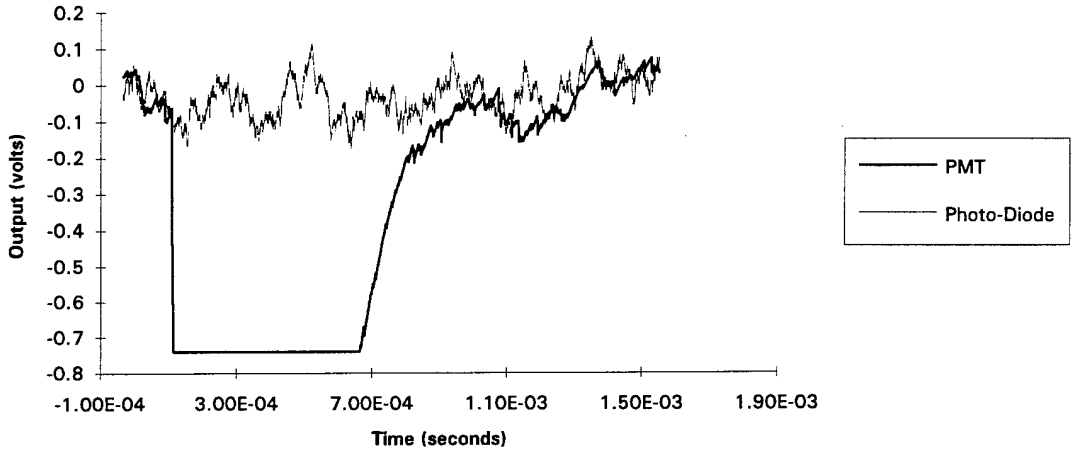

SUNSHADE - 25 DEGREE IMPACT
DATA SET F1, 700 VOLT REMOVED

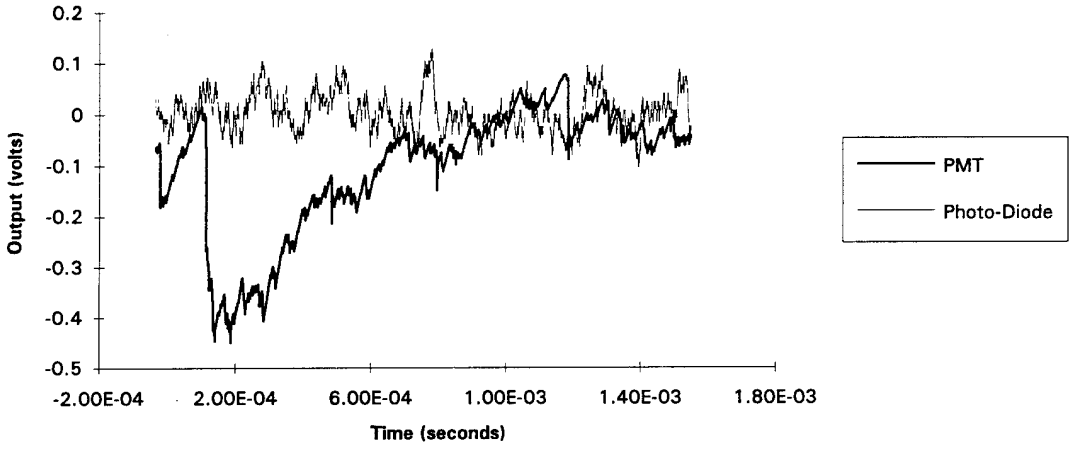

SUNSHADE - 25 DEGREE IMPACT
DATA SET F2, 700 VOLT REMOVED

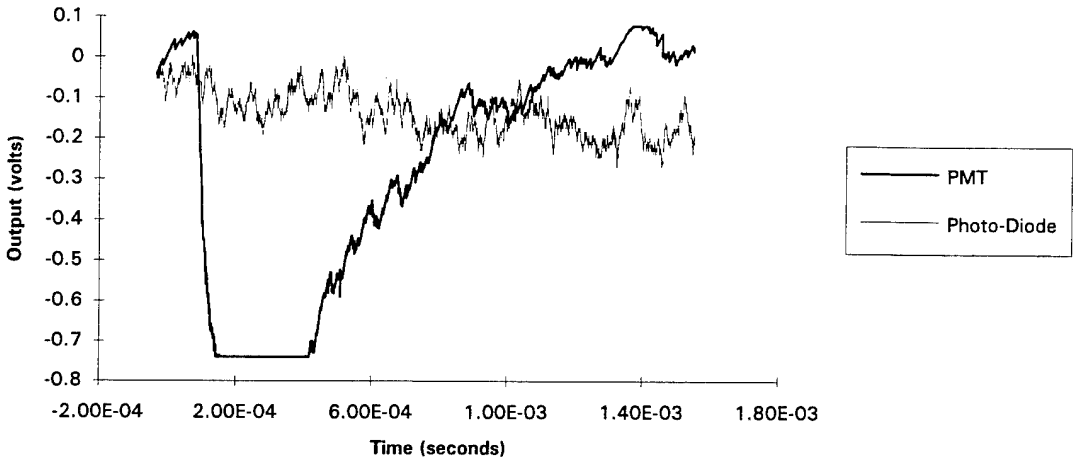

SUNSHADE - 25 DEGREE IMPACT
DATA SET F3, 700 VOLT REMOVED

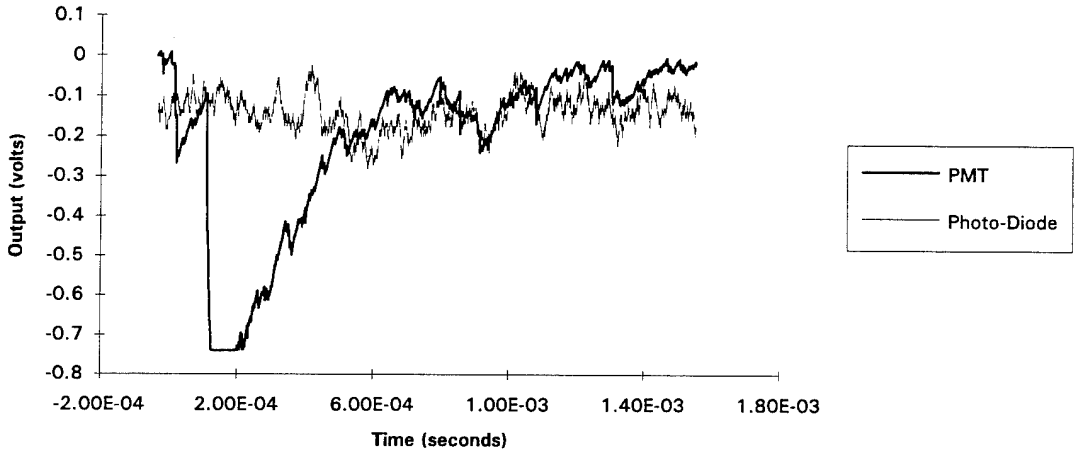

SUNSHADE - 25 DEGREE IMPACT
DATA SET F4, 700 VOLT REMOVED

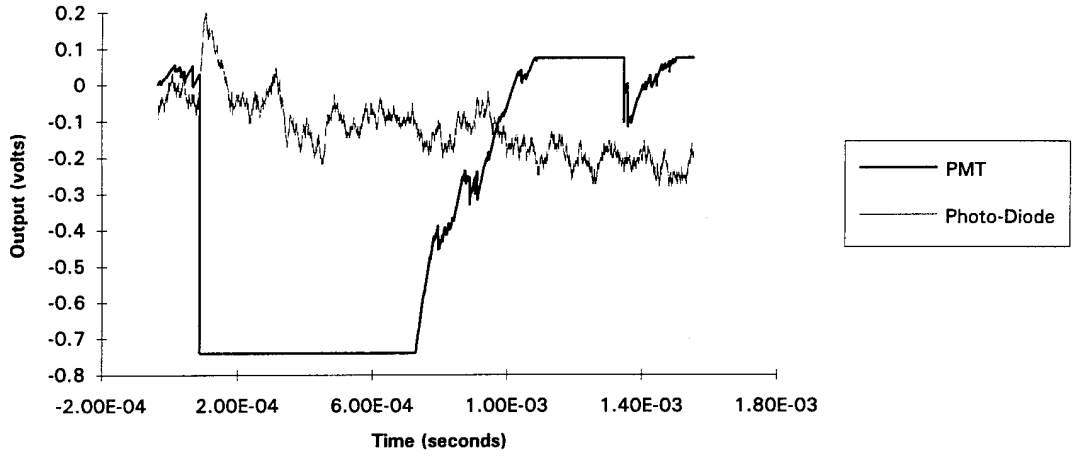

SUNSHADE - 25 DEGREE IMPACT
DATA SET F5, 700 VOLT REMOVED

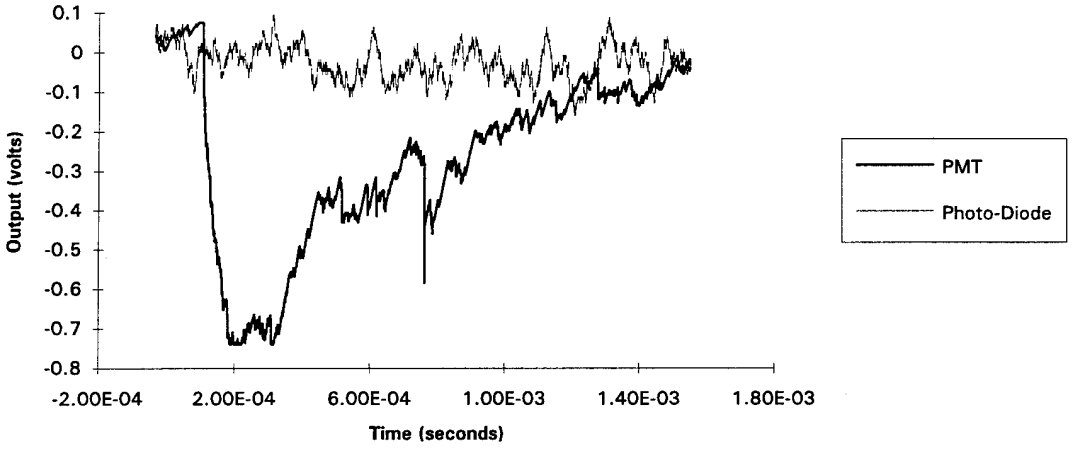

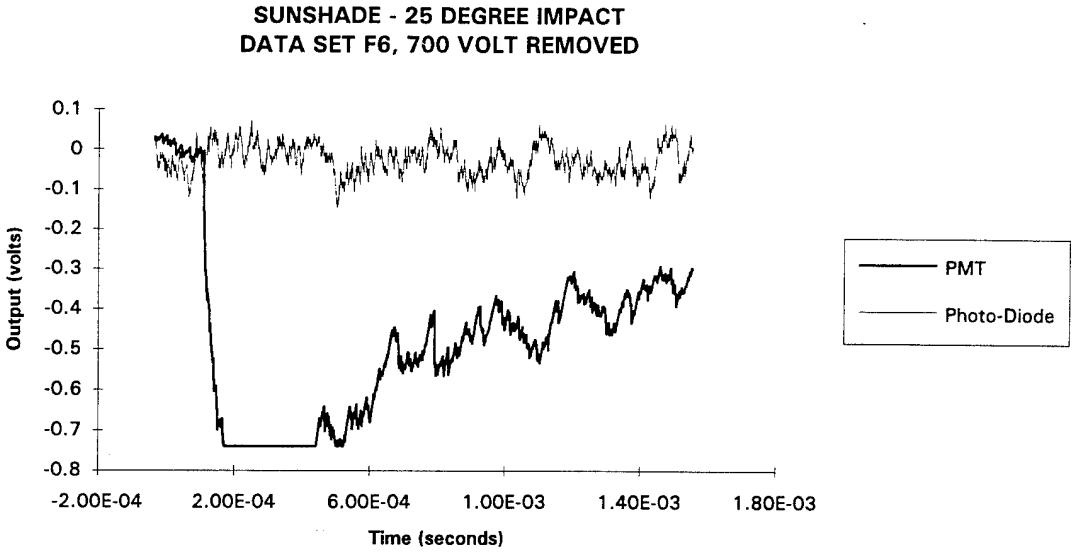
SUNSHADE - 25 DEGREE IMPACT
DATA SET F6, 700 VOLT REMOVED
Output (volts)
0.1
0
-0.1
-0.2
-0.3
-0.4
-0.5
-0.6
-0.7
-0.8
-2.00E-04
2.00E-04
6.00E-04
1.00E-03
1.40E-03
1.80E-03
Time (seconds)
PMT
Photo-Diode

APPENDIX F

SUMMARIZED IMPACT DATA

LENS - NORMAL IMPACT, 700 VOLT APPLIED

Data	Velocity km/sec	Watts Power	Joules Energy	Rise Time Seconds	Diameter micron	Mass g*10^-13	Mass kg	Normalize Mass (J/kg)
A6	8.14	8.87E-09	2.31E-13	3.82E-05	5.54E-01	7.00E+00	7.00E-16	3.30E+02
A7	8.44	1.59E-08	6.41E-13	5.06E-05	5.83E-01	8.14E+00	8.14E-16	7.88E+02
A8	9.49	1.01E-08	5.61E-13	7.64E-05	4.92E-01	4.89E+00	4.89E-16	1.15E+03
A9	9.07	6.37E-09	5.61E-13	2.66E-05	5.07E-01	5.36E+00	5.36E-16	1.05E+03
A10	8.71	1.38E-08	7.51E-13	6.20E-05	5.71E-01	7.65E+00	7.65E-16	9.83E+02
A11	8.02	1.97E-08	1.32E-12	8.42E-05	7.34E-01	1.62E+01	1.62E-15	8.14E+02
A12	9.12	1.09E-08	1.32E-12	4.10E-05	5.34E-01	6.28E+00	6.28E-16	2.11E+03
A13	8.24	9.56E-09	9.15E-13	8.92E-05	5.50E-01	6.83E+00	6.83E-16	1.34E+03
A14	11.22	2.40E-09	3.24E-13	1.18E-04	4.48E-01	3.69E+00	3.69E-16	8.78E+02
A15	8.38	9.20E-09	5.71E-13	6.86E-05	5.86E-01	8.26E+00	8.26E-16	6.91E+02
A16	8.79	1.07E-08	5.71E-13	5.44E-05	5.27E-01	6.01E+00	6.01E-16	9.51E+02
A17	9.23	1.00E-08	9.87E-13	8.92E-05	4.88E-01	4.77E+00	4.77E-16	2.07E+03
A18	10.29	1.45E-09	9.87E-13	3.90E-05	3.76E-01	2.19E+00	2.19E-16	4.50E+03
A19	8.49	1.41E-08	9.87E-13	2.16E-05	5.81E-01	8.05E+00	8.05E-16	1.23E+03
A20	8.22	9.42E-09	9.87E-13	6.50E-05	6.30E-01	1.03E+01	1.03E-15	9.58E+02

3/21/95 4:34 PM
SUMDATAA.XLS

LENS - NORMAL IMPACT, 700 VOLT REMOVED

Data	Velocity km/sec	Watts Power	Joules Energy	Rise Time Seconds	Diameter micron	Mass g*10^-13	Mass kg	Normalize J/kg
A1	8.98	1.88E-08	7.39E-13	5.32E-05	1.52E-01	1.44E-01	1.44E-17	5.13E+04
A2	9.64	1.08E-08	7.46E-13	8.80E-05	1.15E-01	6.24E-02	6.24E-18	1.20E+05
A3	8.29	1.77E-08	8.19E-13	5.94E-05	2.02E-01	3.38E-01	3.38E-17	2.43E+04
A4	8.35	1.91E-08	8.19E-13	4.32E-05	1.59E-01	1.66E-01	1.66E-17	4.92E+04
A5	7.96	3.89E-09	7.46E-13	6.56E-05	7.56E-01	1.78E+01	1.78E-15	4.20E+02
B3	8.12	2.84E-08	1.39E-12	6.70E-05	7.54E-01	1.76E+01	1.76E-15	7.90E+02
B4	13.51	5.18E-09	1.39E-12	1.80E-05	3.38E-01	1.59E+00	1.59E-16	8.74E+03
B5	8.61	1.31E-08	1.39E-12	5.40E-05	6.11E-01	9.39E+00	9.39E-16	1.48E+03
B6	8.71	5.13E-09	1.39E-12	5.90E-05	4.47E-01	3.67E+00	3.67E-16	3.79E+03
B7	8.94	6.61E-09	1.39E-12	3.36E-05	2.60E-01	7.26E-01	7.26E-17	1.91E+04
B8	9.67	4.38E-09	1.39E-12	4.40E-05	4.39E-01	3.47E+00	3.47E-16	4.00E+03
B9	8.27	1.59E-08	1.39E-12	4.24E-05	3.96E-01	2.54E+00	2.54E-16	5.46E+03
B10	8.42	1.28E-08	1.39E-12	8.14E-05	3.73E-01	2.13E+00	2.13E-16	6.53E+03
B11	10.1	3.98E-09	1.39E-12	8.14E-05	1.91E-01	2.84E-01	2.84E-17	4.89E+04
B12	8.34	7.66E-09	1.39E-12	8.14E-05	2.53E-01	6.67E-01	6.67E-17	2.08E+04
B13	8.25	8.86E-09	1.39E-12	8.86E-05	2.75E-01	8.52E-01	8.52E-17	1.63E+04
B14	8.35	1.85E-08	1.39E-12	8.66E-05	3.05E-01	1.16E+00	1.16E-16	1.19E+04
B15	8.33	1.23E-08	1.39E-12	8.14E-05	3.19E-01	1.34E+00	1.34E-16	1.04E+04
B16	8.06	3.81E-09	1.39E-12	8.14E-05	2.59E-01	7.14E-01	7.14E-17	1.94E+04
B17	8.1	2.66E-09	1.39E-12	6.18E-05	2.58E-01	7.07E-01	7.07E-17	1.96E+04
B18	10.33	1.09E-08	1.39E-12	3.06E-05	2.20E-01	4.35E-01	4.35E-17	3.19E+04
B19	8.05	1.29E-08	3.02E-12	1.79E-04	3.40E-01	1.61E+00	1.61E-16	1.88E+04
B20	9.09	1.01E-08	2.32E-12	1.79E-04	3.01E-01	1.12E+00	1.12E-16	2.06E+04

SUNSHADE, 25 DEGREE IMPACT, 700 VOLT REMOVED

Data	Velocity km/sec	Watts Power	Joules Energy	Rise Time Seconds	Diameter micron	Mass g*10^-13	Mass kg	Normalize Mass (J/kg)
C1	8.20	7.35E-08	3.42E-12	5.40E-05	8.17E-01	2.24E+01	2.24E-15	1.53E+03
C2	8.08	5.41E-09	3.42E-12	4.25E-05	7.81E-01	1.95E+01	1.95E-15	1.75E+03
C3	8.34	1.99E-08	3.42E-12	7.10E-05	7.64E-01	1.83E+01	1.83E-15	1.87E+03
C5	8.09	1.66E-08	3.42E-12	8.95E-05	4.76E-01	4.43E+00	4.43E-16	7.73E+03
C6	7.75	7.41E-10	3.42E-12	2.06E-03	6.56E-01	1.16E+01	1.16E-15	2.95E+03
C7	7.57	8.50E-11	3.42E-12	2.06E-03	7.01E-01	1.42E+01	1.42E-15	2.42E+03
* C8	7.59	1.99E-08	8.93E-13	8.96E-05	6.65E-01	1.21E+01	1.21E-15	7.39E+02
C9	9.84	4.43E-09	8.73E-12	1.10E-04	4.44E-01	3.59E+00	3.59E-16	2.43E+04
C10	9.75	5.19E-09	8.73E-12	6.40E-05	4.47E-01	3.66E+00	3.66E-16	2.38E+04
C11	7.67	3.87E-08	9.27E-12	6.55E-05	9.16E-01	3.15E+01	3.15E-15	2.94E+03
C12	8.11	7.61E-09	9.27E-12	5.55E-05	5.56E-01	7.05E+00	7.05E-16	1.31E+04
C13	12.06	4.02E-09	8.73E-12	9.00E-05	3.39E-01	1.60E+00	1.60E-16	5.47E+04
C14	8.76	1.95E-09	1.11E-11	1.34E-03	5.28E-01	6.05E+00	6.05E-16	1.83E+04
C15	30.35	9.22E-12	9.99E-12	1.34E-03	1.66E-01	1.89E-01	1.89E-17	5.29E+05
C16	7.57	1.10E-09	1.13E-11	1.34E-03	4.97E-01	5.06E+00	5.06E-16	2.23E+04
C17	7.79	2.36E-09	1.13E-11	3.03E-04	6.88E-01	1.34E+01	1.34E-15	8.44E+03
C18	7.97	1.43E-08	1.13E-11	1.13E-04	5.11E-01	5.48E+00	5.48E-16	2.06E+04
C19	8.47	2.87E-10	8.51E-12	1.34E-03	6.18E-01	9.70E+00	9.70E-16	8.77E+03
C20	25.67	1.46E-08	8.51E-12	6.45E-05	1.62E-01	1.76E-01	1.76E-17	4.83E+05
* E10	38.39	3.12E-08	1.12E-13	7.20E-06	1.31E-01	8.01E-02	8.01E-18	1.40E+04
E11	8.28	1.11E-08	1.46E-13	1.90E-05	5.91E-01	7.27E+00	7.27E-16	2.00E+02
E12	8.84	1.48E-08	1.34E-12	8.88E-05	4.56E-01	3.39E+00	3.39E-16	3.94E+03
E13	8.2	4.50E-09	1.34E-12	8.14E-05	4.23E-01	3.17E+00	3.17E-16	4.21E+03
E14	10.94	3.25E-11	1.96E-12	6.52E-04	4.07E-01	2.39E+00	2.39E-16	8.21E+03
E15	8.15	8.42E-09	1.96E-12	8.00E-05	4.25E-01	2.70E+00	2.70E-16	7.24E+03
E16	8.09	6.74E-09	1.96E-12	6.36E-05	6.32E-01	8.92E+00	8.92E-16	2.20E+03
* E17	8.09	1.95E-08	3.16E-13	3.24E-05	5.56E-01	5.82E+00	5.82E-16	5.44E+02
E18	8.02	1.28E-09	4.70E-12	4.40E-05	4.70E-01	3.66E+00	3.66E-16	1.28E+04
E19	9.24	4.55E-09	4.70E-12	1.90E-05	4.49E-01	3.20E+00	3.20E-16	1.47E+04
* E20	8.19	6.48E-08	6.61E-13	2.04E-05	6.30E-01	8.86E+00	8.86E-16	7.46E+02
F1	8.03	4.04E-09	8.92E-14	2.90E-05	4.80E-01	3.91E+00	3.91E-16	2.28E+02
* F2	10.47	1.40E-08	4.71E-13	6.75E-05	3.26E-01	1.23E+00	1.23E-16	3.83E+03
* F3	8.22	9.35E-09	1.42E-13	3.04E-05	5.75E-01	6.73E+00	6.73E-16	2.11E+02
* F4	10.01	2.74E-08	2.99E-13	2.18E-05	4.43E-01	3.08E+00	3.08E-16	9.71E+02
F5	8.32	9.57E-09	4.86E-13	7.54E-05	4.93E-01	4.21E+00	4.21E-16	1.15E+03
* F6	7.13	1.13E-08	3.69E-13	6.52E-05	5.53E-01	6.06E+00	6.06E-16	6.10E+02

3/21/95 4:36 PM
SUMDATAC.XLS

* - Estimated power, energy, and risetime

SUNSHADE, 25 DEGREE IMPACT, 700 VOLT APPLIED

Data	Velocity km/sec	Watts Power	Joules Energy	Rise Time Seconds	Diameter micron	Mass g*10^-13	Mass kg	Normalize Mass (J/kg)
F7	8.88	8.53E-09	4.71E-13	7.72E-05	5.11E-01	4.69E+00	4.69E-16	1.00E+03
F8	32.84	5.57E-09	4.71E-13	1.68E-05	1.32E-01	7.06E-02	7.06E-18	6.67E+04
F9	9.32	3.90E-09	4.71E-13	5.52E-05	4.70E-01	3.68E+00	3.68E-16	1.28E+03
* F10	28.33	2.49E-08	2.87E-14	2.30E-06	1.52E-01	1.08E-01	1.08E-17	2.65E+03
F11	8.68	3.10E-09	2.17E-13	6.54E-05	4.03E-01	2.30E+00	2.30E-16	9.40E+02
F12	8.27	4.01E-09	2.41E-13	5.20E-05	4.64E-01	3.52E+00	3.52E-16	6.85E+02
F13	14.48	2.84E-09	8.49E-13	1.86E-04	2.92E-01	8.80E-01	8.80E-17	9.65E+03
* F14	9.58	1.61E-08	1.46E-13	1.81E-05	4.84E-01	3.99E+00	3.99E-16	3.65E+02
F15	8.7	4.70E-09	1.36E-12	1.98E-04	4.75E-01	3.78E+00	3.78E-16	3.59E+03
F16	16.37	3.65E-09	1.11E-12	1.98E-04	2.48E-01	5.44E-01	5.44E-17	2.04E+04
F17	9.84	3.40E-09	1.11E-12	2.00E-07	4.17E-01	2.55E+00	2.55E-16	4.35E+03
F18	8.36	3.58E-09	1.11E-12	8.64E-05	4.67E-01	3.60E+00	3.60E-16	3.08E+03
* F19	8.33	2.24E-08	1.12E-13	1.00E-05	6.35E-01	9.03E+00	9.03E-16	1.24E+02
F20	8.08	6.42E-09	1.11E-12	8.64E-05	6.33E-01	8.94E+00	8.94E-16	1.24E+03
G1	8.03	9.63E-09	5.25E-13	8.64E-05	6.05E-01	7.81E+00	7.81E-16	6.72E+02
G2	8.26	9.07E-09	7.54E-13	1.25E-04	5.89E-01	7.23E+00	7.23E-16	1.04E+03
G3	8.71	5.14E-09	7.12E-13	1.49E-04	4.98E-01	4.35E+00	4.35E-16	1.64E+03
G4	9.59	4.86E-09	7.12E-13	5.44E-05	3.92E-01	2.13E+00	2.13E-16	3.33E+03
G5	8.1	8.10E-09	7.12E-13	3.26E-05	5.90E-01	7.27E+00	7.27E-16	9.79E+02
G6	8.26	5.89E-09	7.12E-13	1.05E-04	5.89E-01	7.23E+00	7.23E-16	9.84E+02
G7	8.18	7.08E-09	8.64E-13	1.32E-04	6.26E-01	8.64E+00	8.64E-16	9.99E+02
G8	8.3	6.29E-09	8.64E-13	5.42E-05	6.30E-01	8.79E+00	8.79E-16	9.82E+02
* G9	8.68	2.12E-08	2.09E-13	1.97E-05	7.85E-01	1.71E+01	1.71E-15	1.22E+02
G10	8.62	3.85E-09	8.64E-13	5.82E-05	4.98E-01	4.37E+00	4.37E-16	1.98E+03
G11	8.46	4.47E-09	8.75E-13	1.58E-04	5.38E-01	5.48E+00	5.48E-16	1.60E+03
G12	8.3	8.85E-09	1.37E-12	1.58E-04	5.59E-01	6.18E+00	6.18E-16	2.21E+03
G13	8.29	5.88E-09	1.02E-12	1.65E-04	4.87E-01	4.07E+00	4.07E-16	2.49E+03
G14	10.82	5.23E-09	1.02E-12	2.56E-05	3.44E-01	1.44E+00	1.44E-16	7.06E+03

* - Estimated power, energy, and risetime

3/21/95 4:37 PM
SUMDATAF.XLS

MICRO-PARTICLE DETECTOR

Data Set	Velocity km/sec	Diameter micron	Mass x 10^-13 gram	Mass gram	Mass kg	Max. Peak Volts	Normalized Volts/kg	Mass * Vel. g - km/s	Max. Peak Volts
D1	8.47	4.38E-01	2.58E+00	2.58E-13	2.58E-16	42.88	2E+17	2.19E-12	42.88
D2	8.34	4.60E-01	2.97E+00	2.97E-13	2.97E-16	42.88	1E+17	2.48E-12	42.88
D3	10.33	4.12E-01	2.14E+00	2.14E-13	2.14E-16	39.36	2E+17	2.21E-12	39.36
D4	9.23	5.26E-01	4.47E+00	4.47E-13	4.47E-16	42.56	1E+17	4.13E-12	42.56
D5	9.45	4.38E-01	2.56E+00	2.56E-13	2.56E-16	43.2	2E+17	2.42E-12	43.2
D6	9.33	4.34E-01	2.50E+00	2.50E-13	2.50E-16	46.4	2E+17	2.33E-12	46.4
D7	8.81	5.28E-01	4.48E+00	4.48E-13	4.48E-16	42.88	1E+17	3.95E-12	42.88
D8	8.60	5.46E-01	5.00E+00	5.00E-13	5.00E-16	42.56	9E+16	4.30E-12	42.56
D9	8.15	4.74E-01	3.28E+00	3.28E-13	3.28E-16	40.96	1E+17	2.67E-12	40.96
D10	8.00	6.24E-01	7.47E+00	7.47E-13	7.47E-16	40.96	5E+16	5.98E-12	40.96
D11	10.03	4.20E-01	2.27E+00	2.27E-13	2.27E-16	44.16	2E+17	2.28E-12	44.16
D12	8.24	5.58E-01	5.29E+00	5.29E-13	5.29E-16	43.2	8E+16	4.36E-12	43.2
D13	8.32	6.00E-01	6.60E+00	6.60E-13	6.60E-16	43.2	7E+16	5.49E-12	43.2
D14	8.50	5.82E-01	6.02E+00	6.02E-13	6.02E-16	42.56	7E+16	5.12E-12	42.56
D15	8.27	5.20E-01	4.29E+00	4.29E-13	4.29E-16	43.52	1E+17	3.55E-12	43.52
D16	9.10	4.42E-01	2.63E+00	2.63E-13	2.63E-16	42.56	2E+17	2.39E-12	42.56
D17	8.13	5.78E-01	5.93E+00	5.93E-13	5.93E-16	43.2	7E+16	4.82E-12	43.2
D18	9.91	4.36E-01	2.55E+00	2.55E-13	2.55E-16	46.72	2E+17	2.53E-12	46.72
D19	8.03	4.72E-01	3.20E+00	3.20E-13	3.20E-16	45.12	1E+17	2.57E-12	45.12
D20	8.23	5.90E-01	6.26E+00	6.26E-13	6.26E-16	44.48	7E+16	5.15E-12	44.48

3/21/95 4:39 PM
SUMDATAD.XLS